Universidad Zaragoza
1542

Proyecto Fin de Carrera

Solidificación de Aminoácidos en la Captura de CO_2

Tomo 2/2: Anexo. Memoria en inglés

Autor

Irene Gallo Stampino Martínez-Berganza

Director

Dr. Philip L. Fosbøl

Ponente

Dr. Rafael Bilbao Duñabeitia

Escuela de Ingeniería y Arquitectura (EINA)

2012

Preface.

This report serves as my master's thesis which is the completion of my master in chemical engineering. The thesis is the result of my work in the period February-June 2012 at the Department of Chemical and Biochemical Engineering at CERE (Center of Energy Resources Engineering).

This report contains information about the techniques used in order to capture CO_2 and especially about solvents (as amino acids) used in CO_2 absorption. The purpose of the report is to study the solidification of some glycinates during the sequestration of carbon dioxide.

I would like to thank my supervisor Philip Fosbøl for his guidance and feedback, and for teaching me how to improve my work and how to be open-minded. Also thanks to Zacarias Tecle for his help in the lab during the measurements and Martin Bjørner for being so kind and help me with my final report. Moreover I wish to thank my family and friends for supporting me and for always listening to me.

Summary.

CO_2 capture processes may help to reduce the emission of CO_2 to the atmosphere from e.g. power production. Amino acids are one category of chemical molecules which may help to improve the technology. Solidification of the liquids may be an important process obstacle or even a benefit.

In this work freezing points and solubilities have been measured in order to determine the solidification of amino acids. Sodium and potassium glycinate amino acids were considered, both pure aqueous solvents and CO_2 loaded solutions. The analyzed concentration range was 0 to 0.83 mass fractions of the amino acid. The following pure sub-systems were measured: glycine-water, sodium hydroxide-glycine-water, potassium hydroxide-glycine-water. The following loaded systems were measured: sodium bicarbonate-glycine-water, potassium bicarbonate-glycine-water, sodium bicarbonate-sodium hydroxide-glycine-water, and potassium bicarbonate-potassium hydroxide-glycine-water. Besides this, loaded potassium piperazine solutions were also analyzed.

Over 400 solutions were prepared and analyzed in the temperature range -35°C to 100°C. Additional information was obtained by using techniques as powder X-Ray diffraction and microscopy to obtain additional information on crystal structures.

Freezing and solubility points for potassium systems were easier to determine compared to sodium systems. Some freezing points could not be measured because of their viscous aspect, which is not a desired property in CO_2 capture. Viscosity for both sodium systems and potassium systems was approximately the same.

It can be concluded that by adding CO_2 the freezing point increases, so the solidification of the glycinates will occur at higher temperatures as more amount of carbon dioxide is added.

The piperazine measurements were more time-consuming as most of the samples needed to be warmed up. Three different solvents were prepared: 2.2 molal PZ, the 3.6 molal PZ and 4.6 molal $KHCO_3$. Different solidification behaviors and phases were observed while analyzing these systems compared to the sodium systems and the potassium systems.

Problem formulation.

Aqueous amines are typical solvents used in CO_2 capture. There is a potential to improve the solvent and construct a capture process which uses less energy and becomes more cost effective. A concern for many of the solvents is their hazardous nature. Either the solvent or the degradation products are poisonous. One solution to this is to apply amino acids. The benefit is their nutritious nature and lower potential for the formation of degradation products.

A brief literature study will be performed on the use of amino acids in CO_2 capture. There need to be a focus on glycinate solvents. Chemical properties are very important during the modeling of CO_2 capture. These could be e.g. vapor-liquid, solid-liquid, heat capacity, or heat of absorption data. Therefore a summarizing literature study on physical-chemical properties of glycinate should be performed.

The main part of the project will be the experimental measurement of potassium glycinate phase behavior. There is a possibility to continue the measurements and examine piperazine in order to see the effect of this activator in the carbon dioxide capture.

Previously at DTU there has been a short study on possible and unknown formation of glycinate hydrates. Here the work is continued in order to find new and unknown precipitation phenomena.

Method.

A general but short introductory study will be performed on CO_2 capture, to learn and understand the concepts of CO_2 capture and their use in power production.

A literature study on glycinate properties will performed using the resources available at the Technical University of Denmark (DTU) like the local DADS service, CAS SciFinder, or ISI web of science. Knowledge available at DTU will be used in the work too.

Newly constructed equipment at the Center for Energy Resources (CERE) at DTU, will be used in the determination of the compatibility between amino acids and water by measuring freezing and solubility points. These reveals the boundary condition at which solid may form. Additional information may be obtained by microscopy, powder X-Ray diffraction, or similar qualitative methods. There may be a need to use principle analysis techniques in the laboratory like, weighing, filtration, evaporation, drying, and titration to accomplish the goal of measuring the properties.

Contents.

1. Introduction. 7
1.1. Global warming. 7
1.2. CO_2 emissions and concentration. 8
1.3. Protocols. 10
2. CO_2 capture and storage (CCS) techniques. 11
2.1. Capture. 11
2.2. Transport. 11
2.4. CCS costs. 13
3. Combustion techniques for CO_2 capture. 14
3.1. Pre-combustion. 14
3.2. Oxy-fuel combustion. 15
3.3. Post-combustion. 16
4. Post-combustion techniques. 17
4.1. Absorption (“scrubbing”). 17
4.2. Carbonation/calcination. 18
4.3. Adsorption. 18
4.4. Membranes. 18
4.5. Other techniques. 19
4.6. Energy penalty impacts. 19
5. Solvent based CO_2 capture. 20
5.1. Amines. 21
5.2. Ammonia. 22
5.3. Ionic Liquids. 22
5.4. Amino acids. 23
6. The amino acid solvent. 23
7. Glycinates for CO_2 capture. 24
7.1. Introduction. 24
7.2. Physical chemical properties. 25
7.2.1. Sodium glycinate. 25
7.2.2. Potassium glycinate. 28
7.2.3. Vapor-Liquid Equilibrium (VLE). 29

7.2.4. Solid-Liquid equilibrium (SLE).....30
8. Experimental method. 31
8.1. Freezing point. 31
8.2. Solubility. 35
9. Experimental overview and calculations.....35
9.1. Calibration. 36
9.2. Glycine-water system. 38
9.3. Sodium hydroxide and sodium bicarbonate systems. 40
9.3.1. Sodium hydroxide-glycine-water system (NaOH-Gly-H_2O).....40
9.3.2. Sodium bicarbonate-glycine-water system ($NaHCO_3$-Gly-H_2O). 50
9.3.3. Sodium bicarbonate-sodium hydroxide-glycine-water system. ($NaHCO_3$-NaOH-Gly-H_2O).....53
9.4. Potassium bicarbonate and potassium hydroxide systems.....61
9.4.1. The purity of the KOH chemical. 61
9.4.2. Titration. 61
9.4.3. KOH concentration. 62
9.4.4. Potassium hydroxide-glycine-water system (KOH-Gly-H_2O).....62
9.4.5. Potassium bicarbonate-glycine-water system ($KHCO_3$-Gly-H_2O). 73
9.4.6. Potassium bicarbonate-potassium hydroxide-glycine-water system ($KHCO_3$-KOH-Gly-H_2O).....78
9.5. Comparison between sodium and potassium systems. 92
9.6. Piperazine. 94
9.6.1. Solvent: 2.2 molal PZ. 95
9.6.2. Solvent: 3.6 molal PZ. 96
9.6.3. Solvent: 4.6 molal $KHCO_3$. 100
10. Discussion and conclusions. 103
The sodium glycinate system 104
The potassium glycinate system.....104
Comparison of the sodium and potassium glycinate systems 105
Comparison to literature.....105
The piperazine system 105
11. Reference list. 106

1. Introduction.

1.1. Global warming.

Actually, climate change is one of the global problems we have to be worried about. Climate change is due to both human activity and natural causes, although these may explain only a part of climate change.

The main problem of climate change is the increase of the called greenhouse gases (GHG), which can absorb or emit longwave radiation to the atmosphere. Approximately 40% of the energy that reaches the Earth's surface from the Sun is reradiated as longwave radiation, and 75% of this longwave energy is absorbed by vapor water, carbon dioxide, methane and other greenhouse gases (nitrous oxide, ozone, hydrofluorocarbons (HFCs), perfluorocarbons (PFCs)). Therefore, about 50% of the longwave radiation is reradiated back to the Earth and turned into heat energy. In this process, greenhouse gases contribute to raise the heat energy released in the Earth's surface and in the lower atmosphere [1].

The concentration of greenhouse gases is controlled by the carbon and nitrogen cycles. About the carbon cycle, this permit to keep the balance between atmospheres emitted carbon and the carbon trapped by plants, the ground and carbon sinks (oceans and forests). With the beginning of the industrial era this cycle has been interrupted by human activities like carbon extraction for combustion and gases emissions to the atmosphere. These changes lead to an increase of carbon dioxide concentration of more than 75% since the pre-industrial era [2, 3]. As shown in Figure 1, 6.5 Gt (billion of tons) of carbon are obtained by burning fossil fuels, and 1.6 Gt of carbon are obtained by deforestation and agriculture. Only 4.5 Gt of carbon are absorbed by CO_2 sinks (2 Gt are absorbed by vegetation and 2.5 Gt are absorbed by oceans) so 3.5 Gt of carbon end in the atmosphere every year.

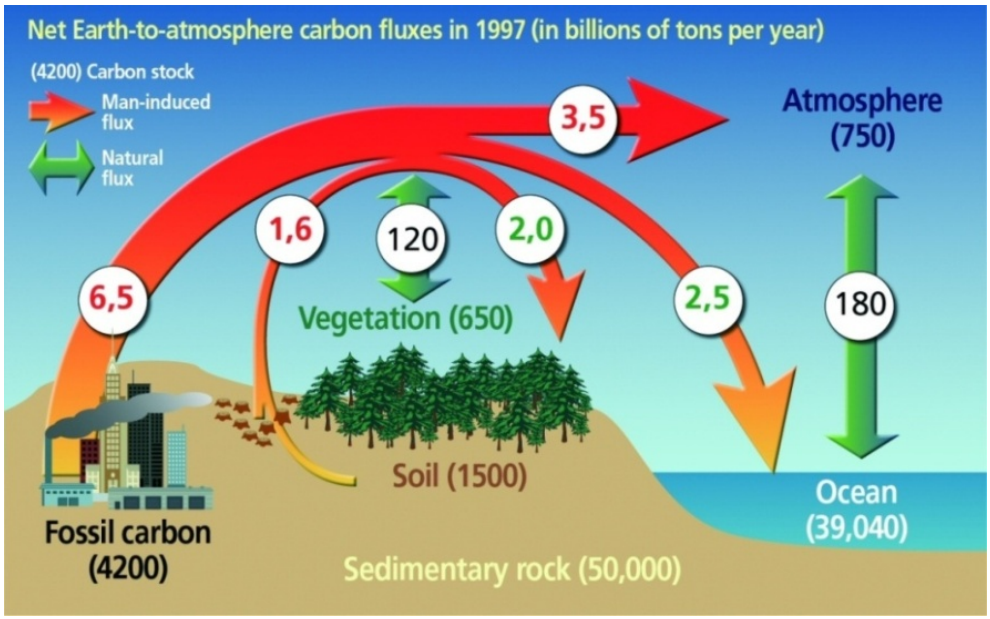

Figure 1. Carbon cycle. Source: [4].

Since the beginning of the Industrial Revolution, human beings have not taken care of gases emissions, causing an increase in gases concentrations, and now we are trying to decrease the consequences of these emissions in the Earth.

1.2. CO_2 emissions and concentration.

The most relevant greenhouse gas is carbon dioxide. Carbon dioxide is a colorless, odorless mixture of two oxygen atoms and one carbon atom linked by a covalent bond. Even though carbon dioxide is asphyxiating in high concentrations and it can be harmful for human health, it's benign in low concentrations and it's treated in some industrial activities.

About the concentration of greenhouse gases and especially carbon dioxide, if we compare the concentration of CO_2 (Figure 2) to the concentration of other gases like sulfur dioxide or oxides of nitrogen (conventional air pollutant, Figure 3), the second one stabilizes. Moreover, conventional air pollutant remains in the atmosphere for hours or days, but carbon dioxide remains for 100 years or more.

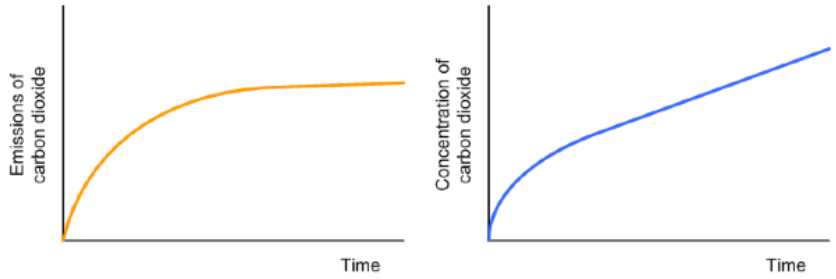

Figure 2. Emissions and concentration of carbon dioxide. Source: [5].

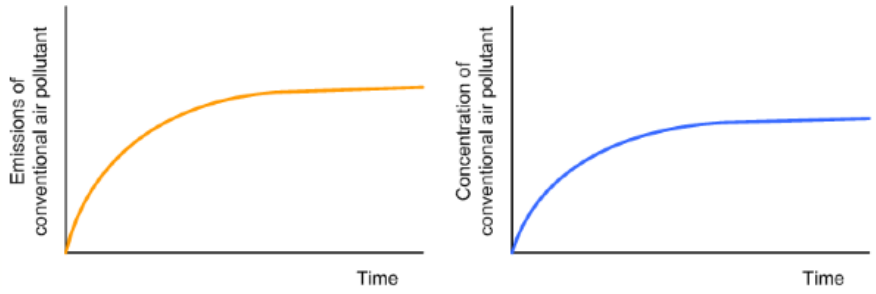

Figure 3. Emissions and concentration of conventional air pollutant. Source: [5].

So if we don´t reduce the greenhouse gases emissions the concentration of these gases will rise, increasing the global warming. If we reduce the atmospheric concentration we will achieve a decrease of 80% of greenhouse gases emissions. We don't know exactly how much reduction we have to achieve, but it´s certain a very deep reduction [5].

As explained before, the concentration of carbon dioxide from fossil fuel combustion has been rising since the Industrial Revolution. Table 1 shows the evolution of the concentration of carbon dioxide (CO_2) in the last years.

Table 1. CO_2 concentration. Source: National Oceanic and Atmospheric Administration (NOAA-ESRL) [6].

Year	CO_2 (ppm)	Notes
1959	315.97	The first year with a full year of instrument data
1987	349.16	The last year when the annual CO_2 level was less than 350 ppm

1992	356.38	Earth Summit in Rio de Janeiro
1997	363.71	Kyoto Protocol
2006	381.90	
2007	383.77	
2008	385.59	
2009	387.38	Copenhagen Accord
2010	389.78	
2011	391.57	

In Figure 4 it is shown the increase of the concentration of carbon dioxide year over year. This data were taken in the Mauna Loa Observatory in Hawaii [6].

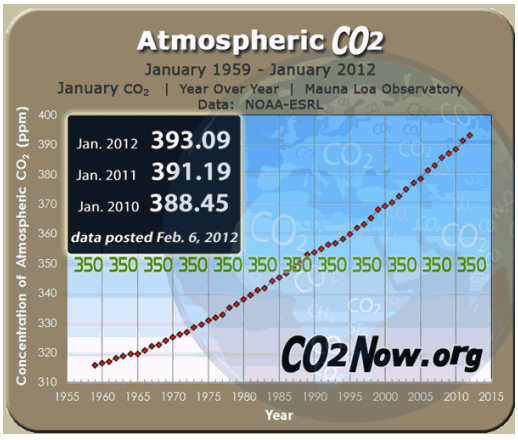

Figure 4. Atmospheric CO_2 concentration vs year. Source: [6].

In order to maintain the atmospheric CO_2 concentration below the 350 ppm (parts per million) barrier as soon as we can, the CO_2 emission must be reduced in a sudden way that this have to be close to zero. Table 2 shows the increase of CO_2 concentration depending on the decades.

Table 2. CO_2 concentration total increase and annual rate of increase. Source: [6].

Decade	Total increase (ppm)	Annual Rate of Increase (ppm per year)
1962-1971	8.88	0.89
1972-1981	13.95	1.40
1982-1991	15.10	1.51
1992-2001	16.00	1.60
2002-2011	20.72	2.07

For the period 2002-2011 the growth rate of atmospheric CO_2 was 2.07 ppm per year, the highest growth rate on record and over twice the annual rate for the period 1962-1971.

To conclude, as time passes both total increase and annual rate of increase are rising, so we have to stop this tendency.

It has been demonstrated that the economical development of developed countries is related with the increase of energy demand, so the need of energetic fuels such as fossil fuels will keep rising provided that new economical and environmental efficient technologies aren't investigated.

Just a small number of countries contribute to emit most of the greenhouse gases in the World. The 25 largest emitters, that cover 75% of the world's population and 90% of gross domestic product (GDP), count with approximately 85% of global greenhouse gases emissions [7].

To fight against climate change, policies are needed to be established to reduce greenhouse gases, and also to improve sinks. Comparing with current rates, by 2100 stabilization of CO_2 in the atmosphere at a level of 550 ppm would need a reduction of 7-70 % in global emissions compared to current rates, as reported by IPCC [8], to avoid harmful damages of climate change.

The most important activity that generates greenhouse gases emissions is energy generation; that is because the great majority of the energy is produced by fossil fuels like coal or natural gas. As for coal, the type of coal that more emissions of greenhouse gases per unit of energy produce is lignite (brown coal). Burning coal generates 70% more CO_2 emissions than natural gas, but on the other hand coal is less expensive and it's the most available fossil fuel. "Globally, energy related CO_2 emissions have risen 145-fold since 1850—from 200 million tons to 29 billion tons a year—and are projected to rise another 54 percent by 2030", as explained by the United Nations Environment Programme (UNEP) [7].

Fossil fuel emissions have risen by more than 1200% in the last 100 years. In 2005 carbon emissions from fossil fuel combustion and cement production were 28% higher than in 1990 (Kyoto Protocol base year). About carbon dioxide emissions, between 60 and 70% of them are caused by fossil fuels [2].

While burning fossil fuels, besides energy generation, gases as carbon dioxide are released. One possibility to reduce carbon dioxide emissions is to capture it and then storage it underground, so that no more carbon dioxide is released into the atmosphere.

If we continue to spend fossil fuels at the same speed as we actually do, we will not be able to fight against global warming crisis, besides if we continue to use our lands in such a way the emissions rise instead of absorb atmospheric carbon dioxide, it will know that we are not doing enough efforts to fight against climate change.

1.3. Protocols.

In 1997 an agreement was reached in Kyoto (Kyoto Protocol) in which sets limits on emissions of greenhouse gases. The target was to decrease the greenhouse gases emissions (carbon dioxide, methane (CH_4), nitrous oxide (N_2O), sulfur hexafluoride (SF_6), hydrofluorocarbons (HFCs), perfluorocarbons (PFCs)) for 2012 about 5.2% of 1990 levels.

Furthermore, in 1998 'The Greenhouse Gas Protocol' was launched. This protocol consists of multiple stakeholders such as nongovernmental organizations (NGOs) and governments and other parts organized by the World Resources Institute (WRI) and World Business Council for Sustainable Development (WBCSD). The aim of this group is to develop standards and accounting tools and coverage to manage lower emissions of greenhouse gases and to make sure that these tasks are accomplished [9].

In order to reduce greenhouse gases emissions, it has been put into practice the following alternatives [10]:

- improve the energy efficiency and reduce the demand.

- use renewable energies (solar, wind, thermal, geothermal, etc.).

- use nuclear energy.

- CO_2 capture and storage (CCS).

It has been determined that fossil fuels will still be needed and that renewable energies will not be enough to replace fossil fuels in a short-medium term. Moreover, since with the first two measures is not possible to reduce the large amounts of carbon dioxide emissions, the alternative to take is to capture and store the carbon dioxide.

There are many reasons why coal and power industries and society would benefit from the use of CO_2 capture equipments in industrial plants. First of all, "the fastest way to reduce CCS costs is via 'learning by doing'", as Hawkins et al. explained in the report "What to do about coal" [11]. The faster the understanding of the system is, the quicker this technology will grow and its price will decrease. In addition, the installation of CO_2 capture equipment as soon as possible will produce a long-term savings. Finally, the rapid implementation will allow the continued use of fossil resources without emitting carbon dioxide into the atmosphere beyond the tolerable limits. It's also known that CCS method requires more fossil fuels to run a fossil-based power plant which is equipped with CCS than a conventional non-CCS plant, if they produce the same net output of electricity [12].

2. CO_2 capture and storage (CCS) techniques.

CO_2 capture and storage gives information about the set of technologies to capture the carbon dioxide emitted by industrial and energy sources before entering the atmosphere, compressing and storing it in secure geological formations and guarantee that the carbon dioxide remains stored there indefinitely. Actually, this technology is not large-scale integrated, basically because of the high costs of this technology. So we have to optimize economically actual processes in order to promote these technologies. Besides, it has to be taking into account that a new technology cannot be supported as a long-period solution without social approval.

CO_2 capture and storage (CCS) seems to be an essential technology for reducing carbon dioxide emissions since it presents a great display and since there is a very high capacity and number of storages all over the world; the process counts with three parts, explained below.

2.1. Capture.

This system is intended to separate CO_2 from the other combustion gases, thereby generating a concentrated stream of CO_2 from a stationary emission source.

2.2. Transport.

Captured CO_2 is taken to the location where it has to be storage. The two most commonly used routes are pipeline transport and road or water transport. Pipelines are the most suitable way of transport. CO_2 pipelines are operated at high pressure (80-150 bar) to guarantee high densities. The pressure must be above the supercritical pressure (74 bar) in order not to have the liquid-gas transition. The advantage of having CO_2 in the supercritical state is that it has both liquid and gas characteristics: it maintains the compressibility of a gas and also has some liquid properties (density). In water transport, CO_2 must be in liquid phase (14 to 17 bar, -25 to -30°C). One of the advantages of this transport is its flexibility; on the other hand, it's more expensive due to liquefaction [13]. If the CO_2 is dry (less than 10 ppm of water), pipelines are made of conventional carbon steel, reducing costs and avoiding hydrate crystallization. Depending on the plant type and the capture system the pipes feed stream may contain impurities such as N_2, O_2, H_2S and/or SO_3. With this mixture, the operational pressure is approximately of 90 bar in CO_2 with impurities, instead of being of 73 bar in pure CO_2 [14].

2.3. Storage.

CO_2 is set in an appropriate deposit; another option is using it for carbonate drinks. Nonetheless, the carbon dioxide market is limited, so it is required to storage it [10].

The three main storage ways considered are:

- Depleted oil fields, by injecting water, natural gas, CO_2 and/or solvents to enhanced oil recovery (EOR).

- Deep saline aquifers, where waste water is the most common fluid used to be injected into aquifers, but CO_2 or natural gas can also be injected. They are a good storage source due to their big size; they are also present in a lot of countries. Nowadays some projects are available, as CO_2 injection at Sleipner in the North Sea, or In Salah in Algeria [15].

- Carbon reservoirs, although sometimes they cannot be easily exploited. In several situations, methane is found in these reservoirs. Nevertheless, it has been observed that when carbon dioxide is injected, carbon layers may act as methane sources, so carbon dioxide may be stored.

There are some investigations about man-made underground cavities, but these kinds of storage have two problems: small capacity and geographical limitations. Instead of these problems, they can be used as temporary storage [15].

Potential problems of the carbon dioxide capture and storage are [3]:

- Cleaning: not only CO_2 but also all emissions are included.

- Safety: it is very important to avoid any possible leakage from reservoirs because it can be harmful for human health. In case of pipeline leakage, asphyxiation risk has to be minimized [16].

- Economical: this process will have more costs. Carbon dioxide separation consumes a lot of energy, so it's the step that more costs needs. Haszeldine reported that "historical examples of CO_2 separation, if scaled-up, could consume 25 to 40% of the fuel energy of a power plant and be responsible for 70% or more of the additional costs in CCS" [14]. For this reason, it will be necessary to have a well-defined policy so that this process could be more competitive with the rest of processes.

- Carbon dioxide capture and storage process is less efficient than fossil fuels consumption, and it will end in a major consumption of fossil fuels.

- It is also needed to discuss if the risks about CO_2 storage are comparable to other alternatives for mitigating carbon dioxide emissions. The most important risks are in the transportation and storage of carbon dioxide.

- Finally, but not lees important than the previous points, social acceptance is also important.

The priorities for the development of future technologies, in terms of environmental impact and investment, will focus on minimizing the energy required to capture carbon dioxide, as well as improvements in process efficiency.

In both industrial large-scale and small-scale, carbon dioxide is separated in some plants as natural gas and ammonia processing. However, there is still no application in large-scale (plants of about hundreds of megawatt), which are the major carbon dioxide emitters. If design and construction of these plants don't start now, they will not be operated by 2014, so they will lose social and commercial credibility by 2020 [14].

Before carbon dioxide capture, it has to be taken into account the entire process since fuel combustion starts. In order to produce electricity from steam, the fuel (coal or biomass) is mixed with air and ammonia to carry out combustion. Besides electricity, it's also obtained a flue gases stream (N_2, O_2 in lower quantities, NO_x, SO_x, H_2O y CO_2 and other gases in less proportion). This stream is passed through an electrostatic separator (ESP) which separates the particles and the gas stream; then the gas stream is carried into a DeSOx process. The resulting gas stream (N_2, O_2, CO_2, H_2O), has roughly 10% of CO_2 in composition, and lead to a CO_2 capture process where a CO_2 stream is obtained, and also a 'clean' flue gases stream (no carbon dioxide), which has approximately 1% of CO_2, so that a 90% of CO_2 separation is achieved.

2.4. CCS costs.

It is important to know that carbon dioxide capture and storage costs are very high, so it is needed to reduce these costs in the near future. First of all, costs depend on the source, location and technology [10], and sometimes there is no need of incentives, or there may be few of them. Moreover, carbon capture and storage is important in terms of CO_2 prices. In general, the biggest cost in the whole carbon dioxide capture and storage process is due to the capture process.

There are several factors that affect CO_2 capture cost: the technology of interest, the system boundary, the technology time frame and maturity and different cost measures, as explained in the IPCC report [17]. About transport, Figure 5 shows costs of onshore and offshore pipelines as a function of the CO_2 mass flow rate. Dotted lines represent high estimates, and solid lines represent low estimates. At low flow rates, the costs are very high, but at high CO_2 flow rates, these costs decrease. So costs depend on the carbon dioxide flow rate.

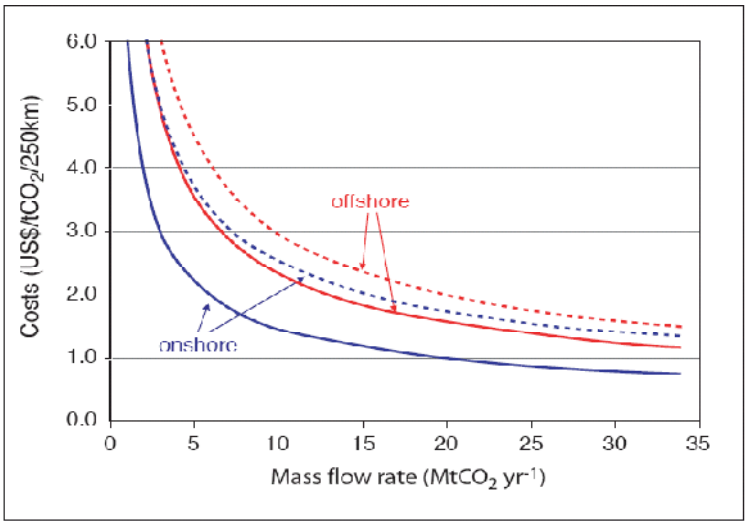

Figure 5. Capture costs onshore and offshore for a nominal distance of 250 km. Source: [3].

3. Combustion techniques for CO_2 capture.

For centuries, combustion has been the main technology to extract and use the energy that is taken from fuel. As current anthropogenic carbon dioxide emissions come from sources as power plants, furnaces in industries and iron and steel production plants, it is needed to mitigate greenhouse gases emissions in order to reduce the amount of gases emitted to the atmosphere. Therefore it is required to change combustion systems in order to capture carbon dioxide.

Critical challenges in carbon dioxide capture are [13]:

- Reducing parasitic energy load.
- Application to existing fleet.
- Scale-up.
- Improving solvents.
- Improving process design.
- Costs.

There are many techniques for carbon dioxide capture, but only three are the most important: pre-combustion, oxy-fuel combustion and post-combustion.

Figure 6 shows the differences between all combustion capture types, and all the processes that are needed for treating air and fuel (coal, gas or biomass), which are explained below.

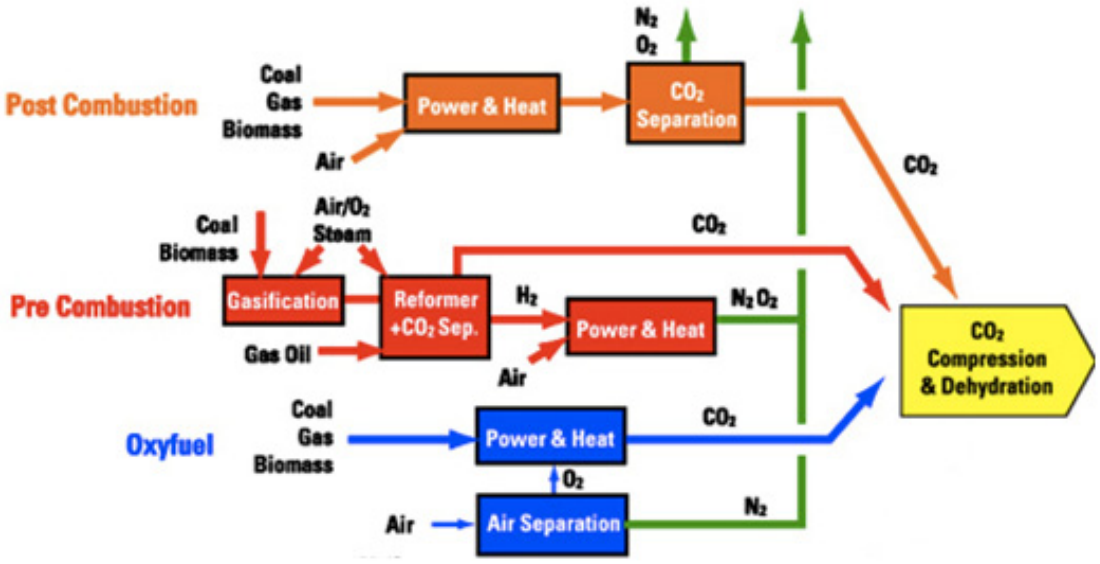

Figure 6. CO_2 capture processes scheme. Source: [18].

3.1. Pre-combustion.

This technology is based on the carbon separation of the fuel before combustion is started. With this process a low content carbon fuel is achieved, and it also has a high H/C ratio [19].

Pre-combustion processes have three different parts: reforming and/or gasification, water-gas shift and CO_2 capture, as it can be seen in Figure 7.

If the fuel is natural gas, a reforming process is necessary, where the flue gas is composed by carbon dioxide and water. In case the analyzed fuel is solid, coal or biomass, this turns into a gas by coal partial oxidation of the fuel in presence of oxygen. The resulting gas, called "syngas", consists essentially of hydrogen, carbon monoxide and light hydrocarbons (methane).

The syngas is contacted with a steam stream and reacts with it to form carbon dioxide and more hydrogen (water-gas shift). In this step is possible to increase the concentration of carbon dioxide, so carbon capture is improved, and the amount of carbon that can be removed is also increasing [13].

After that, carbon dioxide is removed, using either a physical or a chemical solvent, and the hydrogen stream is diluted with nitrogen and used as fuel in a heater or in a combined cycle gas turbine in order to generate electricity [17].

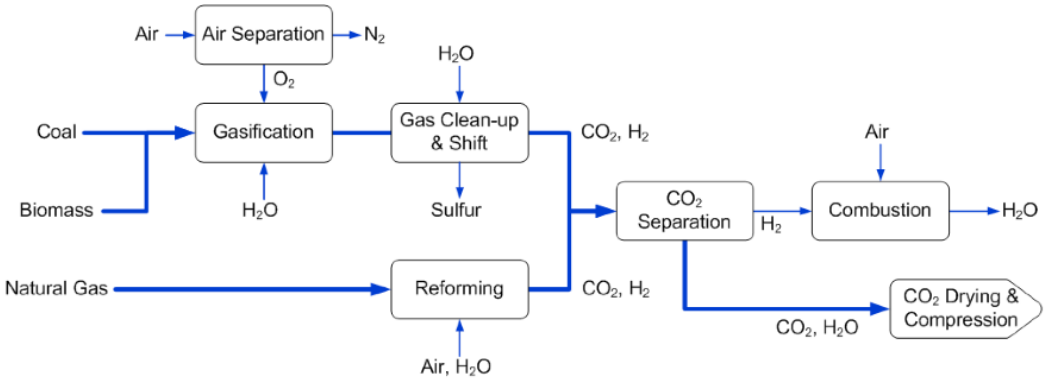

Figure 7. Scheme of the pre-combustion capture. Source: [5].

This technology's main advantage is that is cheaper than post-combustion capture, and it can be used for a lot of different fuels, apart from obtaining several products. In this process it is possible to reduce the amount of impurities like SO_x, NO_x and ashes. Apart from that, pre-combustion leads to a reduction of capture costs compared to post-combustion due to the high pressure and carbon dioxide concentration in flue gases stream [20].

The main disadvantage is the high construction cost. Future studies may come from the development of membranes that allow syngas to be catalytically reformed in order to obtain carbon dioxide at the same time as hydrogen is separated [14]. Normally pre-combustion capture is related with Integrated Gasification Combined Cycle (IGCC) technology [13].

3.2. Oxy-fuel combustion.

In this process, combustion is performed with pure oxygen instead of air. Therefore, the output flue gas stream is formed by water and carbon dioxide. Three components are required for the oxy-fuel combustion for CO_2: the air separation unit (ASU), the furnace and heat exchangers and the CO_2 capture and compression unit [21]. It is also needed another component which is used to clean the flue gas stream (flue gas clean-up). Figure 8 shows the scheme of the oxy-combustion.

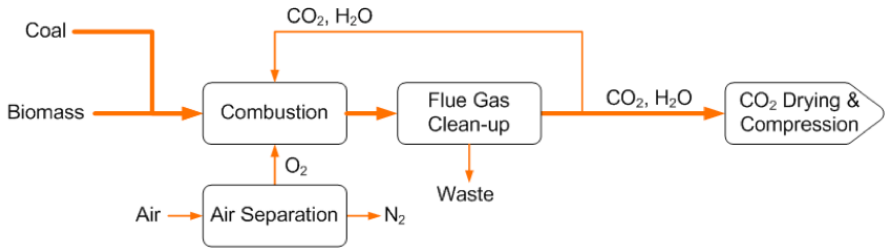

Figure 8. Oxy-combustion capture scheme. Source: [5].

After the combustion is performed, combustion products (water vapor and carbon dioxide) are obtained, so it is not required the CO_2 separation. Instead of it, it is necessary to include an air separation unit to obtain the pure oxygen stream [22]. As there is no nitrogen in the output stream, the concentration of CO_2 in the flue gas is high. In order to control the temperature of combustion it's necessary to re-circulate part of the flue gases stream to the boiler.

Although this process is still under development, some of the advantages of this technology are its dual firing capability, there are no solvents (which makes CO_2 separation easier), its smaller physical size, and it's easier to readapt this process on existing plants (if the boilers are also reconstructed), there is a reduction in the flue gases flow, so it leads to a reduction on separation, compression and storage costs. In this process is obtained a CO_2 rich stream (90-95% CO_2) and also a poor stream in NO_x.

The obstacles of this technology are its high costs in oxygen separation and carbon dioxide separation, very low SO_x is required on burners, and high-temperature resistant materials are requested. Future developments should improve operating temperature and should reduce energy cost in oxygen separation from air [14, 20, 21].

As reported by Haszeldine [14], recent studies in oxy-fuel combustion show the possibility of using burners at 1-MW scale; furthermore 40-MW burners (the world's largest experiments) have been developed to be commercially available from 2015. Nowadays there are two operating pilot plants: Schwarze Pumpe in Germany (since 2008) and Lacq in southwest France (since 2009) [3, 14, 21].

3.3. Post-combustion.

In this process combustion of a fossil fuel is performed, both in a boiler and in a combined cycle, and then takes place the separation of CO_2 from the flue gases stream.

As shown in Figure 9 CO_2 stream is separated from flue gases stream during the fuel (coal, natural gas or biomass) combustion with air. Then the flue gas passes through the flue gas clean-up equipment in which particulate matters are separated from the CO_2 stream. The carbon dioxide flue gas enters in another equipment, where drying and compression are implemented.

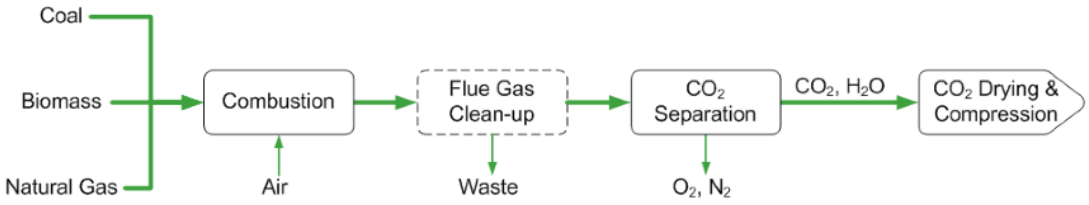

Figure 9. Post-combustion capture scheme. Source: [5].

This process can be carried out in the plant even without modifying the installation, since the CO_2 is captured using a solvent or a membrane [23, 24]. The captured carbon dioxide is stored and the solvent is recycled. For plants that use coal, post-combustion capture is related with subcritical pulverized coal (SCPC), ultra-supercritical pulverized coal (USCPC) and circulating fluidized bed (CFB). This technology also can be associated with Integrated Gasification Combined Cycle (IGCC), although it is more economically effective in pre-combustion [13].

4. Post-combustion techniques.

There are different post-combustion techniques for separating carbon dioxide from the flue gas stream, but the most important are the chemical absorption using a sorbent as amines or ammonia, and the cycle of carbonation/calcination. The other options are less used because of its low development or high cost involved [20].

4.1. Absorption ("scrubbing").

The combustion gases stream, which contains N_2, O_2, CO_2, H_2O, is introduced into an absorption column (called scrubber), where the flue gases stream is put in contact with a liquid absorbent, or solvent, that is CO_2 selective, and turbulent streams make the CO_2 be transferred from the gas stream to the liquid.

Two different streams leave the column: a clean gas stream by the top of the column, and the solvent stream, rich in CO_2, by the bottom of the scrubber. This stream, after passing through a heat exchanger, is introduced into another column in which is contacted with steam to reach the requested temperature to regenerate the solvent. Due to this solvent heating, CO_2 is desorbed.

The liquid is pumped back to the scrubber, while the mixture of steam and CO_2 is cooled to condense the vapor stream and the clean CO_2 stream is removed by the top of this column. The other boiler out stream goes through the heat exchanger and leads to the absorption column [17].

The main problem of this process is the energy needed to produce the vapor that is used during the solvent recuperation. Figure 10 shows the scheme of an amine (solvent) separation process, as explained above. Possible solvents are explained in section 6.

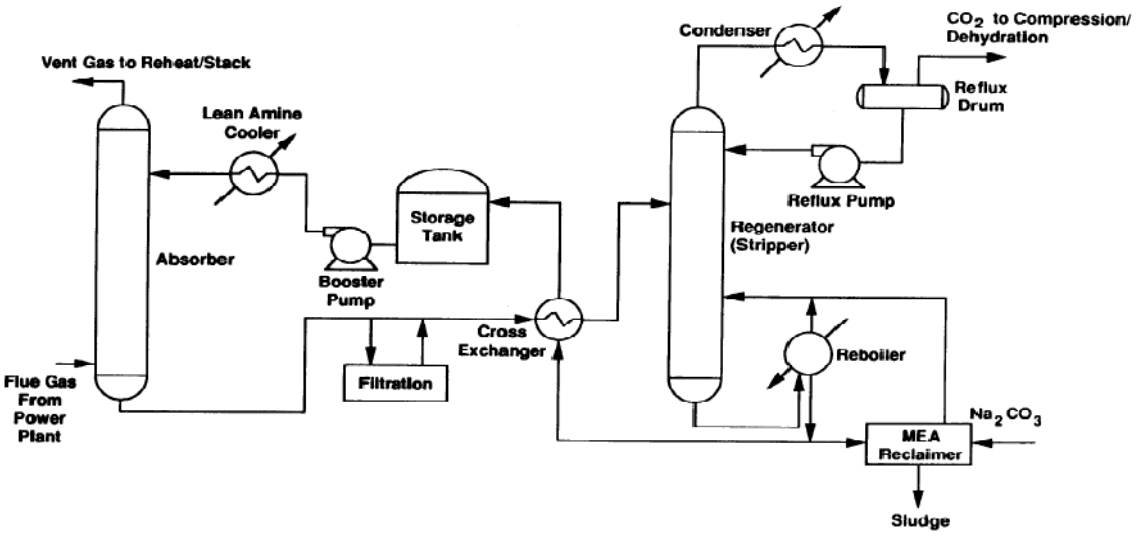

Figure 10. Diagram of the amine separation process. Source: [25].

4.2. Carbonation/calcination.

The mixture of these processes is based on chemical absorption using calcium oxide (CaO) as sorbent, which captures carbon dioxide and reacts with it, resulting in an exothermic reaction and forming limestone ($CaCO_3$).This is known as carbonation. Equation (4.1) shows the reversible reaction for carbonation/calcination.

$$CaO + CO_2 \leftrightarrow CaCO_3 \tag{4.1}$$

This is followed by calcination, which is the reverse process; here the limestone decomposes generating CaO and a concentrated stream of CO_2 is obtained [19, 20, 26, 27].

4.3. Adsorption.

Adsorption consists in using materials that can adsorb carbon dioxide, generally at high temperatures. After that, carbon dioxide is been recovered by temperature changes (TSA) or pressure changes (PSA).

In this process, it can be used either physical or chemical sorbents. Carbon dioxide may be recovered by flue gases streams with a large amount of non reactive sorbents (physical sorbents), including carbonaceous materials and crystalline materials (zeolites). Since CO_2/N_2 selectivity is low, this process is only used when at most 90% CO_2 purity is required.

About chemical sorbents, when limestone is heated to 850°C, carbon dioxide is released and limestone is turned into calcium oxide (CaO), and at 650°C CaO reacts with the carbon dioxide. $CaCO_3$/CaO system is interesting because the amount of CO_2 captured is high, plus it's versatile set when power plants are configured [20, 24].

There are studies about alkali metal-based sorbents, but it is necessary to determinate the exact stability and performance under actual flue gas conditions.

4.4. Membranes.

A component passes through the polymeric membrane by diffusion or sorption by the fluid on the other side of the membrane. This is how the permeation of CO_2 occurs. The driving force can be reached either by pressure or by concentration difference through the membrane [13].

We can discriminate between membrane-based separation and membrane absorption.

The selectivity of the membrane-based separation, which generally consists of thin polymer films, is due to the relative rates at which chemical species permeate, as presented by Herzog et al [24]. The different permeability ranges depend in the relative sizes of permeating molecules or their solubility and/or diffusion coefficients. Since permeability rates vary inversely with membrane thickness, these are made as thin as possible without affecting the mechanical strength. Generally, membrane permeation is pressure-driven.

Regarding membrane absorption, carbon dioxide and nitrogen can transfer easily through membrane pores. The liquid, frequently an amine solution, is the substance that provides selectivity. This system has the advantage that “there are no inherent restrictions to gas and liquid flow rates”, as explained by Herzog et al. [24].

Figure 11 represents the membrane absorption, in which the flue gas is passed through a bundle of membrane tubes; the absorption liquid passes through the shell side of the bundle. Carbon dioxide (red points) passes through the membrane and is absorbed in the absorption liquid, and impurities are blocked from the liquid [28].

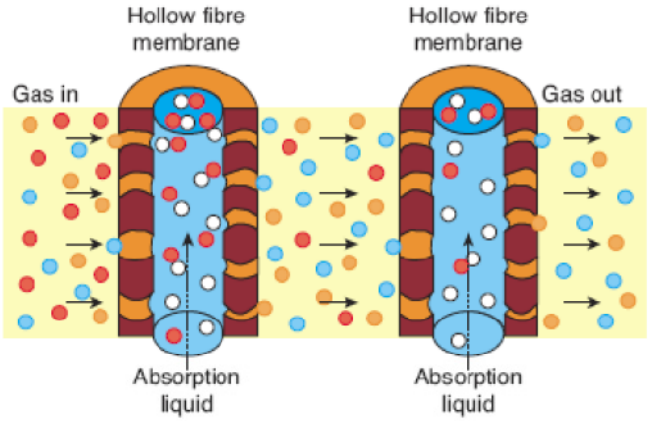

Figure 11. Membrane absorption system. Source: [20].

4.5. Other techniques.

Other techniques have been studied for carbon dioxide capture.

a) Cryogenics distillation system is formed by different compression, cooling and expansion stages, in which flue gases components may be separated in a distillation column [20].

b) Microalgae systems are also under development because of their CO_2 consumption, and also because they avoid the need of compression and carbon dioxide sequestration as they capture the carbon dioxide from air [24].

c) Enzyme-based systems, which is a biologically CO_2 capture system, and is based in natural reactions of the carbon dioxide with organisms [28].

d) Improvements in materials and new concepts, such as solid adsorbents (metal-organic frameworks, functionalized fibrous matrices, ionic liquids), structured fluid absorbents (CO_2 hydrates, liquid crystals, ionic liquids) and non-thermal regeneration methods [24, 28].

4.6. Energy penalty impacts.

The different types of capturing carbon dioxide discussed above need large amounts of energy for operating; thus affecting the efficiency and reduction of the net power when compared to plants without capture system. "Because of the energy consumption for CO_2 separation and compression, the emissions of CO_2 avoided by capturing CO_2 are always less than the amount of CO_2 captured" (equation (4.2)), as explained in the CCS Report [5] and as shown in Figure 12.

$$CO_{2\ avoided} = CO_{2\ emitted\ without\ capture} - CO_{2\ emitted\ with\ capture} \quad (4.2)$$

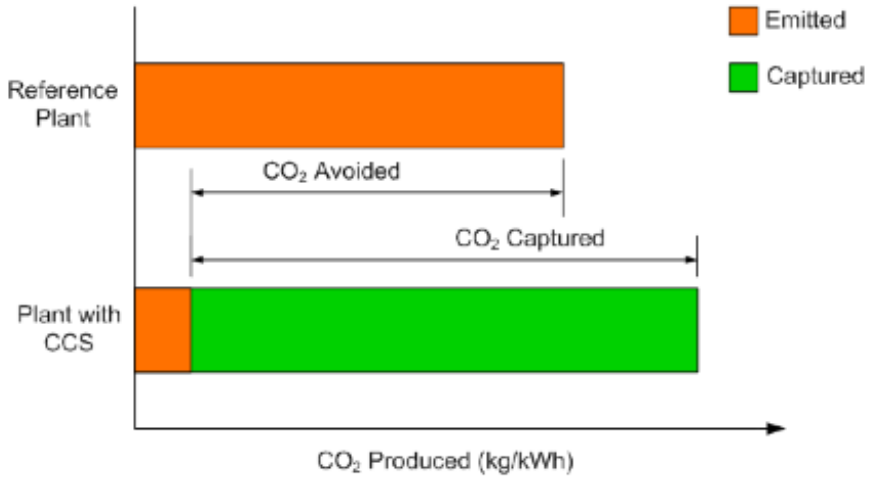

Figure 12. CO_2 produced in plants with and without CCS system. Source: [5].

Moreover, reducing the efficiency of electrical energy involves that production plants with incorporated capture systems consume more fuel and water for the production of waste products (such as ash, slag and sulfur) per unit of electricity compared to a plant without capture system. The energy penalty is defined in the CCS project as "the increase in energy input of the plant per unit of product or output" [5], and quantifies the increase in resource consumption.

5. Solvent based CO_2 capture.

As explained above, many techniques for CO_2 removal have been under investigation. Solvent selection is very important for CO_2 capture because it influences the energy demand and the environmental problem, so it is necessary to enumerate some of the desirable properties required [29].

1) High CO_2 capture capacity of the solvent.

2) Low energy requirement for CCS in order to decrease the energy penalty impacts.

3) The solvent has to have a low cost and it may be available in nature or it should have simple synthesis methods.

4) Even after many cycles the solvent should not lose its solubility.

5) Non-toxic and non-polluting.

6) High CO_2 selectivity.

7) The solvent has to have high capacity and it should have a minimum energy input when releasing the captured CO_2.

Absorbents or solvents that are required to remove carbon dioxide needed to have a "high net cyclic capacity and high reaction/absorption rate for CO_2, as well as high chemical stability, low vapor pressure and low corrosiveness", as indicated by Ma'mun et al.[30].

Water could be used because carbon dioxide is more soluble than nitrogen in it. However, the ability of water to retain carbon dioxide is so low that would require very large volumes of water to have an effective absorption.

There are several solvents under development in post-combustion capture, as shown in Figure 13.

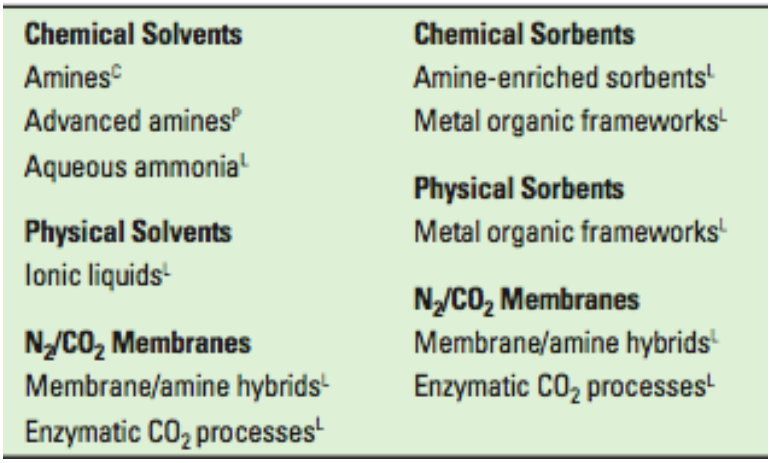

Figure 13. Research pathways in post-combustion for CO_2 capture. Source: [13].

5.1. Amines.

One of the most widely used technologies is the absorption of CO_2 by aqueous amines, such as monoethanolamine (MEA), diethanolamine (DEA), N-methyldiethanolamine (MDEA), etc.; besides, other solvents have been suited for CO_2 removal. The most commonly used solvent is monoethanolamine (MEA) because it can eliminate acid gases such as carbon dioxide or hydrogen sulfide from natural gas streams, although blended-amine systems can be used too, for example N-methyldiethanolamine (MDEA) + diethanolamine (MEA) aqueous systems [31]. In addition, amines can be used with some additives to modify the capture system.

Amines react quickly to form water soluble compounds; they are selective to CO_2 and relatively non-volatile and low-priced. MEA has low molecular weight, high absorbing capacity on a mass basis and reasonable thermal stability and thermal degradation rate. Conversely, MEA also has disadvantages such as the formation of a stable carbamate and the formation of degradation products with COS or oxygen bearing gases, high enthalpy of reaction with CO_2, leading to higher desorber energy consumption, vaporization losses because of high vapor pressure. Likewise amines are corrosive, so it is required more expensive construction materials. In the process, inhibitors were added to reduce degradation of the solvent and corrosion of equipments; besides the solvent strength is low (20-30% by weight of amines dissolved in water), so that the cost of regeneration of the solvent is high and the equipment size is large compared to the size of a coal plant to obtain energy. Furthermore amines can gradually volatilize, which can be a problem, and degrade especially in the presence of oxygen and/or sulfur dioxide, so that fresh feeds are required. In addition, it requires large volumes of solvent and the heating necessary to regenerate the solvent can produce toxic byproducts.

Fosbøl et al. [32] measured the freezing point for aqueous monoethanolamine (MEA), methyl diethanolamine (MDEA), and MEA-MDEA solutions in a concentration range between 0 and 0.4 mass fractions of the alkanolamines.

These amine-based systems have been under investigation in order to improve them by modifying tower packing for reducing pressure drop, reducing energy requirements and solving the corrosive

problem. These are some of the reasons why another solvent is needed to be found, so that these solvents do not require so much energy and become more cost effective.

The mechanism of carbon dioxide absorption (zwitterion[1] mechanism) was reported by Lee et al. [33], so three different reaction steps are taking into account: carbamate formation, bicarbonate formation, and carbonic acid formation. Finally, carbon dioxide has been absorbed by amines. The zwitterion mechanism is explained below.

5.2. Ammonia.

The carbon dioxide absorption using ammonia is under development. The absorption of carbon dioxide in aqueous ammonia solutions is represented by vapor-liquid reactions, in which ammonium bicarbonate (NH_4HCO_3), ammonium carbonate ($(NH_4)_2CO_3$), and ammonium carbamate (NH_2COONH_4) are formed, as reported in equation (5.1) to (5.5) and as explained by Versteeg and Rubin [34].

$$NH_3(aq) + H_2O(l) + CO_2(g) \leftrightarrow NH_4HCO_3(aq) \quad (5.1)$$

$$2\,NH_3(aq) + H_2O(l) + CO_2(g) \leftrightarrow (NH_4)_2CO_3(aq) \quad (5.2)$$

$$(NH_4)_2CO_3(aq) + H_2O(l) + CO_2(g) \leftrightarrow 2NH_4HCO_3(aq) \quad (5.3)$$

$$2\,NH_3\,(g) + \,CO_2(g) \leftrightarrow NH_2COONH_4(aq) \quad (5.4)$$

Salt precipitation reaction. $$NH_4HCO_3(aq) \leftrightarrow NH_4HCO_3(s) \quad (5.5)$$

As reported by Figueroa et al. [28], ammonia-based wet scrubbing is an important process for carbon dioxide capture, but the most important process in ammonia systems is the Chilled Ammonia Process (CAP), which consists in the absorption of CO_2 at low temperature (273-283 K), so ammonia cannot vaporize and the reaction between aqueous ammonium carbonate and ammonium bicarbonate is favored. Under this condition, ammonium carbonate compounds precipitate, as reported by Darde et al. [35]. In this process a low heat is required in the CO_2 desorber, so it is a good advantage for this system. Darde et al. [35] also reported the rate of absorption of carbon dioxide by aqueous ammonia solvent.

Some of the advantages of ammonia-based systems are its reduced CO_2 compressor power, its reduced solvent costs, high carbon dioxide carrying capacity of ammoniated solutions when solids can precipitate, there is no degradation during absorption/regeneration, and low reboiler regeneration energy. However, ammonia-based systems also had some disadvantages, as unwanted side reactions and problems high ammonia levels in the absorber. These problems lead to higher equipment costs and auxiliary loads, so this process is under review [28, 34].

5.3. Ionic Liquids.

Ionic liquids (ILs) are organic salts which contain an organic cation and either an inorganic or organic anion, and their melting point is usually below 100 °C.

[1] Zwitterions are neutral molecules which have a positive and a negative electrical charge at different locations.

They are seen as a good solvent alternative, because of their properties, as reported by Ma et al. [36]. Some of the ionic liquids properties are low vapor pressures, extremely wide liquid ranges, easy assembly, non-flammability, thermal stability, tunable polarity, good electrolytic properties, the facility of dissolving carbon dioxide and stability at temperatures up to several hundred °C and easy recycling [24, 28]. However, about carbon dioxide desorption and the regeneration of ionic liquids this processes need a lot of thermal energy, so this is a problem in terms of costs. Furthermore, ionic liquids are characterized by a high viscosity, so more energy is required, leading to an energy penalty.

5.4. Amino acids.

Other possible solvents are amino acids, which are the main absorbents studied in this report. Amino acids properties and researches are explained in the next section.

6. The amino acid solvent.

Amino acids have been used as promoters in carbonate solutions and amino acid salts were employed for the selective removal of acidic gases such as CO_2 and H_2S. There are several studies reporting data of amino acid salts of a strong inorganic base (for example, potassium or sodium hydroxide); conversely, Aronu et al. [37] investigated the amino acid salts formed of the neutralization of the amino acid with organic bases like amines; these substances are called amine amino acid salts (AAAS).

Some advantages of amino acids are [37, 38, 39, 40, 41]:

- They do not deteriorate in the presence of oxygen, which means that amino acids are more stable to oxidative degradation, especially when removing acid gases from oxygen-rich gas streams, even though they have the same functional groups.

- There is a thermal stability that gives more flexibility to the process.

- The substance is non-volatile, as a salt solution, which helps when working at low pressure and high temperature.

- They have high surface tension.

- Their viscosity is similar to water.

- They can be used in conjunction with simple polyolefin membranes.

- Their volatility is negligible due to the ionic nature if the solutions.

- They have the ability to form solid precipitates during the CO_2 absorption.

- They are not inflammable.

- Amino acids do not cause toxic or environmental problems.

- Amino acids are more expensive than alkanolamines.

Baek and Yoon [42] presented the solubility of carbon dioxide in aqueous solutions of 2-amino-2-methyl-1, 3-propanediol (AMPD), measured over a temperature range of 30-60 °C, partial pressure of carbon dioxide between 0.5 and 3065 kPa and concentrations of the aqueous solutions between 10 and 30 mass% AMPD.

Amino acid salts can also be used in CO_2 removal with or without an activator such as piperazine (PZ), as concluded by Lu et al. [43]; as reported by Vaidya et al. [44], N,N-diethylethanolamine (DEEA) is also used for this function.

Some properties as density, solubility, pH, kinetics parameters and reaction rate constant have been analyzed in literature under different conditions for the following amino acids (Table 3).

Table 3. Amino acids studied in CO_2 capture.

Amino acids	reference	Amino acids	reference
sarcosine	[38],[41],[45]		
Taurine	[45]	**β-alanine**	[38],[41]
6-Aminohexaionic acid	[38]	**ι -proline**	[38],[41]
ι-arginine	[38]	**$_{DL}$-alanine**	[46]
ι -Aspartic acid	[38]	**□-leucine**	[46]
ι -Glutamic acid	[38]	**ι -isoleucine**	[46]
ι ι -Methionine	[38]	**ι -serine**	[46]
ι -Phenylalanine	[38]	**$_{DL}$-phenylalanine**	[46]

7. Glycinates for CO_2 capture.

7.1. Introduction.

Recently, the use of glycinates, as potassium or sodium glycinate, in carbon dioxide capture is under investigation. So glycine is used as a promoter (or activator) in order to improve the absorption rate.

Glycine is the simplest and smallest of the amino acids, and it's the only amino acid that does not have optical isomers. As explained in "Capturing CO_2 with Sodium Glycinate" [47], when glycine is in water solution, it exists as a zwitterion ($^{-}$COO-CH_2-NH_3^+), which is completely non-reactive towards carbon dioxide because of its protonated amino group. On the other hand, when the acid group titration with sodium or potassium hydroxide takes place, a primary amine is formed (equations (7.1) and (7.2)).

$$NaOH + {}^{-}COO - CH_2 - NH_3^+ \rightarrow NaOOC - CH_2 - NH_2 + H_2O \quad (7.1)$$

$$KOH + {}^{-}COO - CH_2 - NH_3^+ \rightarrow KOOC - CH_2 - NH_2 + H_2O \quad (7.2)$$

The zwitterion mechanism proposed by Caplow (1968) is the one used for the CO_2 absorption in amino acid aqueous salts. Alkaline salt of amino acid are expected to react through a zwitterion mechanism, such as amines, due to the similar functional groups [48]. The first step involves the reaction between carbon dioxide and the amino acid salt (for example potassium glycinate), in order to obtain a zwitterion (${}^{-}OOC^{+}H_2N - CH_2 - COO^{-}K^{+}$), as shown in equation (7.3).

$$CO_2 + H_2N - CH_2 - COO^{-}K^{+} \rightarrow {}^{-}OOC^{+}H_2N - CH_2 - COO^{-}K^{+} \quad (7.3)$$

Then, the zwitterion is deprotonated by a base which is in the solution; this base can be water, hydroxide ions (OH^-) and amino acid salt ($K^+ {}^-OOC - CH_2 - NH_2$).

Finally, because of the presence of hydroxide ions in the solution, during the absorption carbon dioxide reacts also with them, so the reaction which takes place is the following one (equation (7.4)):

$$CO_2 + OH^- \xrightarrow{k_{OH}} HCO_3^- \tag{7.4}$$

For the sodium glycinate the zwitterion mechanism is supposed to be identical.

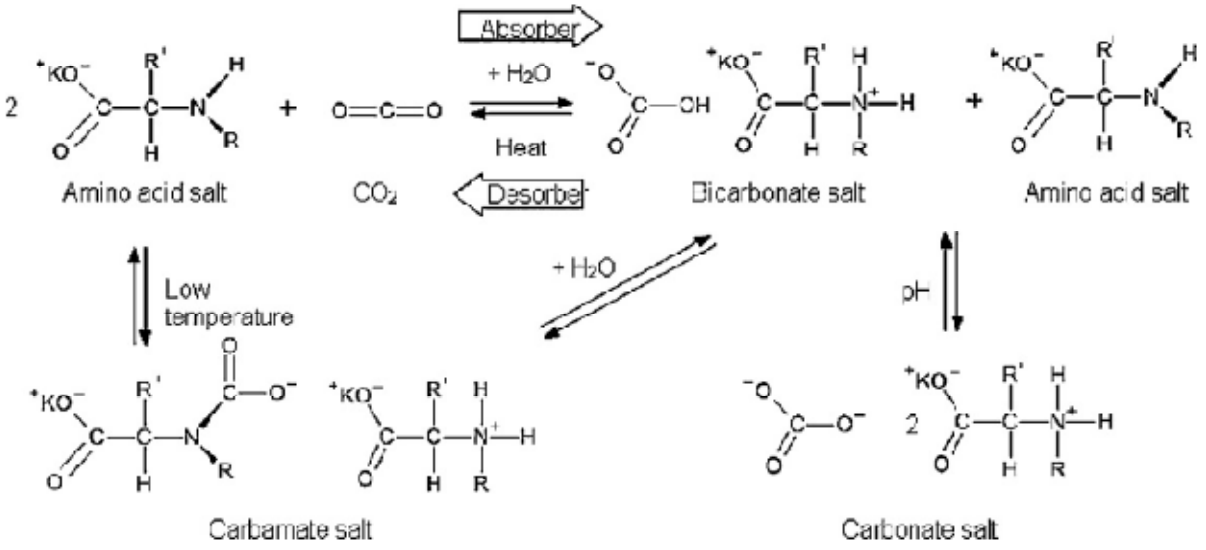

Figure 14. Reaction scheme in the amino acid salt solution. Source: [49].

Figure 14 shows the reaction scheme in the amino acid salt solution explained above [49]. After the formation of the amino acid salt, this neutralized amino acid salt reacts with carbon dioxide by forming carbamate and bicarbonate salts. In case of having primary or secondary amines and low temperature, carbamate and a protonated amino are formed. Carbamate can suffer hydrolysis, so it is bicarbonate is formed. In case of having tertiary amines or sterically hindered secondary amines, bicarbonate is formed [50]. By using amino acids it is possible to remove the protonated amine from the absorption liquid, so a higher uptake of carbon dioxide is obtained. The process which is based on amino acid precipitation is called DECAB process.

7.2. Physical chemical properties.

Regarding carbon dioxide diffusivity, N_2O analogy can be used due to the similar properties between N_2O and CO_2, as configuration, molecular volume and electronic structure [51]. In this report, this analogy has not been taking into account.

7.2.1. Sodium glycinate.

Sodium glycinate is a highly-reactive, non-volatile, resistant to oxidation primary amine. It is very important to know the physicochemical properties of amino acids.

Table 4. Sodium glycinate solubility data in CO_2 capture.

α [$kmol_{CO2}$*$kmol^{-1}_{SG}$]	ΔT [K]	ΔP [kPa]	[SG]	Reference
0.114-0.300	303.15-323.15	89.0039-97.0997	1.056-3.466 [$kmol/m^3$]	[33]
	303.15-323.15		1.056-6.217 [$kmol/m^3$]	[52]
0.275-1.075	303.15-323.15	0.1-213.5	10% wt-30%wt Aqueous SG	[53]
0.888-1.275	313.15	92-2505	10 % wt Aqueous SG	[54]

As shown in Table 4, sodium glycinate solubility data were reported in different articles. Carbon dioxide loadings used in this reports take values from 0.114 to 1.275 $kmol_{CO2}$/ $kmol_{SG}$; temperatures are included between 303.15 and 323.15 K; about pressures, there is a wide range of operation (0.1-2505 kPa).

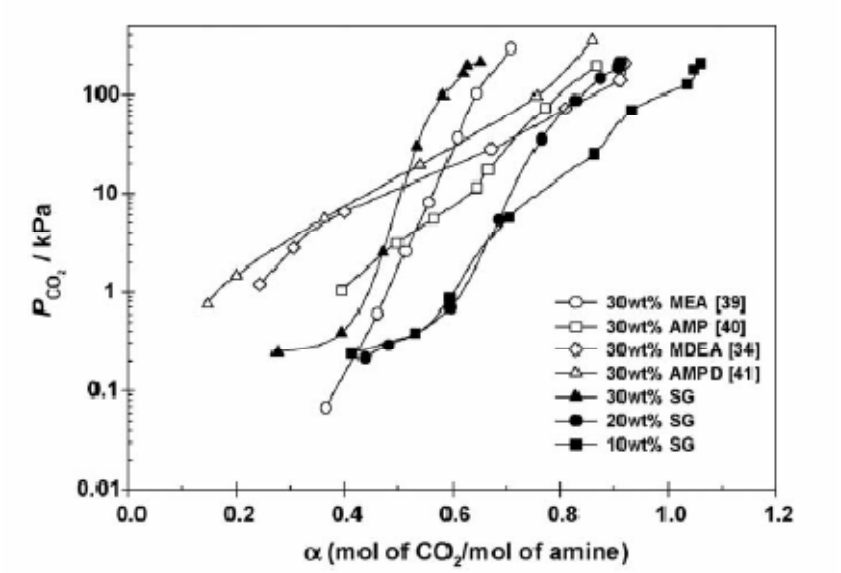

Figure 15. Solubility of CO_2 in aqueous sodium glycinate solutions with other aqueous absorbents under the same conditions (313.15 K). Source: [53].

In Figure 15 is shown the comparison of carbon dioxide solubility in aqueous sodium glycinate solutions with other aqueous absorbents at 313.15 K. Comparing sodium glycinate in different mass percentages and at the same pressure, carbon dioxide is less soluble in 30% mass sodium glycinate than in 10 or 20% mass, although at reduced pressures CO_2 is more soluble in 30% mass sodium glycinate. Furthermore, CO_2 is less soluble in 30% mass sodium glycinate than in the other absorbents.

Concerning solubility, Lee et al. [33 table 1, 52 table 1] presented some Henry's constant data of the CO_2 absorption in aqueous sodium glycinate solutions. In these reports, it is shown that solubility is inversely proportional to Henry's constant. In addition, Mazinani et al. [55] experimentally examined the effect of sodium glycinate on the solubility of CO_2 in MEA solutions in a range of temperature of 298-313 K and over CO_2 partial pressure ranging from 0 to 35 kPa, for molar ratio of sodium glycinate from 0.2 to 0.8 in a total blend concentration of 2.5 M. They also studied other properties as density and viscosity at the same conditions of solubility measurement.

Table 5. CO_2 diffusivity in aqueous sodium glycinate.

α [$kmol_{CO2}$* $kmol^{-1}_{SG}$]	ΔT [K]	ΔP [kPa]	[SG] [$kmol/m^3$]	Comment	Reference
0.114-0.300	303.15-323.15	89.0039-97.0997	1.056-3.466	Physical solubility and CO_2 diffusivity data of N_2O and CO_2	[33]
	298-318	25.73-101.3	1.0-3.0	Absorption data for various SG concentrations	[56]
	303.15-323.15		1.056-6.217	Physical Solubility and Diffusivity of N_2O and CO_2 in aqueous SG	[52]

As reported in Table 5 the operational temperature range analyzed covers from 298 to 323.15 K. Instead, partial pressures range (25.73-101.3 kPa) is not as wide as sodium glycinate concentration´s range (1-6.217 $kmol/m^3$).

Properties as density, viscosity, surface tension, freezing point, CO_2 absorption rate, alkalinity and pH have been studied by different authors [54, 56, 57, 58]. About pH, this is an important property that affects on the solubility data since amino acids appear in different forms when they are in solution [46]. Other important properties are the enthalpy of absorption and the enthalpy of desorption; the second one informs about the energy required in the solvent regeneration [59]. In Table 6 are shown the enthalpy of absorption data measured by Salazar et al. [48].

Table 6. Enthalpy of absorption data.

α [mol_{CO2}*mol^{-1}_{SG}]	ΔT [K]	ΔP [MPa]	SG [mass fraction]	Reference
0.173-1.493	313.15-323.15	12	0.1	[48]

In the article "Determination and Calculation of Physical Properties for Sodium Glycinate as a CO_2 Absorbent" [60] Park et al. measured the solubility of sodium glycinate in 25 g of water at different temperatures. This study was taken into account while doing the measurements. Furthermore Park et al. investigated the heat of vaporization, which is the energy needed to transform a substance into a gas at a given pressure, and Table 7 summarize the results obtained in this study.

Table 7. Heat of vaporization data.

Boiling Temperature [°C]	Vapor Pressure [hPa]	[SG] [%wt]	Reference
31.91-120.51	50-1010	10.0-60.0	[60]

Song et al. [61] estimated the regeneration energy of CO_2 absorption in sodium glycinate, being the regeneration energy the summation of the enthalpy of reaction, the sensible heat and the heat of vaporization. Lee et al. [62] researched about sodium glycinate solutions in a pilot plant, and they obtained data about physical properties of these solutions as heat of formation and free energy of formation.

7.2.2. Potassium glycinate.

Regarding potassium glycinate, some researches lead to indicate that "potassium glycinate reacts with about twice the rate of MEA, and at higher concentrations, at three times the rate" [47].

Table 8. Solubility of CO_2 in aqueous solutions of potassium glycinate.

α [mol_{CO2}*mol^{-1}_{PG}]	ΔT [K]	ΔP [kPa]	[PG] [mol/dm^3]	[MEA] [mol/dm^3]	Comment	Reference
0.069-1.32	293-323	0.54-639	0.1-3	2.51	solubility of CO_2 in aqueous solutions of SG	[63]
0.129-1.357	293-323	0.37-572	0.1-3	2.43		

According to Table 8 CO_2 loadings are covered between 0.069 and 1.357 mol_{CO2}/mol_{PG}, temperatures between 293 and 323 K, pressures between 0.37 and 639 kPa and potassium glycinate concentrations between 0.1 and 3 mol/dm^3. Another reported data is MEA concentration.

Portugal et al. [63] also reported the comparison of CO_2 solubility between potassium glycinate and potassium threonate under certain specific values of temperature (313 K) and concentration (1.0 mol dm^{-3}), which is shown in Figure 16 as a semi-log plot of the solubility of carbon dioxide.

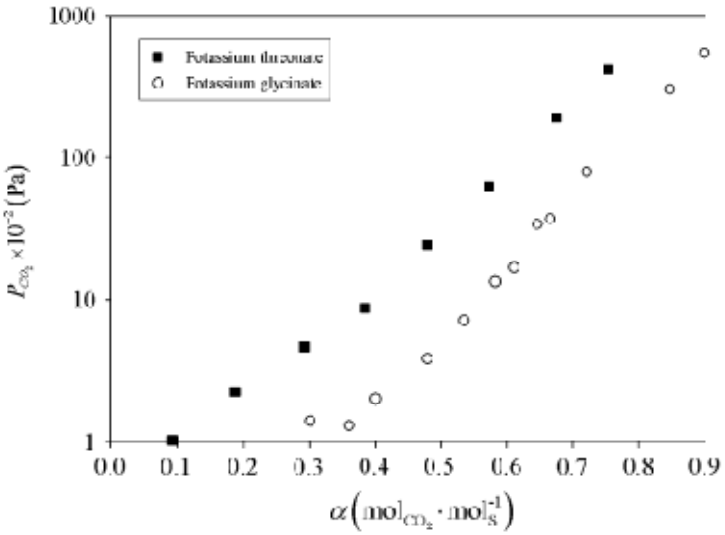

Figure 16. Semi-log plot of CO_2 solubility in aqueous solutions of potassium glycinate and potassium threonate. Source: [63].

According to Figure 16, at constant partial pressure CO_2 loading for potassium glycinate is higher than potassium threonate, so potassium glycinate presents a higher absorption capacity.

Diffusivity is another important property.

Table 9. CO_2 diffusivity in potassium glycinate.

ΔT [K]	[PG] [mol/dm^3]	Comment	Reference
293.15-368.15	0.5 10^{-3}-3.09	length and inner radius of the capillary tube 14.92 m / 5.14 10^{-4} m	[64]
293-313	0.102-2.984	Viscosity and diffusivity of N_2O and CO_2 in potassium glycinate solutions	[40]

As shown in Table 9, in these reports both a wide temperature range (293-368.15 K) and potassium glycinate concentration (0.5 10^{-3}- 3.09 mol/dm^3) have been studied. The difference between CO_2 diffusivity data in sodium glycinate and in potassium glycinate is that there are no values for CO_2 loading and partial pressure for the second one, which is due to the lack of available information about potassium glycinate.

Other properties as viscosity, kinetic data (CO_2 absorption rate, reaction rate constant, etc.) have been reported in different studies [40, 44].

Lu et al. [43] reported data for mixtures of aqueous solutions of potassium glycinate and piperazine as an activator. In this study, they analyzed properties like density, viscosity and surface tension in a range of 288.15 to 323.15 K.

From the open literature consulted we can conclude that there is not much information available about some properties of potassium glycinate, but it is thought that using potassium glycinate instead of sodium glycinate would not make such a difference in the terms of the kinetics of reaction of the amine group with carbon dioxide [47].

7.2.3. Vapor-Liquid Equilibrium (VLE).

When writing this report, relevant topics are the vapor liquid equilibrium (VLE) and the solid liquid equilibrium (SLE). These concepts are needed to be analyzed in CO_2 capture in order to know about the function of amines, amino acids and other substances in CO_2 removal.

Mergler et al. [65] investigated amines systems in order to characterize them; ethylene amine is taken as a base structure, and then was reported the effect of different functional groups in order to vary physical and chemical properties.

Aronu et al. [66] also reported information about VLE measurements for aqueous amine amino acid salt (AAAS) solutions of 3-(methylamino)propylamine/sarcosine (SARMAPA). In this report equilibrium measurements were made by ebulliometric vapor–liquid equilibrium measurements, low temperature equilibrium measurements and high temperature equilibrium measurements.

A VLE example may be found in The Contactor publication [47], as shows Figure 17. At low carbon dioxide loadings, sodium glycinate has about twice the CO_2 partial pressure as MEA, but comparing sodium glycinate with DEA, the last one has a higher CO_2 partial pressure. Moreover, at high loadings it can be seen that sodium glycinate has higher carbon dioxide partial pressure than either MEA or DEA. Though MEA and sodium glycinate have approximately the same heat of absorption of CO_2, it can be said that sodium glycinate requires less regeneration energy than MEA.

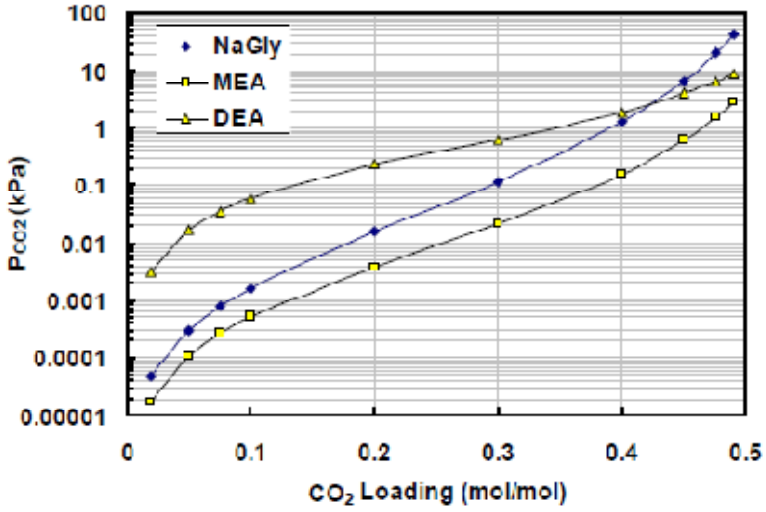

Figure 17. CO_2 partial pressure vs solution loading at 35 °C for various amines. Source: [47].

7.2.4. Solid-Liquid equilibrium (SLE).

Solid-liquid equilibrium is treated as the basis for crystallization processes, and is also important for refrigeration or the transport of liquid gases which solids can be formed. As explained by Jacob et al. [66], "solid-liquid phase equilibria provide the necessary information on the real behavior of systems at low temperatures".

About phase equilibrium, it is important to know the phase rule, developed by Gibbs in 1876, which relates the following terms as the equation (7.5).

$$P + F = C + 2 \tag{7.5}$$

Where:

P: number of phases in the system. As explained by Mullin "a phase is a homogeneous part of a system. Thus, any heterogeneous system comprises two or more phases." [68].

F: degrees of freedom. This term represents the number of variables like pressure, temperature or concentration that can change in magnitude without changing the number of phases. This component is also referred as the variance of the system.

C: number of components, which is "the minimum number of chemical compounds required to express the composition of any phase" [68].

Phase diagrams are employed for representing in two or three dimensions the equilibrium between the phases of the studied system.

8. Experimental method.

8.1. Freezing point.

Freezing point is defined as “the temperature at which a liquid, releasing sufficient heat, becomes a solid. For a given substance, the freezing point of its liquid form is the same as the melting point of its solid form, and depends on such factors as the purity of the substance and the surrounding pressure”[69]. This temperature is a specific property of the substance. When a pure substance is analyzed in order to determine its freezing point, the temperature doesn’t vary during the phase change, as shown in Figure 18 (a). In case of the mixture of the original substance with a second substance, the freezing point of the original substance changes. This situation is relevant for aqueous solutions; when a solute is dissolved in water, its freezing point is lower than the freezing point of the pure substance. This is due to the problem of the molecules of water to fix them to form a pure crystal. In Figure 18 (b) is shown the temperature change with time and the super-cooling occurs; in this case, the temperature shortly drops below the freezing point, and then when crystals are formed, the temperature rises considerably. The freezing point that is needed to be recorded is the temperature at which the first ice crystals are formed [70].

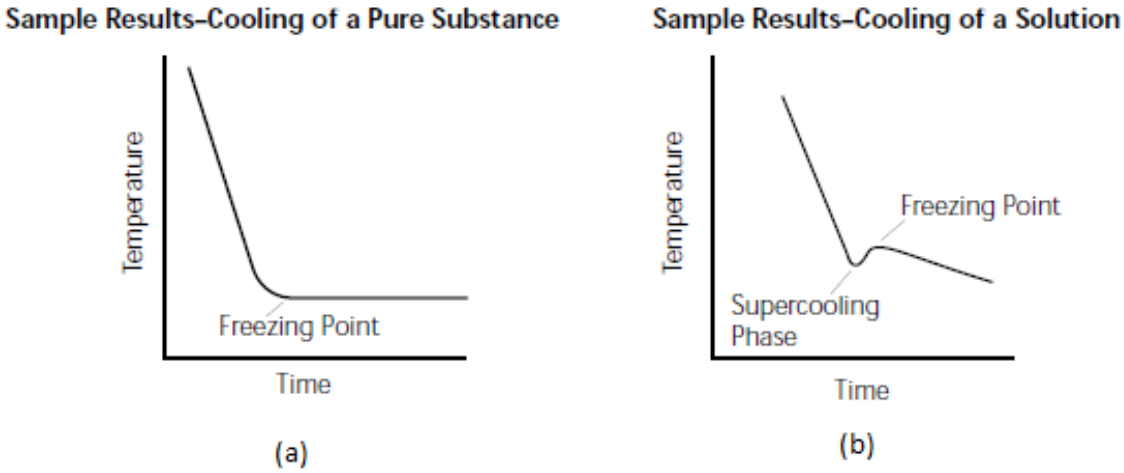

Figure 18. Temperature-time diagram for pure substance (a) and a solution (b).Source: [70].

In order to determine the freezing point of a substance a modified Beckmann apparatus was used. Moreover experiments were done at atmospheric pressure. Figure 19 shows the apparatus carried out by Fosbøl et al. and explained in the article ”Freezing point depression of aqueous MEA,MDEA, and MEA-MDEA measured with a new apparatus” [32]. This setup consists in a Lauda RE 110 thermostatic bath (A) which is used to obtain low temperatures of the refrigerant, the stirrer apparatus and the temperature probe. The temperature probe has different devices as a stirring device (B), beaker glasses (D), a screw lid (E), a rubber stopper (F), a thermometer (G).

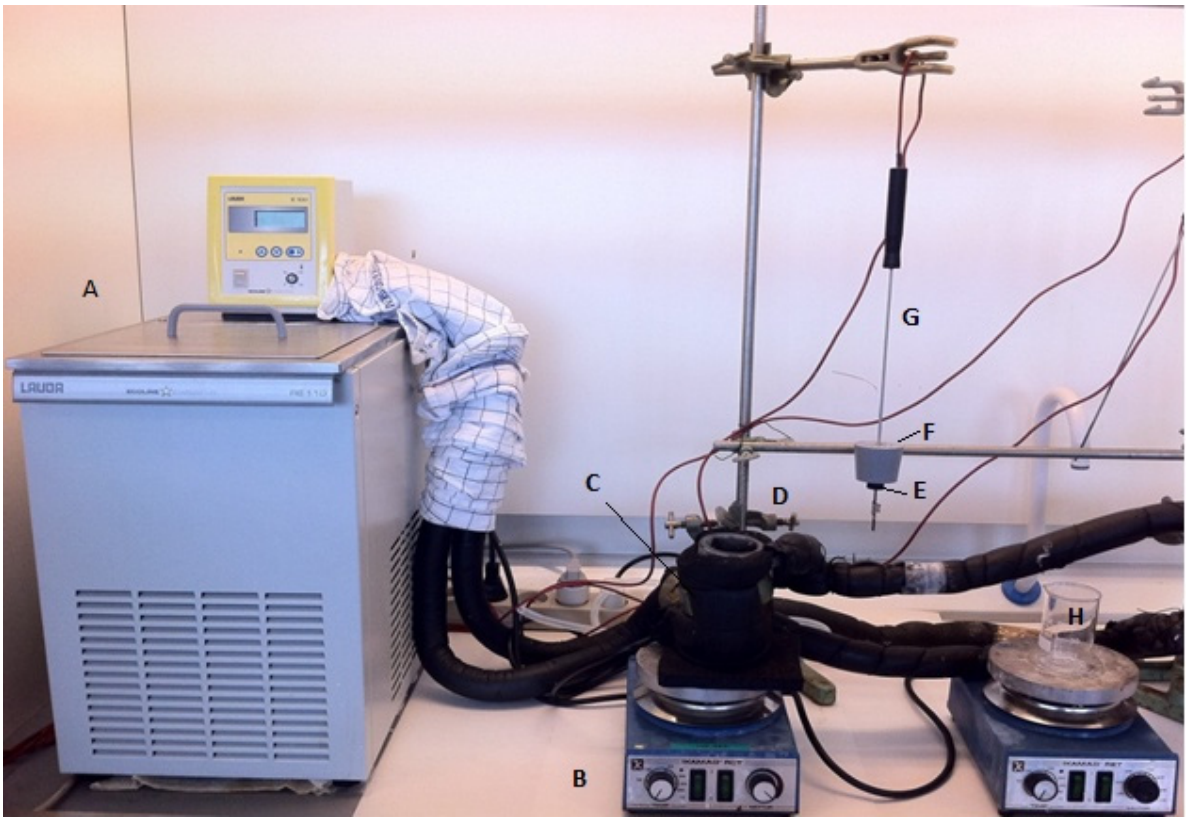

Figure 19. Schematic figure of freezing point depression setup. A, thermostatic bath with ethanol; B, stirring device; C, cooling jacket; D, beaker glass; E, screw lid; F, rubber stopper; G, thermometer; H, beaker glass with ethanol.

As shown in Figure 19 the equipment has two parts: the controlled temperature beaker glass (D) filled with refrigerant (which has a cooling jacket (C) to maintain a constant temperature), and another beaker glass filled with ethanol in order to heat the sample (H). In both systems a stirrer apparatus (B) is placed under these beaker glasses so the sample is always homogeneous. It is necessary to check that the magnet stirrers in both parts of the equipment are stirring the sample. In addition as shown in

Figure 20, distilled water (A), sample glasses (B), and magnets (C) were also used in order to prepare the sample and then analyze it.

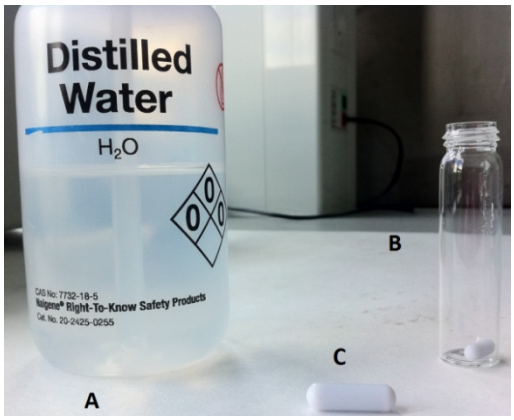

Figure 20. Other useful devices for these experiments. A, distilled water; B, beaker glass with a small magnet; C, magnet.

The preparation of the experiment begins with the weighting of the chemicals, taking in mind that is not appropriate to use volumetric measures since this would require the determination of the density. After mixing the chemicals in the mixing glass, stirring with the magnetic stirrer is the next step; this is done to mix the chemicals and for obtaining a homogeneous solution. If the solution does not become homogeneous, the concentration is above the solubility limit and the freezing point depression cannot be measured at first hand. We will later see how to treat these samples anyway.

Likewise the level of the cooling liquid (ethanol) in the cooling bath has to be checked after stirring the samples. The level should be high enough to cover the sample but not so high that cooling liquid comes into contact with the screw lid of the sample glass in order not to pollute the sample.

The temperature has to be set typically 5°C below the expected freezing point of the sample. Before starting the measurements, it is very important to make sure that the temperature probe and the stirring device are completely dried, so no moisture will dilute and thereby pollute the sample. Then the temperature probe is fixed in the ring stand behind the magnetic stirring apparatus at the cooling jacket.

So as to collect all the data an Agilent 34970A data acquisition unit in connection to a computer was used. A program gives a graph of the temperature versus time, and the scale can also be changed in order to focus on some parts of the figure. The Agilent 34970A unit needs to be calibrated before starting the measurements.

To begin the measurements, the sample glass needs to be filled until 1-1½ cm from the screw lid. If only a small amount of sample is available, the temperature probe needs to be covered with 2 cm of sample approximately, the reason being that the device measures temperature in the lower 1 cm of the probe. In the sample glass there is also a magnet stirrer in order to have a homogeneous solution throughout the measurements. Then the sample glass has to be screwed on the lid attached to the rubber stopper, and the temperature probe monitored on the computer. The sample temperature is recorded every four seconds.

It has to be taken into account that the manual stirring should be uniform during the experiment, and, as explained above, the temperature of the cooling bath has to be set 5°C lower than the expected freezing point. In case the temperature rises and ice is formed, the temperature needs to be reduced 5°C more. On the other hand, if temperature is reduced too fast and the freezing point is not observed, this means that the temperature of the cooling bath was too low and it should be increased during the next measurement.

During an experiment, the temperature will decrease below the freezing point temperature of the sample (in Figure 21, from 0 s to approximately 500 s). When a sub-cooling of 2-5 °C is reached the temperature will rise abruptly (here -19 °C in this test) due to the exothermal crystal formation, and then decrease slowly again due to continuous freeze out of the water and there by continuous concentration change. The freezing point is the maximum temperature measured.

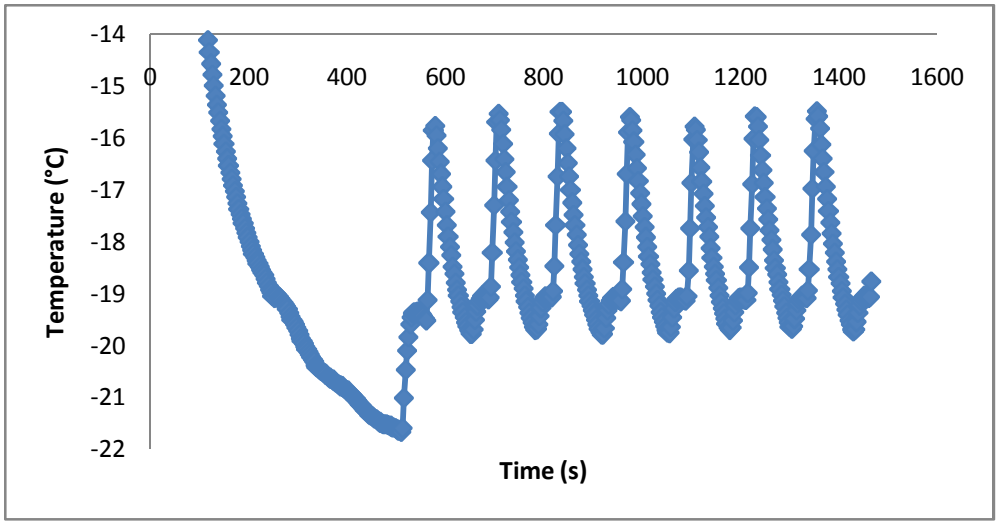

Figure 21. Data collected with the computer.

The first ice formation does not give precise information of the freezing point; that is because of the large sub-cooling required, as shown in Figure 21. In the first measure, an excess of ice formation is obtained, which changes the liquid phase concentration and the measurement is inaccurate. So the correct information will be given by the following measurements. In the previous figure it can be seen that the first freezing point is not correct; that's only used for knowing where the freezing point is, so is used as an approximation of the freezing point [32].

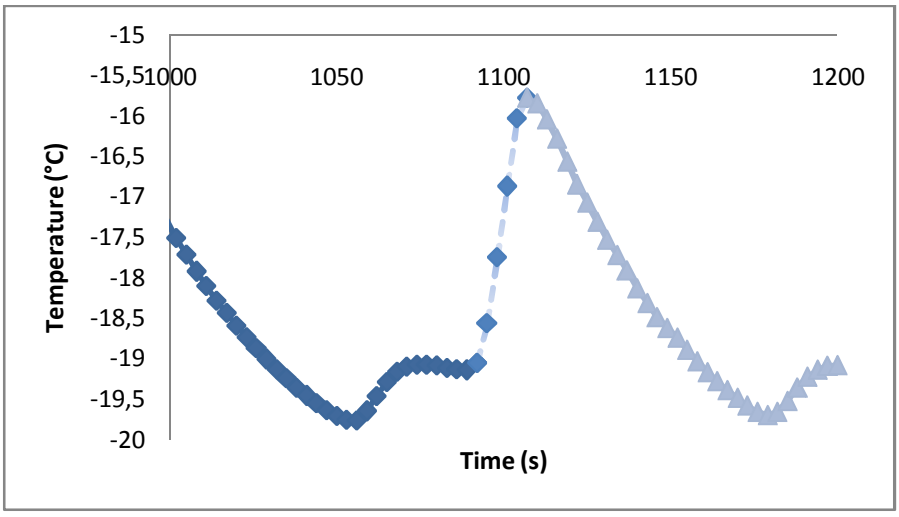

Figure 22. Enlargement of Figure 21 from 1000 to 1200 s.

After noticing the rise of temperature, the temperature probe is taken out of the cooling jacket and kept in a small beaker glass filled with ethanol at room temperature besides the equipment. For the next fifteen seconds the temperature would drop slightly because of the change of the water concentration in the liquid phase (Figure 22). At this point, crystals can be observed, and the sample has to be heated up until only small amount of crystals can be seen (dotted part of the curve in Figure 22). The heating can be done in an ethanol beaker or sometimes just in the air.

It is very important to leave a small amount of ice crystals (seed crystals), so they can be used as nuclei for the formation of new ice in the next experiment. That is the reason why next sub-coolings are not as big as the first one; this phenomena can be observed in Figure 21.

8.2. Solubility.

Determination of the solubility is performed similar to the freezing point determination. The same equipment is used, however the solubility is determined visually; initially the solution is cooled down until precipitation occurs. Then the sample glass is slowly heated up while stirring: this can be done in two different ways depending on the solution: the solution can be melted by holding it in the air at room temperature or by putting it in a small beaker with ethanol which temperature has to be higher than the melting point of the solution. Finally the solubility point is determined as the temperature at which all the crystals disappear, so the solution changes color and becomes clear. Because of the visual determination, the reproducibility of the temperatures is not as accurate as the reproducibility of the freezing points [58].

9. Experimental overview and calculations.

The components used for these experiments were sodium hydroxide, potassium hydroxide, sodium bicarbonate, potassium bicarbonate, glycine, and water. Ethanol was also used as refrigerant in the cooling bath and for heating the solutions in order to determine the solubility point. Furthermore sodium chloride was used for the calibration of the equipment.

In order to calculate the amount of each chemical component used in the different systems, mass, moles and mass fractions were used. As chemicals were weighted (in grams), moles were calculated using the molecular weight of the chemicals.

The amount (moles) of water added to the solution after the reaction, equivalent to moles of sodium or potassium glycinate formed, was calculated taking into account the relation between moles of sodium (or potassium) hydroxide or sodium (or potassium) bicarbonate and moles of glycine (excess or default of glycine, for example). In the case in which the sodium bicarbonate-sodium hydroxide-glycine-water system was analyzed, the moles of water added were the same as the moles of glycine in the sample, since the relation between moles of cation and moles of glycine is one to one (for the potassium system the K:Gly relations 1:1 and 2:1 were studied). The total amount of water in the solution was calculated as moles of water added (formed) plus moles of water in the solution (initial water). In the potassium systems, the purity of potassium hydroxide has to be taken into account.

For the sodium bicarbonate-sodium hydroxide-glycine-water and potassium bicarbonate-potassium hydroxide-glycine-water systems the calculation was set up, so the amount of $NaHCO_3$ and $KHCO_3$ needed to reach the specified loadings were calculated. Then how much NaOH and KOH were needed to add to reach the K: Gly 1:1 or 2:1 relations were calculated.

Two different mass fractions were calculated, and it is very important to understand the difference between both. Mass fraction (wt%) was calculated as mass of sodium (or potassium) glycinate formed divided by total mass. The mass fraction (salt free) was calculated as mass of sodium (or potassium) glycinate formed divided by the sum of mass of total water and mass of sodium (or potassium) glycinate formed. Taking the sodium system, mass fractions were defined as equations (9.1) and (9.2).

$$wt\ frac = \frac{m_{NaGly}}{m_{total}} \quad \left[\!\left[\frac{g\ NaGly}{g\ total}\right]\!\right] \tag{9.1}$$

$$wt\ frac(salt\ free) = \frac{m_{NaGly}}{m_{H2O\ total}+m_{NaGly}} \quad \left[\!\left[\frac{g\ NaGly}{g\ water+g\ NaGly}\right]\!\right] \tag{9.2}$$

In order to compare all the measurements and to have the same concentration scale, all the figures were represented with the same x axis (wt fraction salt free). Representing the measurements in the same scale allows comparing all the results as they take into account the same parameters.

To be more accurate with the results, it was recommended to take three or four freezing point measurements for each sample, so finally an accurate average of temperature was calculated and standard deviations had low values (about ±0.05°C). While determining solubility points standard deviations begin to be higher due to the temperature range used in the calibration (0 to -25°C) does not match with the temperature range for these points.

First of all, the calibration of the equipment was done. After that, various systems were analyzed in order to determine the freezing points of the solutions and also to study the difference between them. Two different amino acids were studied: sodium glycinate and potassium glycinate. For each amino acid, various systems were examined:

- Sodium or potassium bicarbonate-glycine- water: systems with carbon dioxide formation.
- Sodium or potassium hydroxide-glycine-water: systems without carbon dioxide formation, taking into account an excess or default of glycine or cation (sodium or potassium).
- Sodium or potassium bicarbonate-sodium (or potassium) hydroxide-glycine-water: systems with and different CO_2 loadings.

9.1. Calibration.

The first step in order to use the equipment necessary to determine the freezing point is the calibration of the equipment. Solutions of different mass fractions of sodium chloride (NaCl) were prepared (0, 2.5, 5, 7.5, 10, 15, 17.5 and 22 wt% NaCl). For each solution, ten temperature measures were made in order to achieve the lowest standard deviation of the data. Temperature average and standard deviation are displayed in Table 10.

Just to be sure that the previous calibration was good, the measurements were repeated, but this time more samples were prepared: 0, 2.5, 5, 7.5, 10, 12.5, 15, 17.5, 20 and 22 wt% NaCl. Solutions were prepared and analyzed as explained in "8. Experimental method."

Table 10. Sodium chloride and water weights, temperature average and standard deviation for every wt fraction of sodium chloride.

wt% NaCl	m NaCl (g)	m H_2O (g)	Mean T (°C)	T Stddev (°C)	wt% NaCl	m NaCl (g)	m H_2O (g)	Mean T (°C)	T Stddev (°C)
0	0	25.023	-0.013	0.014	**12.5**	3.572	25.003	-8.67	0.015
2.5	0.641	25.072	-1.50	0.007	**15**	4.412	25.009	-11.05	0.014
5	1.316	25.040	-3.03	0.005	**17.5**	5.303	25.018	-13.56	0.023
7.5	2.029	25.012	-4.70	0.035	**20**	6.253	25.020	-16.42	0.018
10	2.779	25.012	-6.54	0.008	**22**	7.051	25.015	-19.06	0.015

With the exception of two cases, all the measurements in Table 10 have standard deviations less than 0.03 °C, which lead to a very good grade of accuracy.

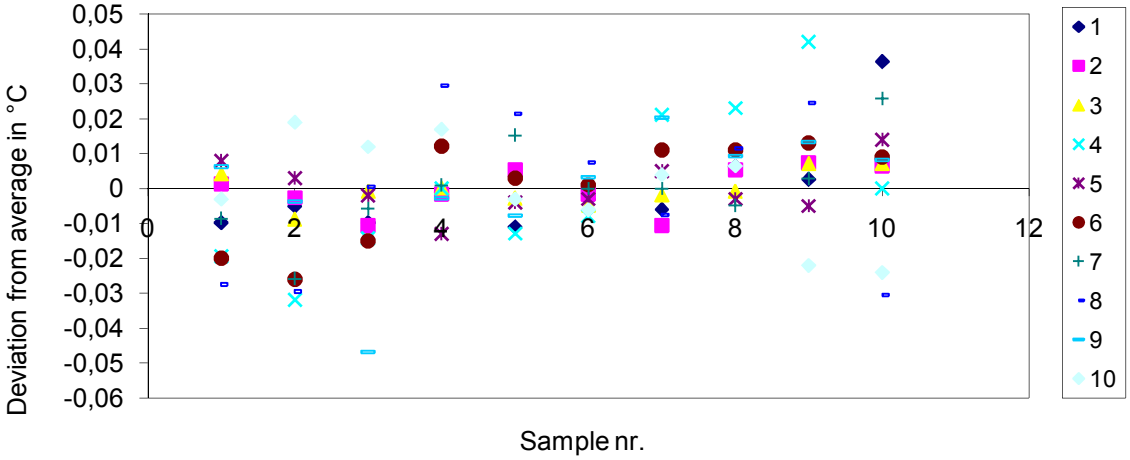

Figure 23. Standard deviations for the samples of Table 10.

As shown in Figure 23 the average of the standard deviation for measuring the freezing point of the prepared samples was good (±0.05°C range), so all the freezing points of the samples had been determined with acceptable accuracy.

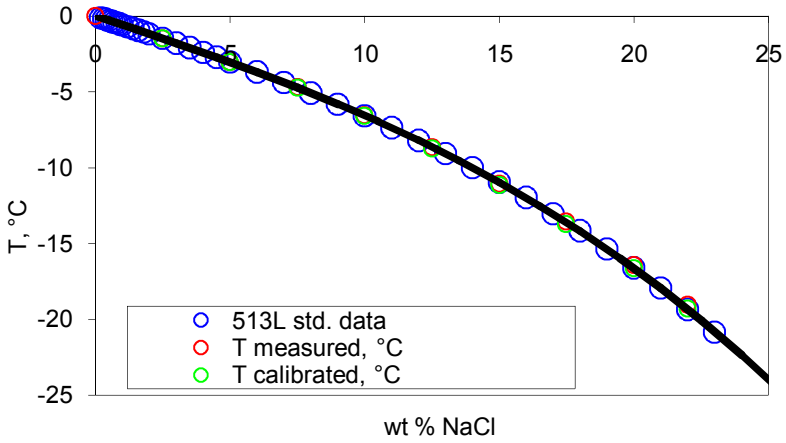

Figure 24. Temperature versus wt% sodium chloride for the measured data and the calibrated data.

Figure 24 shows the similarity of the measured temperature (red) and the calibrated one (green). It can be seen that the measures and the calibration correlation are approximately the same, the red and the green data coincide. This indicates that the original calibration was reasonably good. If the original calibration was bad, both red and blue curves should be far from each other. This is not that case, so it can be concluded that the previous calibration was very accurate comparing with the new data. Furthermore, the new calibrated data (green) should lay on top of the standard database data (blue), as shown in Figure 24.

As a result of the calibration, two new calibration values (M and B) had been determined, which were the values used in the following experiments. For this project the M and B values used were: M=0.96925 and B=-0.44422.

The difference between both calibrations was not so big, so there was no need to repeat the experiments. It also had to be taken into account that the calibration had been done for an average of temperature (from 0 to -25°C), so it could be difficult to obtain good results while working with other temperatures out of this range.

9.2. Glycine-water system.

The glycine-water system was analyzed. Glycine (Gly) mass fractions between 0.01 and 0.275 were prepared and their freezing points were determined. Water was also analyzed in order to determine its freezing point. The measurements were carried out as explained in "8. Experimental method."

From the 0.15 Gly mass fraction as not all the glycine was dissolved, warming the samples was needed, so solubility points were determined. Then glycine mass fractions from 0.15 had to be part of the solubility curve. Crystals for these experiments were amorphous.

Table 11. Temperatures measured and standard deviations for the system glycine-water.

wt % glycine	m H_2O (g)	m Glycine (g)	Mean T (°C)	T stddev (°C)	wt % glycine	m H_2O (g)	m Glycine (g)	Mean T (°C)	T stddev (°C)
1.00	9.035	0.091	-0.2096	0.016	**19.94**	9.035	2.250	24.72	0.633
2.50	9.019	0.231	-0.65	0.005	**20.95**	9.027	2.392	27.54	0.267
5.00	9.008	0.474	-1.24	0.019	**22.41**	9.049	2.613	32.20	0.278
7.50	9.003	0.729	-1.79	0.002	**23.97**	9.013	2.842	37.33	0.102
9.99	9.034	1.002	-2.49	0.032	**24.94**	9.027	3.000	39.60	0.249
15.00	9.002	1.588	-3.31	0.039	**26.43**	9.033	3.245	44.41	0.209
16.00	9.004	1.714	11.31	0.648	**27.50**	9.004	3.415	49.08	0.281
17.99	9.008	1.976	16.21	0.745					

As shown in Table 11 standard deviations up to 0.1°C were obtained at those mass fractions in which heat was needed to be applied in order to dissolve all the precipitate, so when the solubility points were determined; particularly in this system standard deviations had higher values from 16 wt% glycine (Gly). Higher standard deviations values were explained by the temperature range used in the calibration; as these temperatures were not in the calibration range (0 to -25 °C), standard deviations started to increase. The 15 wt% glycine was also the most difficult point to analyze due to it is thought to be near the eutectic point. While working near the eutectic point the measurements could be very difficult to be carried out, and results may also be inaccurate.

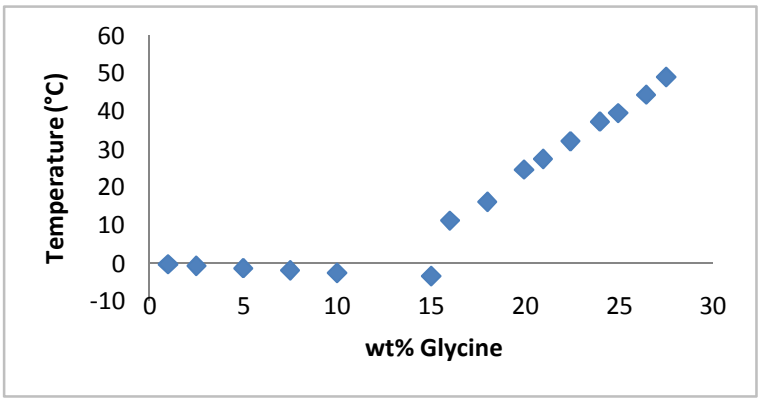

Figure 25. Temperature versus wt% glycine for the measured data.

Figure 25 represents all the data collected for this binary system (glycine-water). Theoretically the 15 wt% glycine point should be in the solubility curve, but experimentally it appears in the freezing curve; this means that this concentration is near the eutectic point. As the 15 wt% Gly has to be on the solubility curve, if a trendline is added, as shown in Figure 26, the eutectic point seems to be near the 12 wt% glycine. Furthermore, in Figure 26 the difference between the freezing curve trendline (linear) and the solubility curve trendline (second order polynomial) is shown.

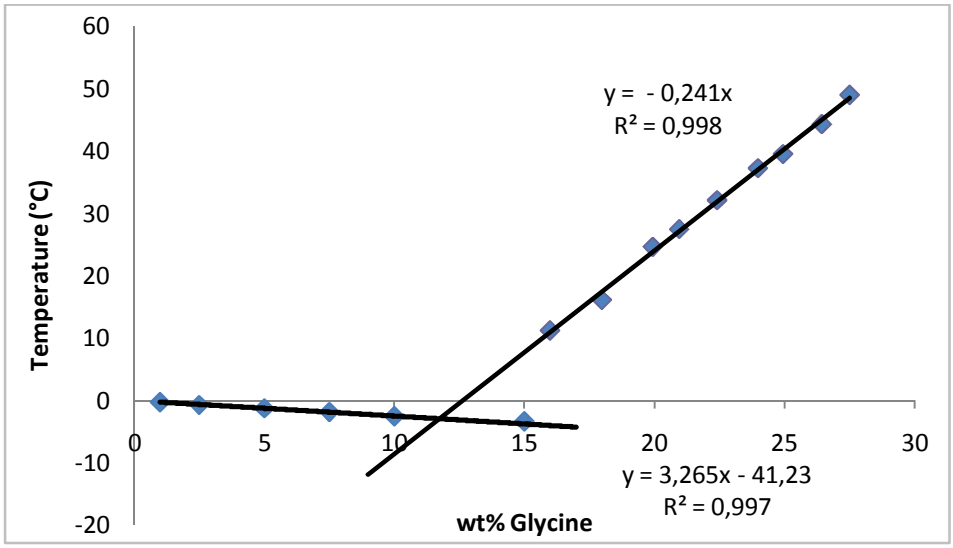

Figure 26. Temperature versus wt% glycine for the measured data.

Figure 26 shows the equations for both trendlines, so the intersection of both trendlines is calculated as:

$$-0.0006x^2 - 0.2413x = 3.2655x - 41.234 \tag{9.3}$$

Solving equation (9.3) the x value (wt% glycine) is calculated as:

$$x = \frac{-(-3.5068) \pm \sqrt{(-3.5068)^2 - 4(-0.0006)41.234}}{2(-0.0006)} \tag{9.4}$$

Equation (9.4) has two solutions: x=5856.4 (not valid) and x=11.73. So according to the experimental measurements the eutectic point has to be located in the 11.73 wt% of glycine.

Looking at the points 17.99 and 26.43 wt% glycine in Figure 26, these differ from the trendline values. This could be because the temperature measurements were not taken very accurately, so their standard deviations were higher than the ones of the other points due to the temperature average was not the same as the one during the calibration.

9.3. Sodium hydroxide and sodium bicarbonate systems.

For all the cases demineralized water was used in order to determine its freezing point and all the samples were measured as reported in "8. Experimental method." Water was also analyzed in order to insure the reproducibility of calibration.

9.3.1. Sodium hydroxide-glycine-water system (NaOH-Gly-H_2O).

The system sodium hydroxide-glycine-water was determined in order to study the formation of sodium glycinate without the additions of carbon dioxide. As a result of the reaction between sodium hydroxide and glycine in a water solution, sodium glycinate and water are formed.

A literature study was performed in order to find works discussing the above system. Only a limited amount of publications could be found, as explained in "7.2.1. Sodium glycinate."

Five new cases were studied; the difference between them was the relation among moles of sodium hydroxide and moles of glycine (n_{NaOH}:n_{Gly}). These experiments were carried out in order to study how the (n_{NaOH}:n_{Gly}) relation affects at the freezing point. From the CO_2 capture point of view it is more interesting to have an excess of sodium hydroxide. The base, sodium hydroxide, captures the CO_2. The amino acid can be thought of as a catalyst or a buffer. The interesting cases would be the systems which have excess moles of sodium hydroxide per moles of glycine relation above 1:1 for example 2 to 1 and 5 to 1.

9.3.1.1. Relation of moles of NaOH per moles of Glycine 1 to 1.

Sodium glycinate mass fractions between 0.01 and 0.83 were studied. No need of warming solutions was necessary as all the chemicals dissolved easily below room temperature. Table 12 summarizes the measured weights, freezing points and standard deviations for these measurements.

Table 12. Temperature measured and standard deviation of the measurements for the system NaOH-Gly-H_2O (nNaOH:nGly 1:1).

wt frac NaGly, salt free	m H_2O (g)	m Gly (g)	m NaOH (g)	Mean T (°C)	T Stddev (°C)
0.0000	9.000	0.000	0.000	0.0372	0.004
0.0100	9.012	0.071	0.038	-0.32	0.005
0.0200	9.031	0.143	0.081	-0.70	0.012
0.0410	9.024	0.301	0.160	-1.44	0.002
0.0647	9.045	0.490	0.266	-2.43	0.007
0.0842	9.029	0.654	0.350	-3.26	0.005
0.1001	9.015	0.792	0.424	-3.99	0.005
0.1206	9.017	0.982	0.523	-5.00	0.005
0.1497	9.055	1.274	0.687	-6.63	0.007
0.1754	9.013	1.544	0.825	-8.19	0.022
0.2013	9.000	1.841	0.984	-9.88	0.018
0.2505	9.025	2.487	1.338	-14.27	0.009
0.3000	9.028	3.251	1.762	-19.55	0.016
0.3496	9.036	4.174	2.238	-26.24	0.055

Table 12 shows that the measured temperatures have standard deviations below or equal to 0.055 °C, so the measurements were taken very accurately. The freezing points of the NaOH-Gly-H_2O system are shown in Figure 27 as laid out in Table 12.

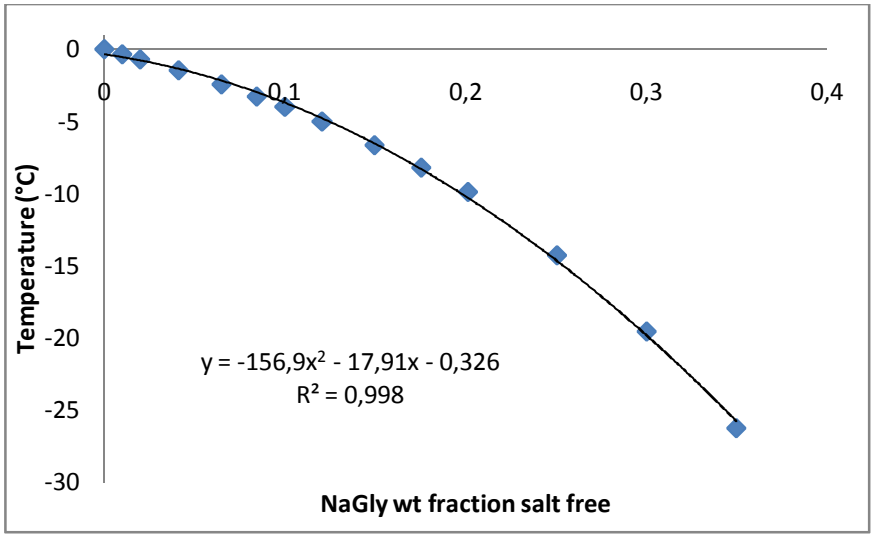

Figure 27. Temperature vs wt fraction in the system sodium hydroxide-glycine-water (nNaOH:nGly 1:1).

As shown in Figure 27 all the points seem to follow a polynomial tendency, which is different from the glycine tendency (linear).

From 35 wt% NaGly to 83 wt% NaGly I tried to analyze the samples but it was very difficult. According to the Korean data [60], from approximately 41 wt% of sodium glycinate, temperatures are located in the solubility curve, as shown in Figure 28.

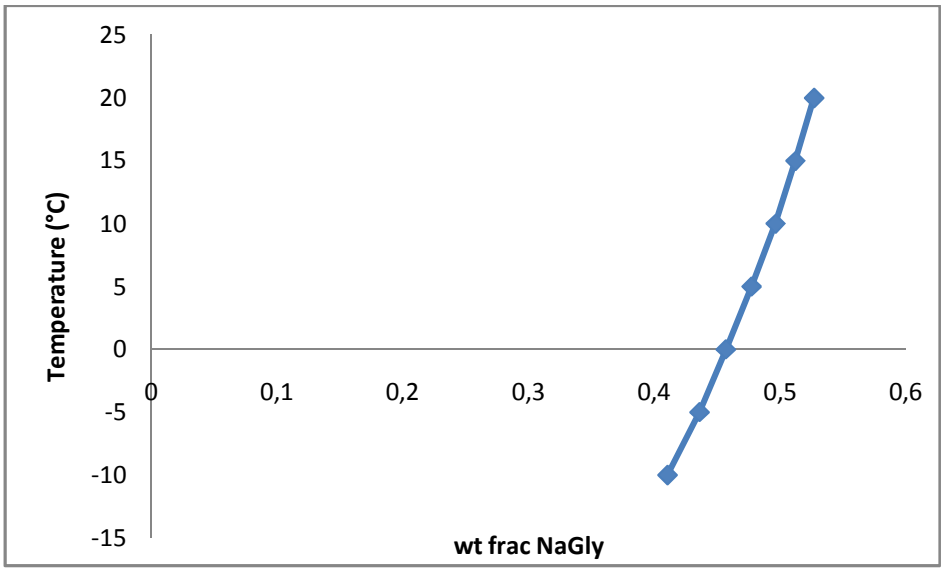

Figure 28. Temperature vs NaGly mass fraction from the study written by Park et al [60].

When 40 wt% NaGly was analyzed, the first problem was to dissolve all the precipitate. When cooling the solution, the cooling bath could not cool the sample as needed. Furthermore, the solution seemed very viscous, like gelatin (Figure 29).

A lot of bubbles were created because of the manual stirring. Even if I cooled the samples to -30°C I could not see crystals forming, so some samples were analyzed by microscope in order to determine if crystals were formed. These analyses showed that there were some tiny crystals, but we couldn't know exactly if these were real crystals or flakes from the Teflon stirrer.

For the 70 wt% NaGly sample, after dissolving the solution, at -10°C the solution was very viscous, and it was also very difficult to stir (like rubber). When analyzing the 83 wt% NaGly, the highest NaGly concentration possible with a small amount of water. Remembering that mixing NaOH and Gly creates water, thereby only a maximum of 83 wt% can be reached. Even if the sodium hydroxide pellets were milled in order to increase the contact surface, the solution could not be dissolved, as showed in Figure 29.

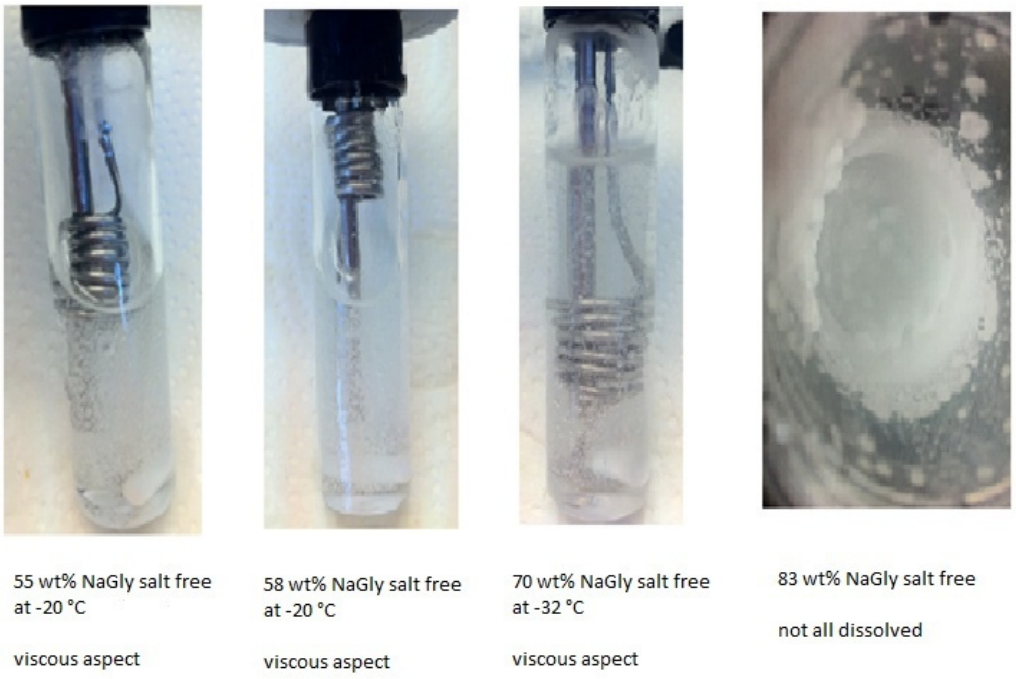

Figure 29. Some solutions of sodium hydroxide and glycine with a n_{NaOH}/n_{Gly} relation (1:1) in water.

As explained above the results obtained in this study were different from the ones obtained by Park et al. [60] as no points in the solubility curve could be determined. So I could not compare my results with the ones in the article written by Park et al.; the experiments of this project didn't agree with the ones of Park et al. [60].

9.3.1.2. Relation of moles of NaOH per moles of Glycine 1 to 2.

In this system an excess of glycine (twice moles of glycine than moles of sodium hydroxide) was taken into account. Sodium glycinate mass fractions from 0 to 0.3923 were analyzed. From 17.16 wt% NaGly solubility points were determined instead of freezing points as the solutions needed to be warmed up to dissolve all the chemicals.

Table 13. Measured temperatures and standard deviation for the system NaOH-Gly-water (nNaOH:nGly 1:2).

wt frac NaGly, salt free	m H_2O (g)	m Gly (g)	m NaOH (g)	Mean T (°C)	T Stddev (°C)
0.0000	9.000	0.000	0.000	-0.202	0.012
0.0254	9.056	0.375	0.098	-1.42	0.011

0.0527	9.019	0.774	0.209	-2.85	0.007
0.0799	9.012	1.231	0.328	-4.46	0.006
0.1127	9.019	1.801	0.483	-6.66	0.012
0.1249	9.030	2.050	0.546	-7.62	0.011
0.1716	9.004	3.005	0.800	12.02	0.408
0.1958	9.035	3.553	0.950	19.50	0.421
0.2235	9.040	4.250	1.133	29.04	0.289
0.2376	9.029	4.612	1.231	32.93	0.182
0.3098	9.031	6.850	1.822	54.59	0.237
0.3923	9.004	10.202	2.723	-	-

As shown in Table 13 for low sodium glycinate mass fractions (0-0.1249) all the measurements had standard deviations values lower than 0.02 °C, so the measurements were taken very accurately. For concentrations above the 0.3923 NaGly mass fraction the solution could not be completely dissolved by heating to approximately 80°C so it was not possible to determine its solubility point.

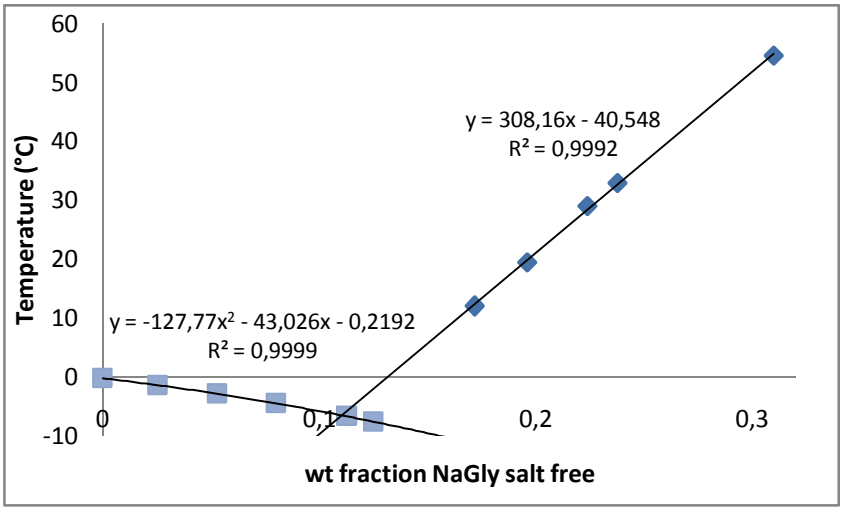

Figure 30. Temperature vs wt fraction in the system sodium hydroxide-glycine-water (nNaOH:nGly 1:2).

In Figure 30 freezing and solubility points are represented. It can be observed that points included from 0 to 0.1249 NaGly mass fractions follow a polynomial tendency; however the solubility curve tendency seems to be linear. The intersection between both curves seems to show that the eutectic point is near the 11.27 wt% NaGly, so the 12.49 wt% NaGly measurement was likely a metastable point precipitating ice.

9.3.1.3. Relation of moles of NaOH per moles of Glycine 2 to 1.

A default of glycine (or excess of sodium hydroxide) was considered in this system. Sodium glycinate mass fractions between 0 and 0.51 planned to be measured. It was very difficult to determine the freezing point for the 22.22 wt% NaGly, but finally the temperature was obtained. No solubility points were obtained during the measurements only freezing points.

Table 14. Measured temperatures and standard deviation for the system NaOH-Gly-water (nNaOH:nGly 2:1).

wt frac NaGly, salt free	M H_2O (g)	m Gly (g)	M NaOH (g)	Mean T (°C)	T Stddev (°C)
0	9.000	0.000	0.000	0.059	0.001
0.0521	9.026	0.388	0.410	-3.54	0.007
0.1049	9.001	0.834	0.887	-8.31	0.017
0.1509	9.014	1.282	1.364	-13.84	0.012
0.2010	9.005	1.839	1.954	-21.63	0.075
0.2223	9.007	2.103	2.239	-26.34	0.052
0.2792	9.005	2.908	3.099	-30.64	0.074
0.3412	9.046	4.009	4.263	-	-
0.4079	9.007	5.503	5.863	-	-
0.4788	9.011	7.720	8.230	-	-
0.5103	9.018	9.011	9.592	-	-

As reported in Tabe 14 from 34.12 wt% NaGly freezing points could not be determined because crystals wouldn't appear even if the sample was cooled to limit of the equipment; furthermore, the solution had a viscous aspect which makes the experiments difficult, since stirring becomes difficult. The 0.2515 NaGly mass fraction was analyzed too; the sample could crystallize, even when I cooled it to -35°C. As the expected freezing point for this solution might be at a temperature under -30°C, the cooling bath had to cool the refrigerant (ethanol) 5°C below the freezing point; so for this solution this equipment could not reach the temperature needed to form crystals.

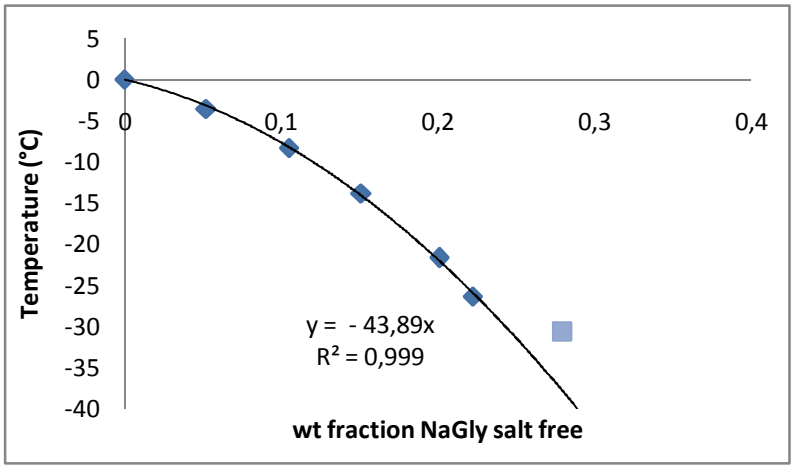

Figure 31. Measured temperature vs sodium glycinate mass fraction for the system sodium hydroxide-glycine-water (nNaOH:nGly 2:1).

For the 27.92 wt% NaGly the sample was not warmed up as all the sodium hydroxide and glycine were dissolved. As shown in Figure 31 the freezing point for the 27.92 wt% NaGly does not continue the trend of the other points; in order to continue the trend its freezing point had to be at approximately -35 °C. Another explanation is that this point is not part of the freezing curve but it is part of the solubility curve, so the eutectic point might be between 22.22 and 27.92 wt% NaGly. But as no other results were determined for the solubility curve of this system, we do not know whether it is a point on the freezing of the solubility curve.

9.3.1.4. Relation of moles of NaOH per moles of Glycine 1 to 5.

The analyzed sodium glycinate mass fractions are collected in Table 15. From 0.0658 NaGly mass fraction, points are located in the solubility curve.

Table 15. Measured temperatures and standard deviation for the system NaOH-Gly-water (nNaOH:nGly 1:5).

wt frac NaGly, salt free	m H_2O (g)	m Gly (g)	m NaOH (g)	Mean T (°C)	T Stddev (°C)
0.0000	9.000	0.000	0.000	0.1617	0.006
0.0142	9.004	0.505	0.054	-1.44	0.006
0.0276	9.035	1.001	0.106	-2.71	0.005
0.0409	9.031	1.502	0.160	-4.19	0.004
0.0524	9.015	1.952	0.208	-5.44	0.002
0.0598	9.019	2.221	0.239	-	-
0.0658	9.051	2.508	0.266	18.81	0.495
0.0757	9.019	2.903	0.309	28.15	0.323
0.0900	9.015	3.502	0.374	38.37	0.672
0.1079	9.019	4.307	0.460	52.36	0.451
0.1229	9.028	5.013	0.535	61.12	0.374
0.1449	9.019	6.101	0.650	-	-

As reported in Table 15 the freezing point for the 0.0598 sodium glycinate mass fraction was not determined; the measurements were hard to take, even if the solution was correctly dissolved at room temperature. This could be because this point is next to the eutectic point.

The standard deviations for the points which form the freezing curve are lower than 0.006°C and the ones that form the solubility curve are up to 0.3°C as can be seen in Table 15. Results are plotted in Figure 32.

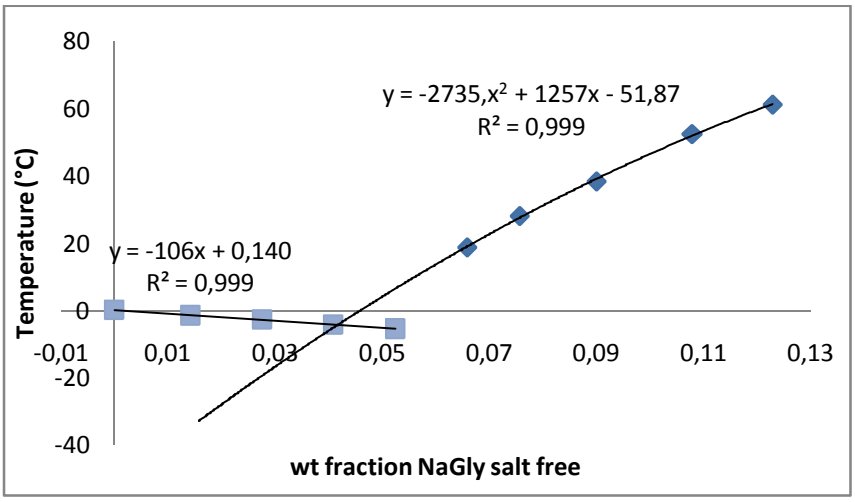

Figure 32. Temperature vs wt fraction of sodium glycinate in the system NaOH-Gly-H_2O in nNaOH:nGly relation 1:5, considering the 5.24 wt% NaGly part of the freezing curve.

As shown in Figure 32, two different tendencies are followed: for the freezing curve the tendency is linear, while for the solubility curve the tendency is polynomial. Moreover, it can be also seen that the

intersection between both curves is placed near the 4.09 wt% NaGly (supposed to be the eutectic point), which means that the point for the 5.24 wt% NaGly may be a metastable point.

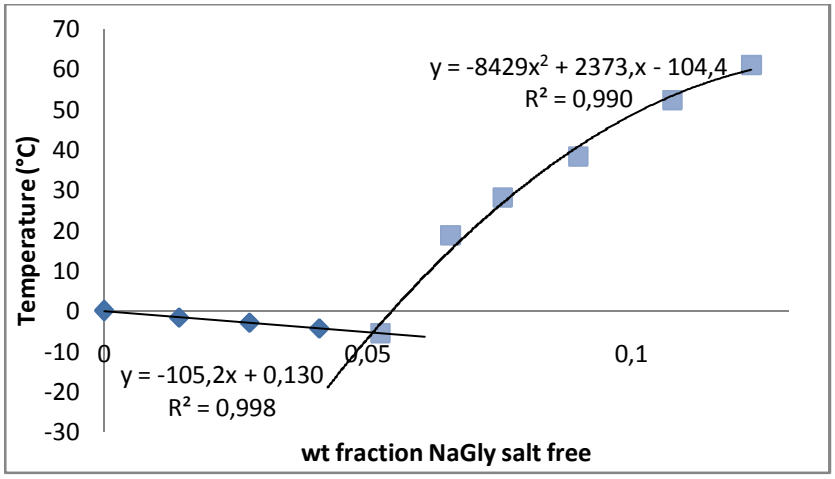

Figure 33. Temperature vs wt fraction of sodium glycinate in the system sodium hydroxide-glycine-water in molal relation 1:5, considering the 5.24 wt% NaGly part of the solubility curve.

If the 5.24 wt% NaGly point is considered as part of the solubility curve (Figure 33), not as the experiments suggested because the sample did not need to be heated, then the intersection of both curves (the eutectic point) seems to be placed near the 5 wt% NaGly. As the experiments with mass fractions between 0.05 and 0.06 NaGly mass fraction were difficult to analyzed, it can be concluded that the eutectic point is in the 0.04-0.05 sodium glycinate mass fractions range.

9.3.1.5. Relation of moles of NaOH per moles of Glycine 5 to 1.

With this system it was tried to determine the influence of a very big excess of sodium hydroxide (five moles of sodium hydroxide per mole of glycine) in the sodium hydroxide-glycine-water system. Different mass fractions were analyzed, and the results for their freezing points are shown in Table 16. From 0.1029 NaGly mass fraction solutions were heated in order to dissolve all the sodium hydroxide and glycine of the samples.

Table 16. Mass fractions of sodium glycinate for the system sodium hydroxide-glycine-water (NaOH:Gly 5:1).

wt frac NaGly, salt free	m H_2O (g)	m Gly (g)	m NaOH (g)	Mean T (°C)	T Stddev (°C)
0.0000	9.000	0.000	0.000	0.138	0.008
0.0149	9.019	0.106	0.276	-2.60	0.006
0.0256	9.053	0.185	0.402	-3.74	0.001
0.0349	9.015	0.254	0.667	-6.39	0.003
0.0413	9.031	0.304	0.802	-8.01	0.008
0.0519	9.017	0.386	0.987	-9.08	0.005
0.0608	9.021	0.457	1.197	-13.03	0.008
0.0720	9.009	0.549	1.438	-16.76	0.017
0.0789	9.018	0.607	1.612	-19.72	0.043
0.0909	9.039	0.712	1.894	-24.51	0.056
0.1029	9.084	0.824	2.136	-17.65	0.085

0.1226	9.052	1.005	2.667	-	-
0.1512	9.007	1.283	3.428	-	-
0.2025	9.063	1.868	4.890	-	-
0.2519	9.030	2.510	6.679	-	-

As shown in Table 16 NaGly mass fractions have very low values, and the standard deviations for the freezing points are low too (standard deviations lower than 0.05°C), so the measurements were carried out with acceptable accuracy. For the solubility points, only one point was determined, and its standard deviation (0.085°C) is higher than standard deviations for the freezing points. For the 0.1029 NaGly mass fraction crystals were formed at approximately -25°C. Four more mass fractions up to 10 wt% NaGly were prepared, but these samples could not be dissolved as they were very viscous, like gelatin.

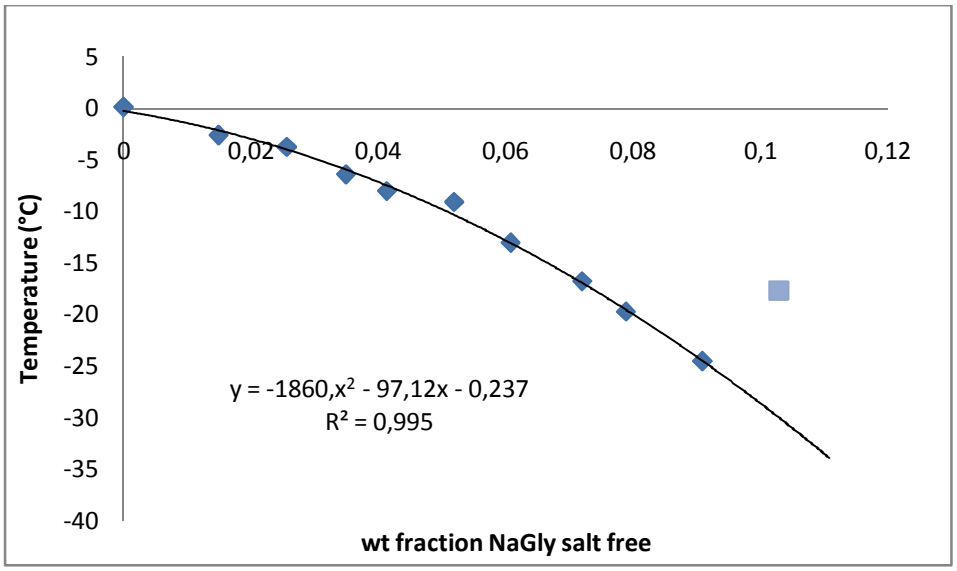

Figure 34. Freezing point for the different mass fraction in the system sodium hydroxide-glycine-water with the nNaOH: nGly relation 5:1.

Figure 34 shows the tendency of the freezing points for the analyzed system. As shown in the figure, the temperature for the sodium glycinate mass fraction 0.0519 did not follow the curve tendency; this could happen because the measurements were not taken very accurately. The 10.29 wt% NaGly temperature was supposed to form part of the solubility curve as it was determined by heating the solution. In case this point forms part of the freezing curve, its freezing temperature should be of approximately -30 °C.

As no results were obtained for the mass fractions above 10 wt% NaGly, no information is available for the solubility curve, so we cannot conclude anything about the solubility curve or the point which sodium glycinate mass fraction is 0.1029.

9.3.1.6. Comparison between all the NaOH-Gly-H_2O systems.

This section wants to recollect all the data for the sodium hydroxide-glycine-water system in order to compare all the measurements and the obtained results. In this section all the results were compared with the n_{NaOH}/n_{Gly} relation 1 to 1.

Figure 35 shows the comparison between the n_{NaOH}:n_{Gly} relation 1:1 and the n_{NaOH}:n_{Gly} relation with an excess of sodium hydroxide. For both cases in which there was an excess of sodium hydroxide (n_{NaOH}:n_{Gly}

2:1 and 5:1) I could not determine the solubility curve. The reason being at higher mass fractions the solutions were very viscous, for some of them even the stirring was almost impossible. Furthermore, only one point which could be determined on the solubility curve.

Conclusively the more sodium hydroxide is added, the more compressed in concentration the freezing curve becomes and the lower the mass fraction is on average. The freezing point decreases on adding NaOH.

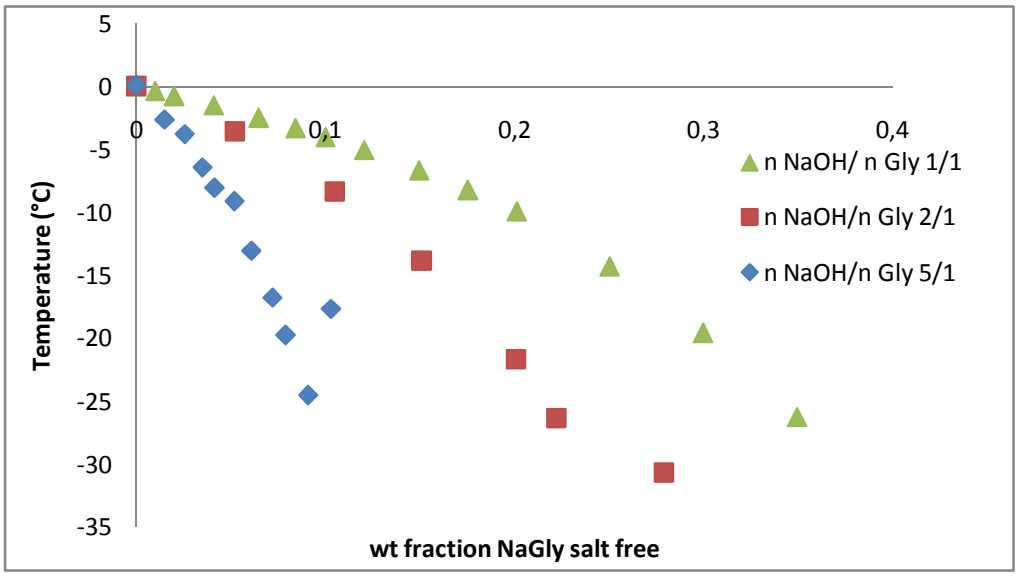

Figure 35. Comparison between the excess of sodium hydroxide systems (2:1 and 5:1) and the former case.

When reducing the sodium hydroxide, the curve also becomes compressed (Figure 36) similar to results of Figure 35. The freezing point also decreases by having a reduced amount of sodium hydroxide.

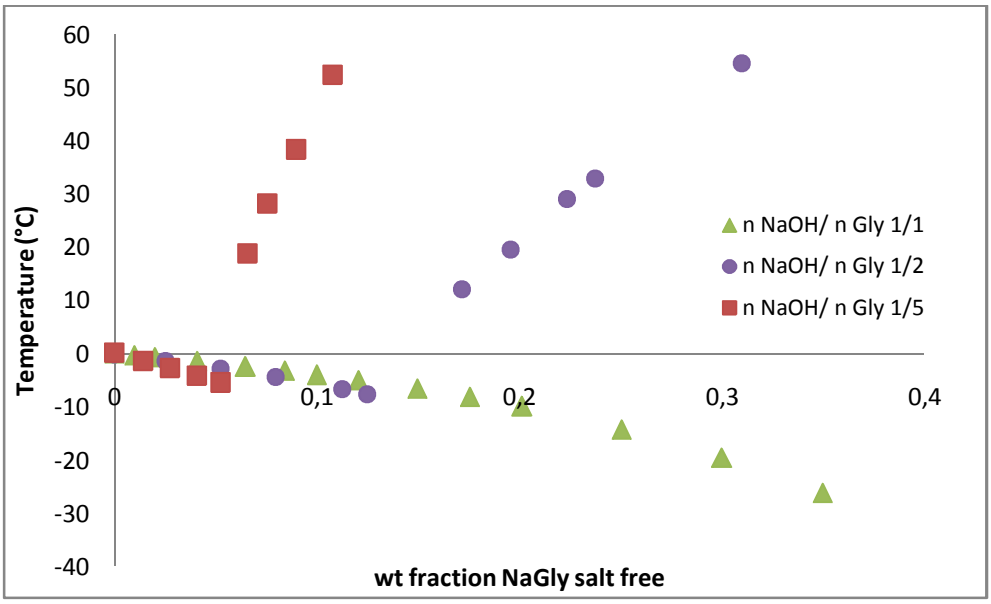

Figure 36. Comparison between the default of sodium hydroxide systems (1:2 and 1:5) and the former case.

Comparing the 1:1 n_{NaOH}:n_{Gly} relation with the 1:2 and 1:5 relation the difference is very big as for the 15 wt% NaGly the tendency of the curve is very different.

In order to compare all the systems, Figure 37 shows all the results obtained for all the experiments.

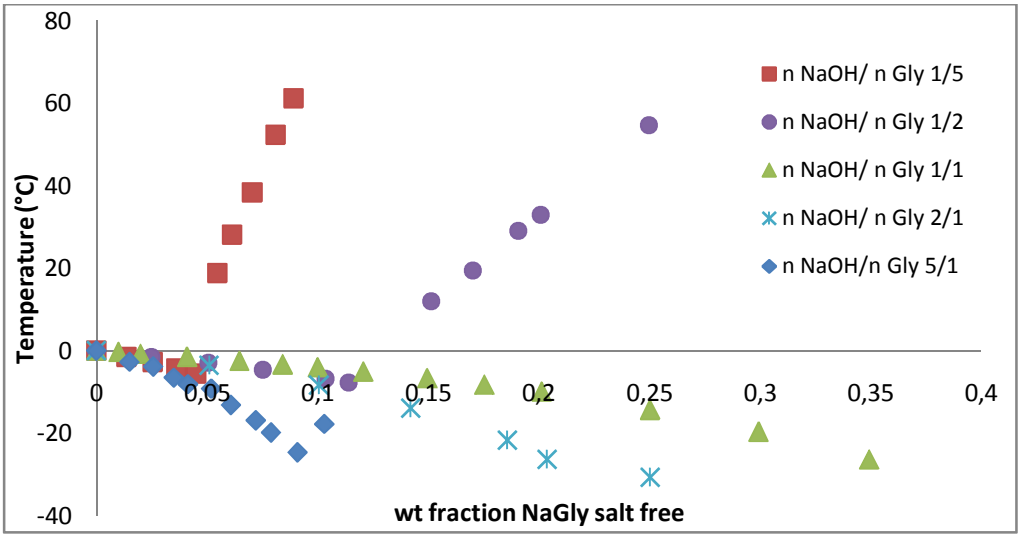

Figure 37. Freezing points for all the sodium hydroxide-glycine-water systems.

For the case which has the 1 to 1 n_{NaOH}:n_{Gly} relation, where sodium hydroxide and glycine were mixed as one mole of sodium hydroxide per mole of glycine (n_{NaOH}:n_{Gly} 1:1), the freezing curve contains mass fractions from 0 to 0.35.

For low mass fractions (below 5 wt% NaGly) the freezing points determined for all the measurements were very similar. Figure 35 shows that for the n_{NaOH}:n_{Gly} relation 2:1 and 5:1 freezing points differed from the n_{NaOH}:n_{Gly} relation 1:1. But in Figure 36 (n_{NaOH}:n_{Gly} relations 1:1, 1:2 and 1:5) the freezing points were quite the same. When bigger NaGly mass fractions were analyzed the behavior of the curve was completely different; this is due to molecular interaction and non-ideality of the liquid phases.

The more excess of both sodium hydroxide and glycine was considered the lower freezing points were obtained.

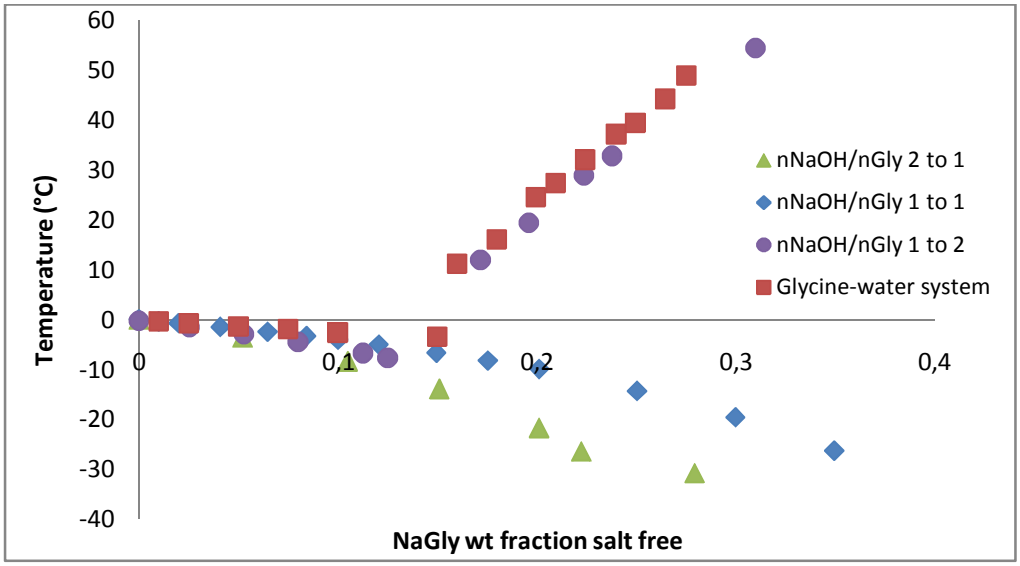

Figure 38. Comparison between the simple system glycine-water and the system sodium hydroxide-glycine-water in different nNaOH/nGly ratios.

Figure 38 shows the comparison between the glycine-water system and the systems in which sodium hydroxide was added for different n_{NaOH}:n_{Gly} ratios. For low mass fractions, comparing the glycine-water system with the n_{NaOH}:n_{Gly} relations, freezing temperatures have similar values, but when mass fractions are higher the systems have different behaviors.

If the 1:1 n_{NaOH}:n_{Gly} relation is compared with the glycine-water system, the tendency is the same from 0 to 0.15 NaGly mass fractions, but from 15 wt% NaGly the tendency is different. Comparing the glycine-water system with the n_{NaOH}:n_{Gly} relation 2:1, from 0.05 NaGly mass fraction the curve is different; as more excess of sodium hydroxide is considered freezing points are lower. Instead comparing the 1:2 n_{NaOH}:n_{Gly} relation with the glycine-water system it can be seen that both curves have the same tendency.

9.3.2. Sodium bicarbonate-glycine-water system ($NaHCO_3$-Gly-H_2O).

In order to study the effect of carbon dioxide on the system, sodium bicarbonate-glycine-water was studied. As a result of the sodium bicarbonate and glycine reaction more water was formed in addition to the water added to the experiment, as shown in equation (9.5).

$$NaHCO_3 + Gly \xrightarrow[H_2O]{} NaGly + CO_2 + H_2O \quad (9.5)$$

Two cases had been under investigation: one mole of sodium bicarbonate per mole of glycine (n_{NaHCO3}:n_{Gly} relation 1:1) and n_{NaHCO3}:n_{Gly} relation 3:1 (excess of sodium bicarbonate or glycine default). For every case pure water was analyzed in order to guarantee the calibration.

9.3.2.1. Relation of moles of $NaHCO_3$ per moles of Glycine 1 to 1.

In this section a stoichiometric moles relation between sodium bicarbonate and glycine was under study; notice that a 1:1 $NaHCO_3$:Gly relation gives a CO_2 loading of 1 mole CO_2/mole Gly. In this case, the same amount of moles both sodium bicarbonate and glycine was added. After making, preparing, and stirring the solutions they were analyzed in the setup. As expected, if the amount of sodium bicarbonate was increased the amount of carbon dioxide increased too. The analyzed concentrations, temperature, and temperature standard deviations can be seen in Table 17. From 13.8 wt% NaGly not all sodium bicarbonate and glycine were dissolved, so warming the samples was needed.

Table 17. Temperature and standard deviation for the system sodium bicarbonate-glycine-water ($nNaHCO_3$:nGly 1:1).

wt frac NaGly, salt free	m H_2O (g)	m Gly (g)	m $NaHCO_3$ (g)	Mean T (°C)	T Stddev (°C)
0	9.000	0.000	0.000	-0.0064	0.015
0.0099	9.037	0.070	0.078	-0.51	0.005
0.0196	9.017	0.142	0.157	-0.98	0.021
0.0410	9.051	0.302	0.338	-1.96	0.052
0.0624	9.011	0.473	0.526	-2.96	0.002
0.0837	9.042	0.650	0.728	-3.81	0.006
0.1054	9.021	0.841	0.940	-4.71	0.006
0.1163	9.012	0.944	1.053	-5.17	0.004
0.1378	9.030	1.152	1.288	-5.61	0.080
0.1731	9.030	1.529	1.702	-7.17	0.051
0.2835	9.084	3.001	3.358	-	-
0.3745	9.021	4.723	5.260	-	-

Standard deviations have very low values, so a good repeatability, often better than 0.05°C, was obtained. This means that the measurements were carried out very accurately.

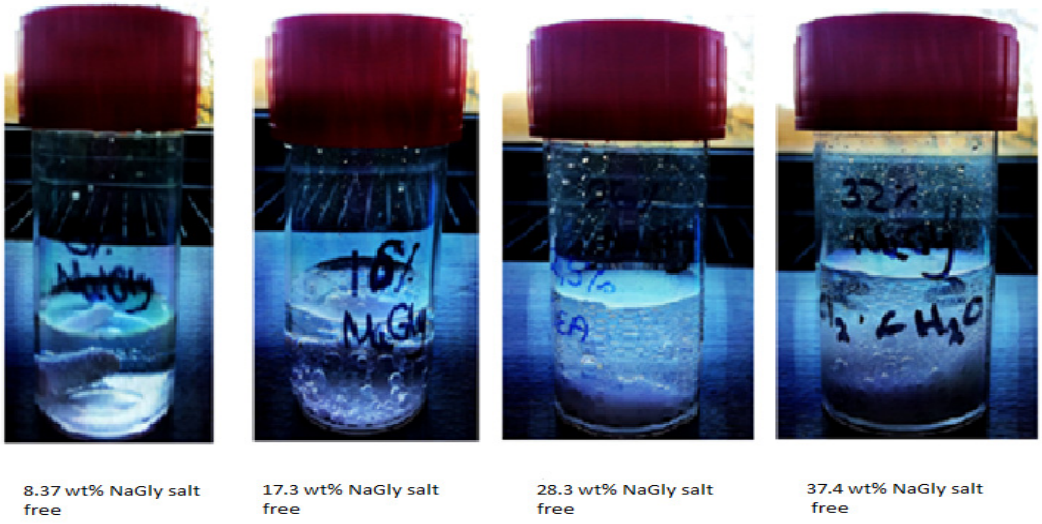

Figure 39. Different samples of the mixture of sodium bicarbonate and glycine (nNaHCO3:nGly 1:1).

Figure 39 shows the different appearance of the solutions when varying the NaGly wt%. Colours have been changed to improve clarity. The main difference between 8.37 wt% NaGly and the rest of the solutions was that bubbles appeared due to the carbon dioxide formation. Furthermore, water was also formed due to reaction, so the solution had more water than the one that was added; the extra water adds up, but the salt in the solutions also makes the liquid expand. This can be seen in Figure 39 comparing the 8.37 NaGly wt% and the 37.4 NaGly wt% solutions.

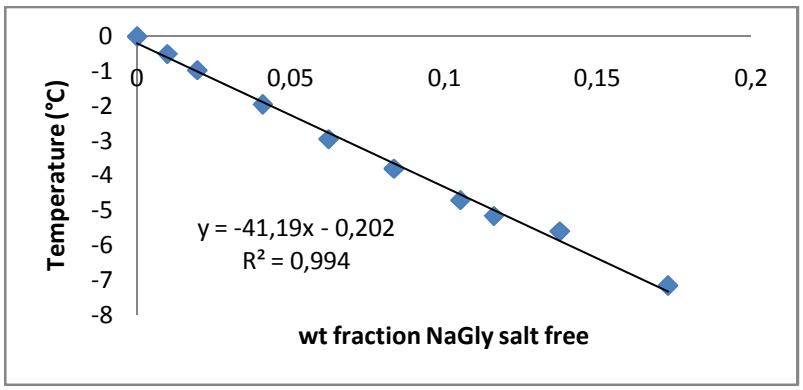

Figure 40. Temperature versus wt fraction of sodium glycinate (nNaHCO3:nGly 1:1).

Temperatures for both sodium glycinate mass fractions 0.1378 and 0.1731 were expected to be in the solubility curve as no heating was needed before the measurement, but as Figure 40 shows, these temperatures were lower than the previous ones. Maybe the problem was that when heating the sample, not all the precipitates were dissolved, so when the solutions were analyzed the measured temperatures were not the correct, so these data could be wrong. It also could be that these points were metastable

points. When adding CO_2 to the system, you can expect the curve to look differently and they should not be strictly comparable to the NaOH-Gly system.

It also has to be taken into account that if we warm too much the samples in order to dissolve all the sodium bicarbonate and the glycine, carbon dioxide may escape to the atmosphere. These samples were heated too much during mixing, that's why the points which have a higher NaGly mass fraction are not represented in Figure 40.

9. 3.2.2. Relation of moles of $NaHCO_3$ per moles of Glycine 3 to 1.

Due to the excess of sodium bicarbonate, more CO_2 was formed. Sodium glycinate mass fractions between 0 and 0.2221 were analyzed. After preparing the solutions, from 0.1279 NaGly mass fraction even if the samples were heated the sodium bicarbonate and the glycine were not dissolved. Figure 41 shows the main difference between low (0.0562) and high (0.2221) NaGly mass fractions, as it can be seen that a lot of sodium bicarbonate and glycine were not dissolved in the bottom of the sample glass. Besides, more bubbles were formed as the wt% NaGly increased.

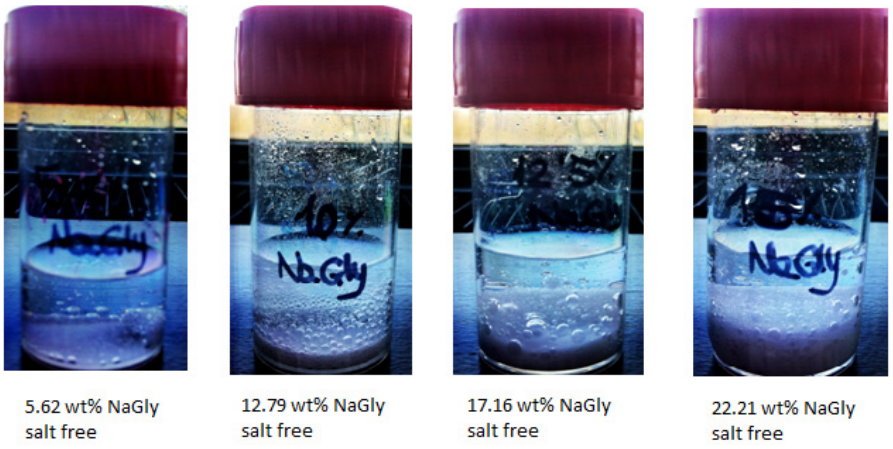

Figure 41. Sodium glycinate samples for each concentration ($nNaHCO_3$:nGly 3:1).

In order to determine more freezing points for other NaGly mass fractions, small amounts of sodium bicarbonate and glycine were used. Table 18 shows all the weights and temperatures obtained during the measurements. From 0.0451 NaGly mass fraction heat is applied in order to dissolve all the sodium bicarbonate and the glycine in the solution.

Table 18. Measured temperature and standard deviation for the system sodium bicarbonate-glycine-water (3:1).

wt frac NaGly, salt free	m H_2O (g)	m Gly (g)	m $NaHCO_3$ (g)	Mean T (°C)	T Stddev (°C)
0.0000	9.000	0.000	0.000	-0.006	0.016
0.0113	9.033	0.080	0.269	-1.24	0.004
0.0142	9.017	0.100	0.337	-1.55	0.006
0.0211	9.021	0.151	0.503	-2.19	0.039
0.0339	9.043	0.247	0.805	-3.34	0.005
0.0451	9.001	0.332	1.109	-3.25	0.064
0.0562	9.032	0.421	1.411	-4.68	0.039
0.0697	9.032	0.531	1.779	-	-

0,1279	9.009	1.051	3.525	-	-
0,1716	9.012	1.502	5.038	-	-
0.2221	9.015	2.103	7.050	-	-

Standard deviations are low down to 0.04°C were obtained for the freezing points; in the case of the solubility points standard deviations have higher values (0.06°C), but this values are not very big (lower than 0.1°C). So the measurements were carried out with a good accuracy.

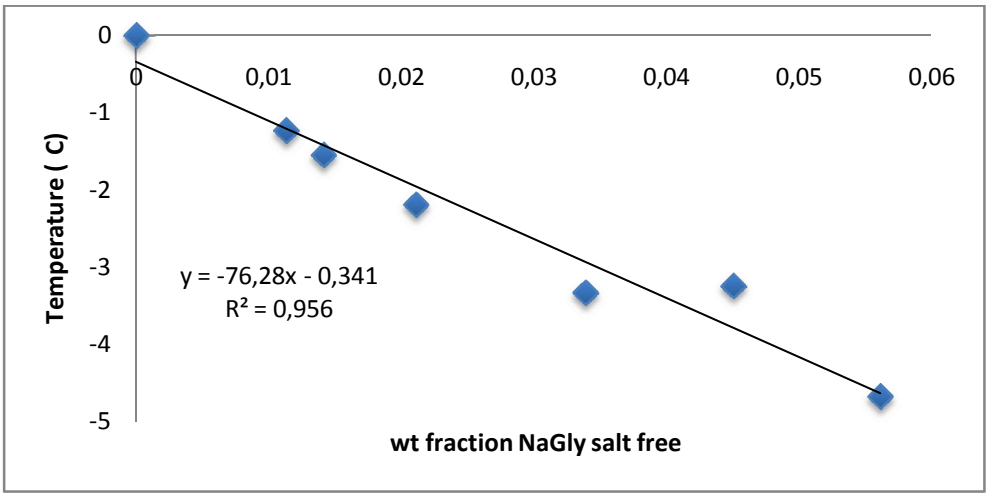

Figure 42. Temperature versus wt% sodium glycinate for the molal relation NaHCO3:Gly 3:1.

Figure 42 shows the trendline for the data. For both 4.51 and 5.62 wt% NaGly freezing points were determined. The deviation of these points from the trendline is observed due to heating and this caused CO_2 evaporation.

9.3.3. Sodium bicarbonate-sodium hydroxide-glycine-water system. ($NaHCO_3$-NaOH-Gly-H_2O)

The system formed by sodium bicarbonate, sodium hydroxide, glycine and water was under investigation. In these cases the relation between moles of sodium bicarbonate and sodium hydroxide and moles of glycine was set constant during the preparation of the experiments: one mole of sodium bicarbonate and sodium hydroxide per mole of glycine (Na:Gly relation 1:1).

The only difference between the three cases was the carbon dioxide loading. The loading was defined as moles of CO_2 per moles of sodium glycinate. Measurements were carried out for three different loadings: 0.1, 0.25 and 0.5. In the previous section (9.3.2.1) 1 loading by sodium bicarbonate was analyzed, so it is also possible to compare this loading with the systems explained below. Water was analyzed for all the systems in order to know its freezing point and taking it into account while plotting the phase diagrams.

9.3.3.1. CO_2 loading: 0.1.

Different sodium glycinate mass fractions between 0 and 0.51 were analyzed in order to determine the freezing and the solubility curves; these results were collected in Table 19. From 0.2691 NaGly mass fraction solutions were warmed in order to dissolve all the sodium bicarbonate, sodium hydroxide and glycine of the sample. Crystals were amorphous for the freezing points and white for the solubility points.

Table 19. Temperature and standard deviation for the 0.1 loading of the system $NaHCO_3$-NaOH-Gly-H_2O.

wt frac NaGly, salt free	m H_2O (g)	m Gly (g)	m $NaHCO_3$ (g)	m NaOH (g)	Mean T (°C)	T Stddev (°C)
0.0000	9.000	0.000	0.000	0.000	0.073	0.003
0.0100	9.021	0.071	0.008	0.035	-0.26	0.008
0.0506	9.019	0.375	0.041	0.177	-1.71	0.005
0.1016	9.033	0.807	0.093	0.387	-3.87	0.019
0.1539	9.034	1.316	0.146	0.619	-6.42	0.002
0.2050	9.004	1.886	0.219	0.886	-9.80	0.020
0.2532	9.023	2.525	0.284	1.209	-13.57	0.049
0.2691	9.025	2.759	0.310	1.320	3.94	0.222
0.2867	9.022	3.031	0.332	1.435	4.54	0.325
0.3045	9.015	3.322	0.373	1.593	5.75	0.274
0.3273	9.019	3.732	0.414	1.777	6.85	0.127
0.3567	9.002	4.304	0.487	2.062	6.37	0.166
0.3809	9.032	4.854	0.547	2.329	8.91	0.161
0.4081	9.009	5.510	0.618	2.637	10.52	0.371
0.4570	4.019	3.101	0.349	1.491	11.30	0.551
0.5087	4.035	4.001	0.449	1.916	-	-

Standard deviations below 0.05 °C were obtained for the measurements with lower amine concentration, but when the NaGly concentration increases, standard deviations are higher. This can be caused by an increase of the viscosity of the solutions, so the mixing of the sample is less efficient.

I tried to analyze the 50.87 wt% NaGly, but once the solution was dissolved, it was very difficult to determine the freezing point. Besides, the solutions had a viscous aspect. For the 0.2050 mass fraction I warmed the sample in order to see if the crystals were the same at -9.8 °C and at 0 °C, but at -9 °C there were no crystals, so at 0°C no crystals were in the sample.

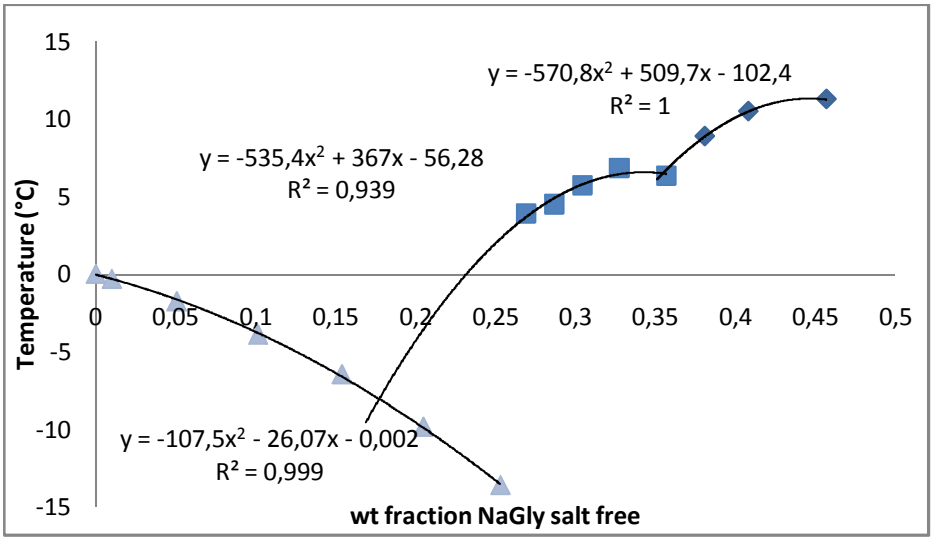

Figure 43. Measured temperature versus mass fraction for the 0.1 loading of the system $NaHCO_3$-NaOH-Gly-H_2O.

Figure 43 represents all the temperatures determined in the laboratory for this loading and system. According to the trendlines in Figure 43 the eutectic point is placed in the 19.28 wt% NaGly. This figure is different from the previous ones; the temperature for the 35.67 wt% NaGly solution was lower than the temperature of the previous point, which makes the curve seem to have a strange gap. This might be because two different compounds (hydrates of sodium glycinate) which formed.

To determine the nature of the crystals in the 0.2691-0.457 NaGly mass fraction range, two samples (30 and 38 wt% NaGly, one for each side of the gap) were taken to the X-Ray machine in order to analyze them and to obtain diffractograms which gives the information to determine the substance of the sample. In order to analyze the samples in the X-Ray equipment, crystals must be formed. Filtering the crystals and obtaining powder was necessary. After analyzing the powder for both solutions in the X-Ray equipment the analyses showed that both solutions had the same substance: gamma-glycine, so the 'bump' of the curve is not due to a crystal change. If the 35.67 wt% NaGly measure is not taken into account, the curve looks as in Figure 44. In this case the eutectic point seems to be near the 13.86 wt% NaGly.

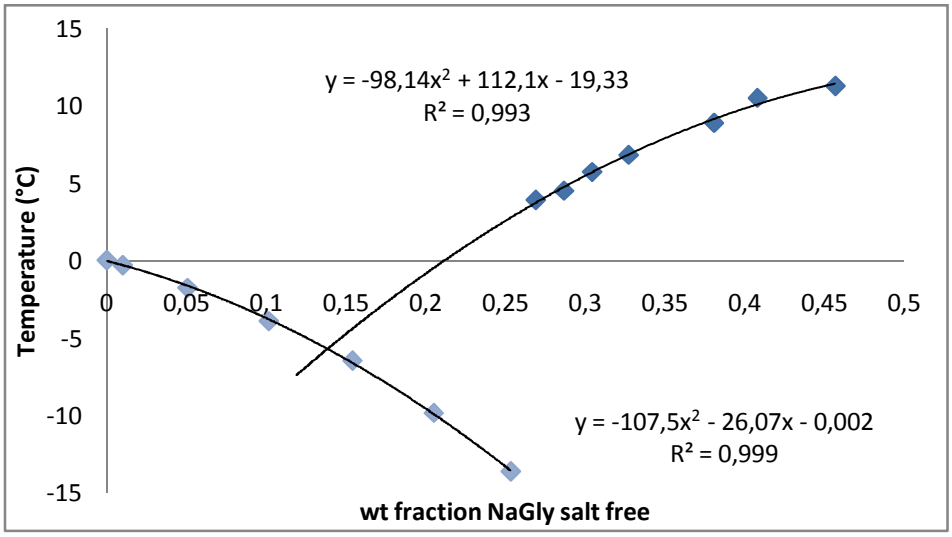

Figure 44. Trendlines for both freezing and solubility curves if the 35.67 wt% NaGly measure is not taken into account.

In order to determine how much water was in the solutions at high NaGly mass fraction, the 0.30 and 0.38 NaGly mass fractions were analyzed by filtering the crystals and evaporating the water in a vacuum oven at 110 °C. It was important to cover the samples with a filtrating paper in order not to waste the crystals when evaporating the water. Three weights were needed to be done: the sample glass and the sample glass with the crystals before and after the evaporation. Table 20 indicates the samples weights for the three systems, and the amount of water that was supposed to be in the solutions when crystals were formed.

Table 20. Samples weights and relation between the molecules of water and the molecules of sodium glycinate.

wt% NaGly	sample Glass (g)	sample Glass + crystals (g)		molecules of H_2O per molecules of NaGly
		before evaporation	*after evaporation*	
30	7.816	8.353	7.9059	26.814
38	7.8313	9.2478	8.3044	10.751

Some assumptions were taken into account. First of all, it was assumed that only water evaporates, which could be wrong as carbon dioxide may be present in the solution, but it was not possible to determine if there was some. Finally, it was assumed that all the remains were sodium glycinate. Under these assumptions, the ratio between molecules of water and molecules of sodium glycinate was calculated. As shown in Table 20, the amount of water for the first mass fraction was very high compared with the one for the second fraction.

9.3.3.2. CO_2 loading: 0.25.

Different mass fractions were analyzed to determine their freezing points, and Table 21 contains all the information. From 0.2571 NaGly mass fraction solutions were needed to be warmed up to dissolve all the precipitates not dissolved. Two different types of crystals could be seen: amorphous crystals (from 0.0499 to 0.2571 NaGly mass fraction) and white crystals (from 0.2685 to 0.3905 NaGly mass fractions).

Table 21. Measured temperature and standard deviation for the solutions prepared for the sodium bicarbonate 0.25 loading.

wt frac NaGly, salt free	m H_2O (g)	m Gly (g)	m $NaHCO_3$ (g)	m NaOH (g)	Mean T (°C)	T Stddev (°C)
0.0000	9.000	0.000	0.000	0.000	0.112	0.030
0.0499	9.028	0.371	0.108	0.149	-1.74	0.002
0.1015	9.019	0.805	0.224	0.319	-3.86	0.016
0.1528	9.013	1.301	0.372	0.520	-6.21	0.006
0.2077	9.013	1.921	0.532	0.760	-9.33	0.017
0.2571	4.020	1.150	0.327	0.456	-13.04	0.022
0.2654	4.009	1.201	0.333	0.472	5.14	0.426
0.2685	4.013	1.223	0.342	0.488	5.41	0.498
0.2844	4.044	1.343	0.377	0.534	7.49	0.411
0.3112	4.080	1.557	0.448	0.625	8.90	0.284
0.3323	4.020	1.705	0.476	0.676	8.52	0.322
0.3492	4.008	1.848	0.515	0.735	7.83	0.513
0.3653	4.020	2.004	0.558	0.800	5.49	0.428
0.3774	4.079	2.155	0.602	0.859	-4.41	0.474
0.3905	4.455	2.507	0.700	0.999	7.65	0.455
0.4197	4.028	2.603	0.744	1.033	-	-
0.4489	4.041	3.000	0.842	1.198	-	-
0.4673	4.147	3.361	0.973	1.342	-	-

When the chemicals were not all dissolved the standard deviation increased (as shown in Table 21); for the freezing points standard deviations have values lower than 0.03°C, and standard deviations up to 0.3°C were observed for the solubility points. Moreover, I tried to measure the 0.4197 NaGly mass fraction but after dissolving all the sodium bicarbonate, sodium hydroxide and glycine at -28°C the temperature of the sample stopped increasing because the cooling bath could not reach lower temperatures than -33°C, so I could not determine its freezing point. Furthermore, the solution was very viscous. On the other hand, the 44.89 wt% NaGly sample was not completely dissolved, end even if a lot of energy was applied the solution still remained not dissolved.

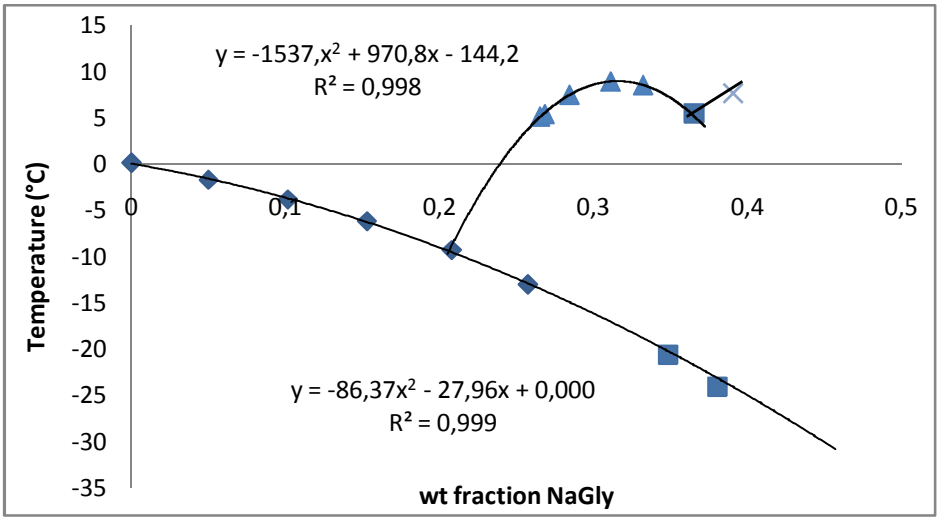

Figure 45. First curve obtained for the system $NaHCO_3$-NaOH-Gly-H_2O (load:0.25).

Figure 45 shows the first temperature values obtained to compose the curve. The strange fact is that points 33.22 and 36.53 wt% NaGly had low temperatures, when they are supposed to have positive temperatures. The explanation for these cases is that ice is precipitating instead of the crystal. So these points are metastable, which indicates that in principle it should not precipitate, but the driving force for precipitating the other component is not big enough. It can also be that not all the precipitate was dissolved before analyzing the freezing point, so the measures were not correctly taken. According to the trendlines plotted in Figure 45 and the equation of the intersection, the eutectic point is the 20.63 wt% NaGly.

The samples for the 33.61 and 36.21 wt% NaGly were repeated, and different freezing points were obtained, so now the curve had a different shape as plotted in Figure 46.

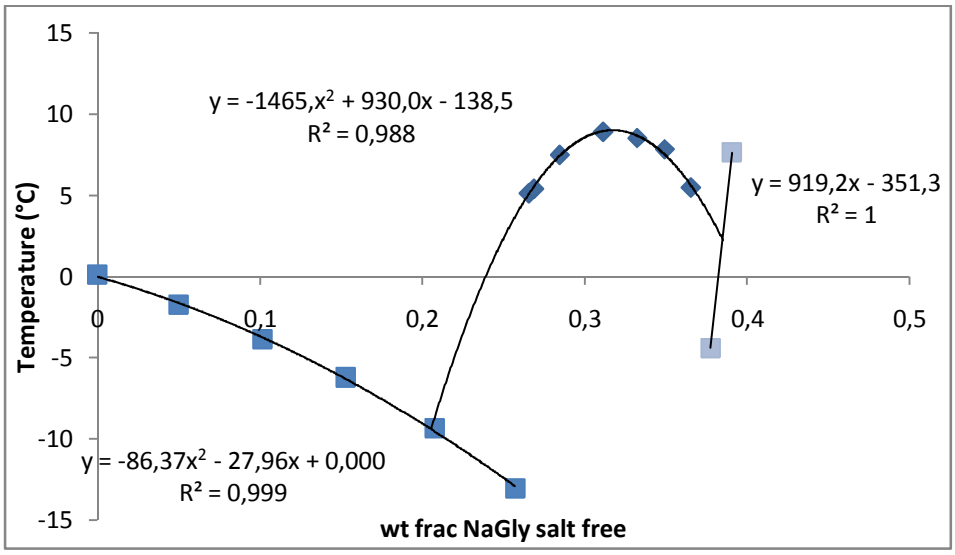

Figure 46. Temperature vs mass fraction NaGly for the system $NaHCO_3$-NaOH-Gly-H_2O (load:0.25).

As shown in Figure 46, the eutectic point seems to be the same as for the Figure 45, but calculating it as the intersection of the trendlines the mass fraction is 0.2053 NaGly mass fraction (very similar at the previous one). So the 25.71 wt% NaGly is a metastable point. But again, something strange happens for the

point 37.74 wt% NaGly; its freezing point is negative, when the trendline situate it at a positive temperature. All the trendlines are polynomial, except for the one that joins the two last points.

The same X-Ray experiments as for the CO_2 loading 0.1 were needed to be done in order to determine the substance at high NaGly mass fractions. Two NaGly mass fractions for both sides of the gap (30 and 39.05 wt% NaGly) had to be analyzed, but in this case there was a problem: the temperatures at which crystals disappeared were lower than room temperature (5-10°C). As the measurements for the X-Ray equipment were done at room temperature and there was no possibility to analyze samples at lower temperatures, the solutions could not be analyzed. The observed melting point at 5-10°C indicates that this could be a hydrate of some sort. It could be a good idea to further investigate this in the future.

9.3.3.3. CO_2 loading: 0.5.

Table 22 collects the weightings, freezing points and temperature standard deviations for the sodium bicarbonate loading of 0.5. Above the 20.93 wt% NaGly the solution needed to be warmed up because not all the sodium bicarbonate, sodium hydroxide and glycine could dissolve a room temperature. Crystals were amorphous at low NaGly mass fractions (0.01-0.3355) and white for high NaGly mass fractions (0.3468-0.4371).

Table 22. Temperature and standard deviation for the sodium bicarbonate 0.5 loading.

wt frac NaGly, salt free	m H_2O (g)	m Gly (g)	m $NaHCO_3$ (g)	m NaOH (g)	Mean T (°C)	T Stddev (°C)
0.0000	9.000	0.000	0.000	0.000	0.150	0.010
0.0101	9.013	0.071	0.040	0.018	-0.28	0.006
0.0531	9.035	0.396	0.214	0.108	-1.77	0.005
0.1032	9.021	0.820	0.459	0.218	-3.55	0.002
0.1558	9.002	1.331	0.745	0.356	-5.66	0.004
0.2093	9.065	1.952	1.091	0.518	-7.86	0.081
0.2374	9.004	2.301	1.289	0.614	-9.45	0.144
0.2649	9.097	2.717	1.522	0.720	-12.02	0.089
0.2932	4.028	1.401	0.796	0.373	-13.61	0.122
0.3220	4.034	1.625	0.908	0.439	-16.22	0.266
0.3355	4.003	1.725	0.957	0.457	-16.64	0.119
0.3468	4.005	1.825	1.037	0.484	7.96	0.438
0.3664	4.007	2.008	1.120	0.530	14.10	0.650
0.3787	4.047	2.152	1.203	0.571	19.50	0.020
0.4371	4.069	2.856	1.617	0.762	-	-

Standard deviations lower than 0.01°C were obtained for the freezing points (low NaGly mass fractions). But for highly concentrated solutions standard deviations up to 0.02°C were observed. However it can be said that the measurements were taken very accurately as standard deviations did not have values up to 0.6°C.

I tried to measure the temperature for the 43.71 wt% NaGly, but I couldn't dissolve all the sodium bicarbonate, sodium hydroxide and glycine in the solution.

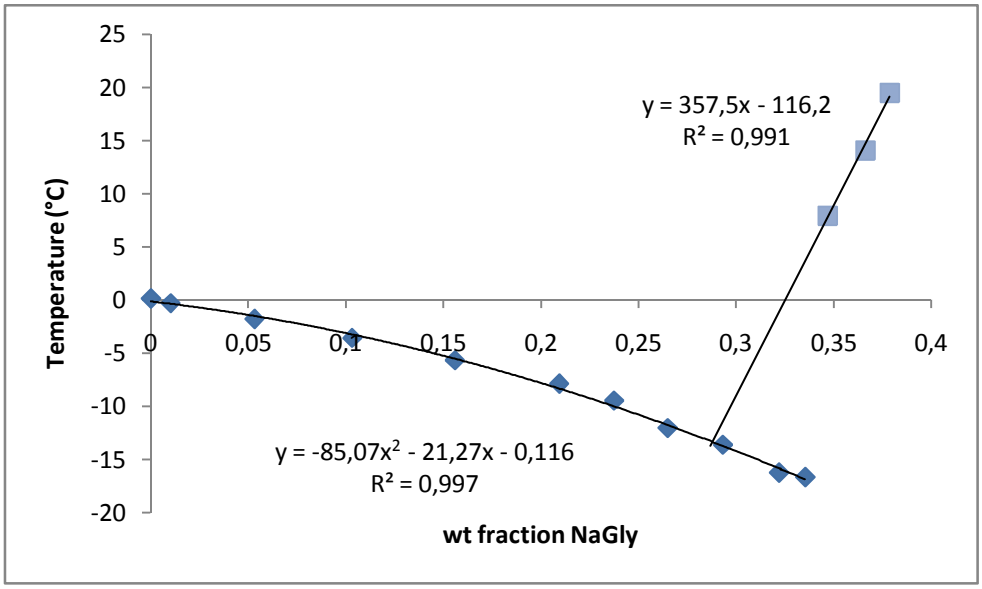

Figure 47. Temperature vs wt fraction NaGly for the sodium bicarbonate 0.5 loading.

The freezing curve tendency is polynomial, while the solubility curve tendency is linear. As shown in Figure 47 the intersection between both tendencies is placed near the 0.29 sodium glycinate mass fraction, so the eutectic point seems to be at 28.80 wt% NaGly. So the 29.32, 32.20 and 33.55 wt% NaGly points are metastable points as they have to belong to the solubility curve.

9.3.3.4. Comparison between all the $NaHCO_3$-NaOH-Gly-H2O systems.

In order to compare the results obtained in this section for the different CO_2 loadings, Figure 48 was plotted.

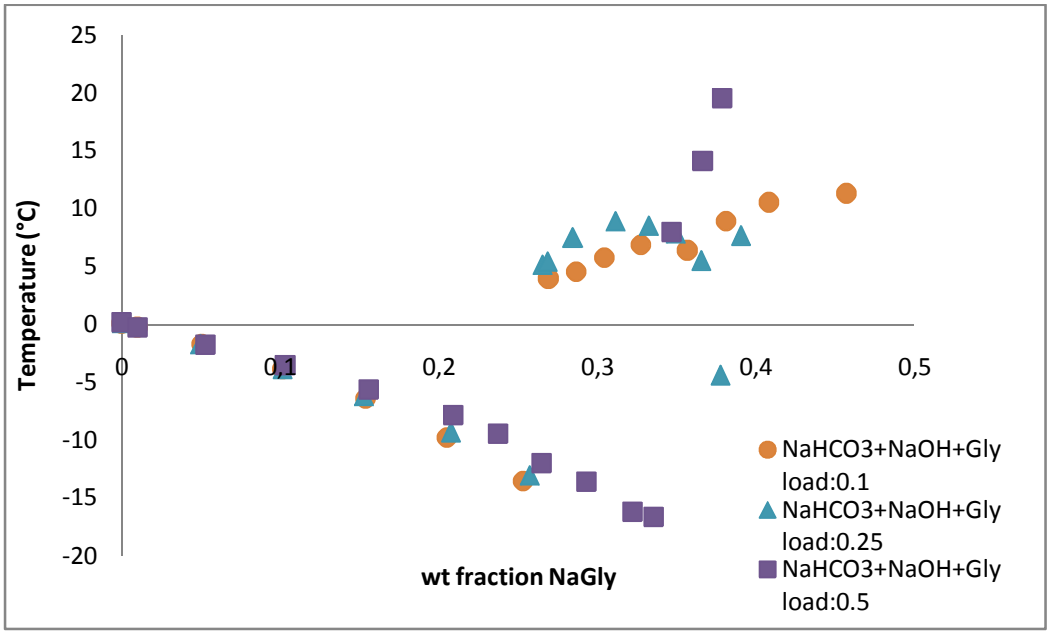

Figure 48. Temperature vs wt fraction NaGly for different $NaHCO_3$ loadings for the system $NaHCO_3$-NaOH-Gly-H_2O.

Figure 48 shows that at low NaGly mass fractions (0-0.25) all curves had the same tendency, besides for all the experiments the freezing point had the same values. But when the mass fraction is increased (from 0.25 to 0.5), the curves had different tendencies. However, the carbon dioxide loadings 0.1 and 0.25 had the same tendency, presenting a gap at approximately 35 wt% NaGly. But, as explained above, the same substance was obtained during the tests in the X-Ray equipment, so there may be no gap.

Figure 49 also considered the sodium hydroxide-glycine-water and the sodium bicarbonate-glycine-water systems, a part from the different CO_2 loadings.

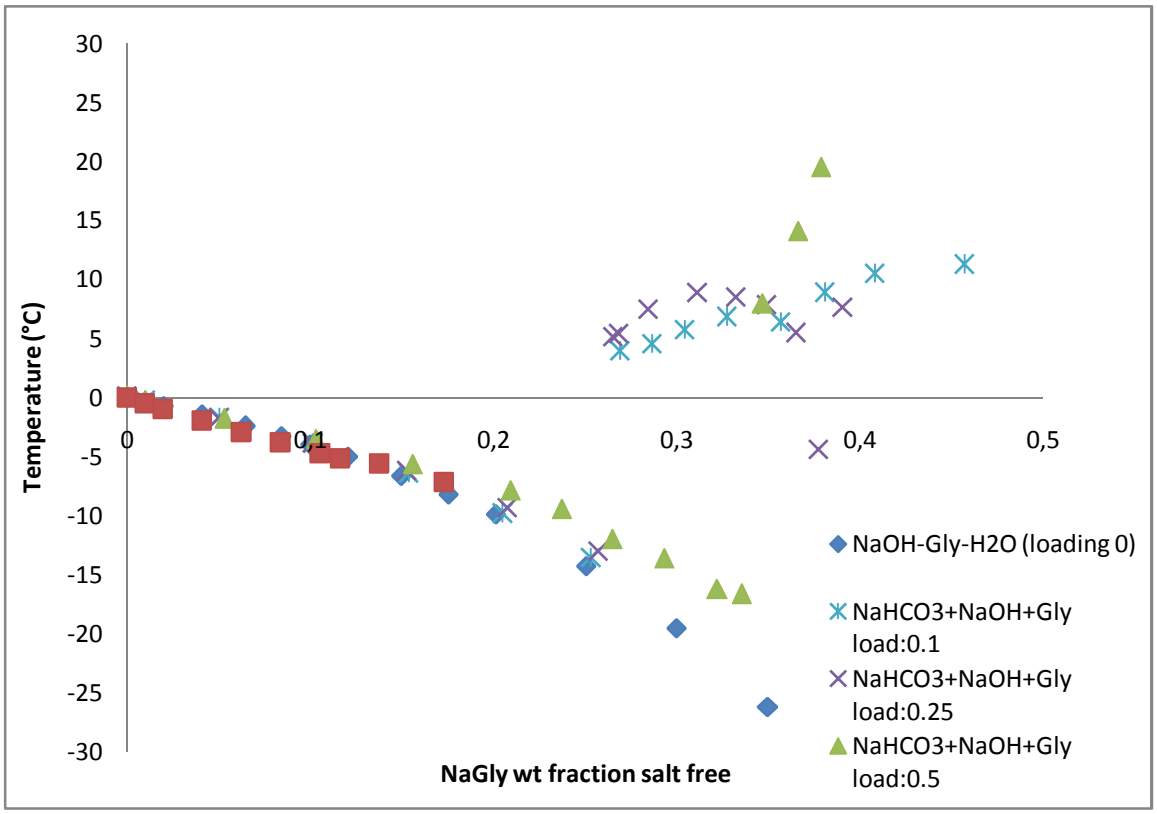

Figure 49. Comparison of the $NaHCO_3$-NaOH-Gly-H_2O system with the NaOH- Gly-H_2O system and the $NaHCO_3$-Gly-H_2O system.

The $NaHCO_3$-Gly-H_2O system represents the system with a loading of 1 mol CO_2/mol NaGly. Comparing this system with the three different loadings (0.1, 0.25 and 0.5), the freezing curve is the same for all the systems, but the solubility curve varies. As shown in Figure 49 at low NaGly mass fractions freezing points are similar; but from 0.2 NaGly mass fraction freezing points are different.

In order to know exactly the substance at high NaGly mass fractions, some solutions were prepared to be analyzed in the X-Ray equipment. Results are commented in section discussion and conclusions.

9.4. Potassium bicarbonate and potassium hydroxide systems.

9.4.1. The purity of the KOH chemical.

In this part of the study, potassium is used as the cation in the solutions. It is added to the liquids in terms of potassium hydroxide (KOH). The chemical supplier of DTU was unable to supply high purity KOH without absorbed water. The chemical purity need to be taken into account.

9.4.2. Titration.

Titration or titrimetry was used in order to calculate the concentration of the potassium hydroxide solution. Three compounds are needed for this volumetric analysis: the reagent (titrant or titrator), the analyte (titrand) and the indicator [71].

Different titration techniques exist, but in this report the important one was the acid-base titration. Two solutions were needed: an acid solution (standardized hydrochloric acid) and a base solution (the sample potassium hydroxide). As the potassium hydroxide is solid, it is needed to be dissolved into an aqueous solution. The concentration of the hydrochloric acid is known (0.1 M), the amount potassium hydroxide is also know, but concentration need to be determined.

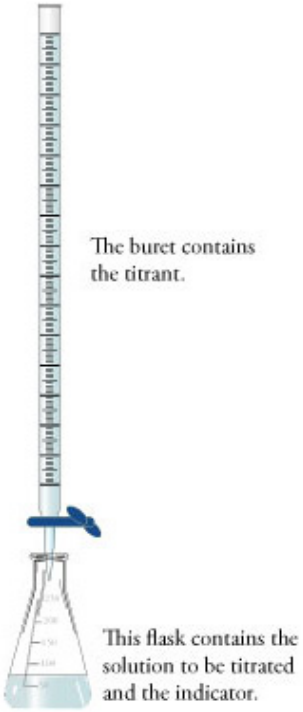

Figure 50. Setup for the titration. Source: [71].

As shown in Figure 50 the system is formed by two parts: a burette and an Erlenmeyer flask. Potassium hydroxide is under investigation in the Erlenmeyer flask, and the hydrochloric acid is in the burette. Furthermore, a small amount of indicator (phenolphthalein) is added in order to determine when the reaction is completed by changing color.

At the beginning, the solution in the Erlenmeyer flask is basic due to the hydroxide ions from the potassium hydroxide; as more hydrochloric acid is added, hydroxide ions react with the H_3O^+ ions, by the following reaction (equation (9.6)):

$$OH^-(aq) + H_3O^+(aq) \rightarrow H_2O\ (l) \quad (9.6)$$

When all the potassium hydroxide has reacted the solution pH becomes quickly neutral and acidic by and additional small amount hydrochloric acid. By this change the indicator changes color as function of the H_3O^+ ions.

Phenolphthalein molecules are colorless, but when a base is added its conjugated base colors the solution fuchsia. Initially, the solution had a fuchsia color due to the phenolphthalein, and as more acid is added, the solution turned to colorless.

9.4.3. KOH concentration.

First of all, the potassium hydroxide solution was weighted. The amount of equivalent used hydrochloric acid was determined by titration. All the results were collected in Table 23.

Table 23. Amount of potassium hydroxide and water weighted and volume of hydrochloric acid added during titration.

m KOH (g)	m H_2O (g)	Vol(mL) HCl added
0.4608	5.3071	70

By calculating the moles of potassium hydroxide (equation (9.7)) and hydrochloric acid ((equation (9.8)), and knowing that the relation between both is one, the purity of the potassium hydroxide was calculated as equation (9.9):

$$n_{KOH} = \frac{0.4608\ (g)}{56.11\left(\frac{g}{mole}\right)} = 0.00821\ moles\ of\ KOH \quad (9.7)$$

$$n_{HCl} = 0.07(L) \cdot 0.1\left({}^{mole}/_{L}\right) = 0.007\ moles\ of\ HCl \quad (9.8)$$

$$\%purity\ KOH = \frac{0.007}{0.00821} \cdot 100 = 85.24\ \% \quad (9.9)$$

The potassium hydroxide purity used in all the experiments is the one calculated above (85.24 wt% purity). As reported for the sodium system, for all the systems studied the freezing point of distilled water was obtained, and the method to determine the freezing point was reported in section 8. Experimental method.

9.4.4. Potassium hydroxide-glycine-water system (KOH-Gly-H_2O).

These systems were studied in order to analyze the pure CO_2 capture solvent without CO_2. Additional experiments were also carried out to analyze the impact from CO_2. In this initial study five different relations between cation and glycine were analyzed: 1 to 1 (even stoichiometric relation), 2 to 1, 5 to 1 (excess of cations, so excess of potassium hydroxide), 1 to 2 and 1 to 5 (excess of glycine).

Potassium hydroxide was used, and the purity is determined according to the calculations above, in section “Potassium bicarbonate and potassium hydroxide systems.”

9.4.4.1. Relation of moles of KOH per moles of glycine 1 to 1.

Table 24 shows the weights, and KGly mass fractions of the solutions prepared for this system and the measured freezing points. The high concentration samples 0.5959 KGly mass fractions were heated in order to dissolve the potassium hydroxide and glycine. Precipitated crystals for the lower KGly mass fractions (0.01-0.3468) were amorphous, and for the higher mass fractions (0.5959-0.7241) were white.

Table 24. Weights and mean temperatures measured plus standard deviations for the temperatures analyzed.

wt frac Kgly, salt free	m H_2O (g)	m Gly (g)	m KOH (g)	Mean T (°C)	T Stddev (°C)
0.0000	5.000	0.000	0.000	0.20	0.028
0.0103	5.043	0.036	0.031	-0.18	0.002
0.0502	5.023	0.180	0.156	-1.63	0.004
0.1001	5.033	0.382	0.335	-3.68	0.013
0.1269	5.009	0.506	0.439	-5.03	0.003
0.1513	5.015	0.628	0.544	-6.45	0.010
0.1775	5.000	0.756	0.667	-8.22	0.002
0.2017	5.016	0.897	0.794	-9.99	0.013
0.2501	5.022	1.210	1.063	-13.94	0.005
0.2755	5.027	1.408	1.226	-16.93	0.019
0.3003	5.052	1.608	1.420	-20.04	0.018
0.3468	5.096	2.064	1.812	-26.46	0.011
0.3978	5.068	2.651	2.332	-	-
0.4237	5.045	3.003	2.631	-	-
0.4499	5.019	3.405	2.987	-	-
0.4992	5.028	4.401	3.858	-	-
0.5488	5.050	5.805	5.091	-	-
0.5784	2.042	2.801	2.458	-	-
0.5912	2.155	3.209	2.809	-	-
0.5959	2.009	3.168	3.178	3.44	0.417
0.6325	2.032	4.014	3.519	9.56	0.543
0.6595	2.047	5.006	4.389	23.81	0.413
0.6804	2.030	6.001	5.271	32.87	0.344
0.7002	3.037	11.020	9.652	39.03	0.344
0.7241	2.047	10.001	8.783	47.66	0.304

It was very difficult to determine the freezing point for the 0.3468 KGly mass fraction since the freezing point was very low, at the limit of the equipment capacity. I tried to measure the freezing point for the 0.3978 KGly mass fraction, but at -33 °C no crystals were formed and the cooling bath couldn't cool below -36°C. The freezing point was expected to be at approximately -34°C. Furthermore, the solution was very viscous.

For the potassium glycinate mass fractions between 0.5784 and 0.5912 it was impossible to form a precipitate. The freezing points were expected at very low temperatures, and the cooling bath could not reach these temperatures. Consequently these measurements could not be determined. Furthermore, the solutions were very viscous.

At high KGly mass fractions, crystals were formed at positive temperatures: for example, the 65.94 wt% KGly, formed at 8°C, and the 70 and the 72.14 wt% KGly, crystals formed at approximately 26°C.

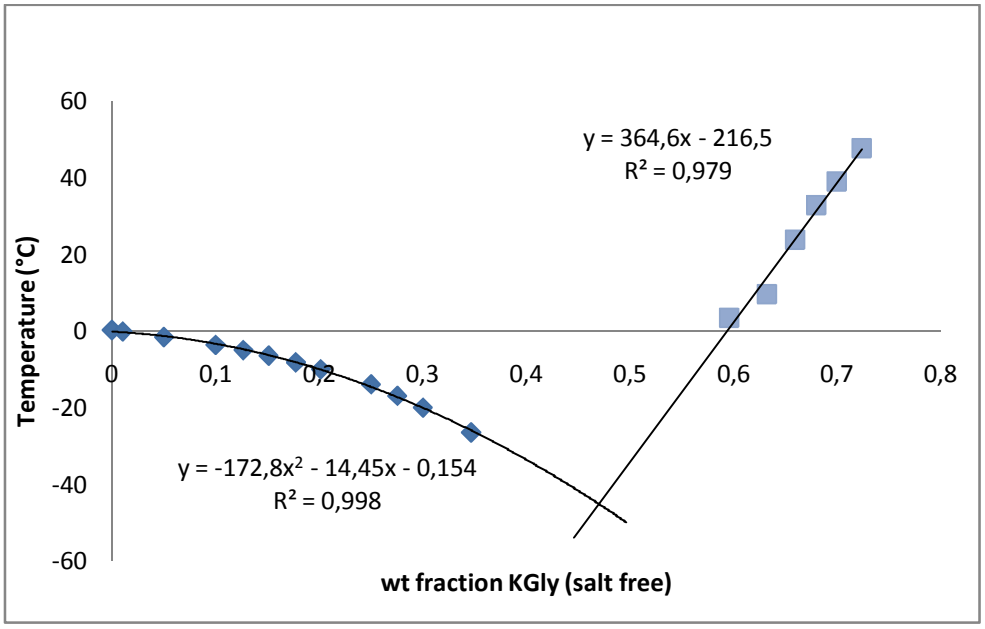

Figure 51. Freezing points for the mass fractions analyzed for the KOH-Gly-H2O system (stoichiometric mole relation).

Figure 51 shows the freezing and solubility points determined in the laboratory. As it can be seen in the figure, from 0.4 to 0.6 KGly mass fractions no data was recorded although it was tried. This is due to the impossibility to obtain such low temperatures (-40/-50 °C) and due to the difficulty of measurement in the vicinity to the eutectic point. The tendencies for the freezing and the solubility curve were different (polynomial and linear respectively). From these tendencies it can be seen that the eutectic point seems to be at approximately 0.47 KGly mass fraction.

9.4.4.2. Relation of moles of KOH per moles of glycine 1 to 2.

In order to determine the influence of an excess of glycine, the potassium hydroxide-glycine-water system with the relation of moles of potassium hydroxide per moles of glycine (n_{KOH}/n_{Gly}) 1 to 2 was analyzed. The results are shown in Table 25. From 0.2136 KGly mass fraction the samples were needed to be warmed up to dissolve all the chemicals. Precipitates were amorphous for low KGly mass fractions (0.01-0.18) and white at high KGly mass fractions (0.2-0.32).

Table 25. Mean temperatures and standard deviations for the analyzed KGly mass fractions for the KOH-Gly-H_2O system (nKOH/nGly 1/2).

wt frac KGly, salt free	m H_2O (g)	m Gly (g)	m KOH (g)	Mean T (°C)	T Stddev (°C)
0.0000	5.000	0.000	0.000	0.221	0.039
0.0112	5.037	0.076	0.033	-0.24	0.006
0.0313	5.032	0.214	0.095	-1.33	0.004
0.0539	5.016	0.365	0.169	-2.30	0.002
0.0770	5.041	0.557	0.250	-3.73	0.006
0.1003	5.039	0.761	0.336	-5.10	0.009
0.1265	5.017	1.004	0.438	-6.97	0.006
0.1504	5.016	1.232	0.540	-8.82	0.002

0.1757	5.022	1.482	0.657	-10.77	0.003
0.1827	3.024	0.958	0.416	-11.43	0.020
0.2003	5.050	1.786	0.784	4.65	0.135
0.2136	3.015	1.162	0.510	6.47	0.272
0.2270	5.035	2.110	0.927	12.87	0.518
0.2339	5.027	2.202	0.965	17.53	0.460
0.2490	5.047	2.412	1.059	22.99	0.478
0.2631	5.038	2.605	1.147	27.06	0.546
0.2890	5.009	3.004	1.315	35.65	0.220
0.3000	3.007	1.919	0.838	38.66	0.290
0.3252	3.035	2.217	0.965	43.61	0.875

Standard deviations lower than 0.15°C were observed for the points in the freezing curve; though for the points in the solubility curve their standard deviations are higher than 0.2°C, as shown in Table 25.

From 0.2136 KGly mass fraction the samples were needed to be warmed, but for the 0.2003 KGly mass fraction the sample was not heated but while taking the measurements white crystals appeared and the temperature is above 0 °C. After heating the solutions, they were cooled down to -15/-16°C till crystals were formed. In the solution of 0.3252 KGly mass fraction after warming the sample and before analyzing it the solution was left in order to decrease its temperature, and at room temperature thin crystals were formed.

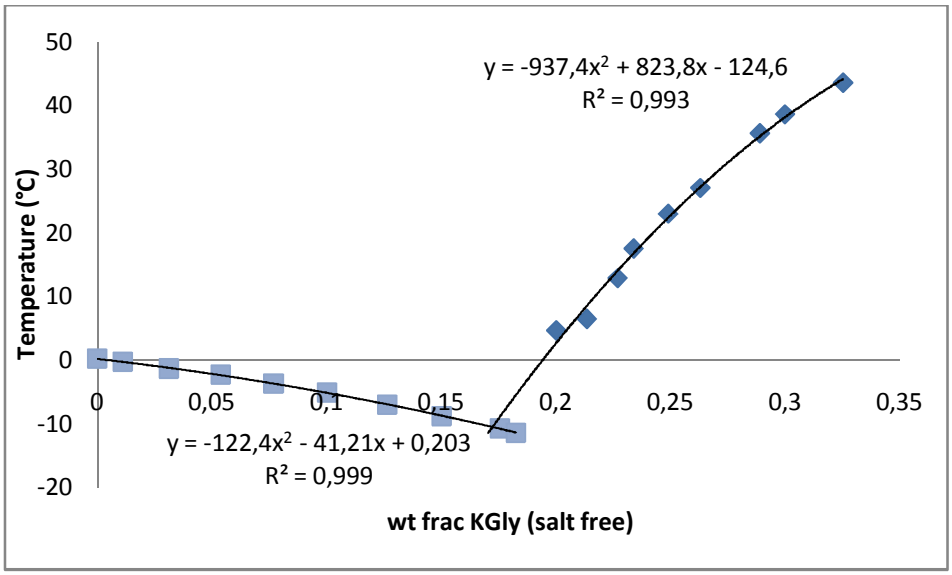

Figure 52. Temperatures measured for different KGly mass fractions for the KOH-Gly-H_2O system with an excess of glycine.

Figure 52 shows the data obtained during the experiments for the potassium hydroxide-glycine-water system with double moles of glycine with regard to one mole of potassium hydroxide. It can be seen that the temperature for the 0.2003 KGly mass fraction deviates from slightly from the trendline. During the measurements the solution was not heated in order to dissolve the sample. The deviation may indicate that heating of the sample influences the determined solubility curve in some way. This could be related to the evaporisation of water during heating. The 0.2136 KGly mass fraction also deviates slightly from the solubility curve. The standard deviation is higher than the others and the accuracy of this point could maybe be improved in the future.

If the measurement at 20.03 wt% KGly is not taken into account in calculation of the trendline, the results of Figure 52 will look like the outcome in Figure 53.

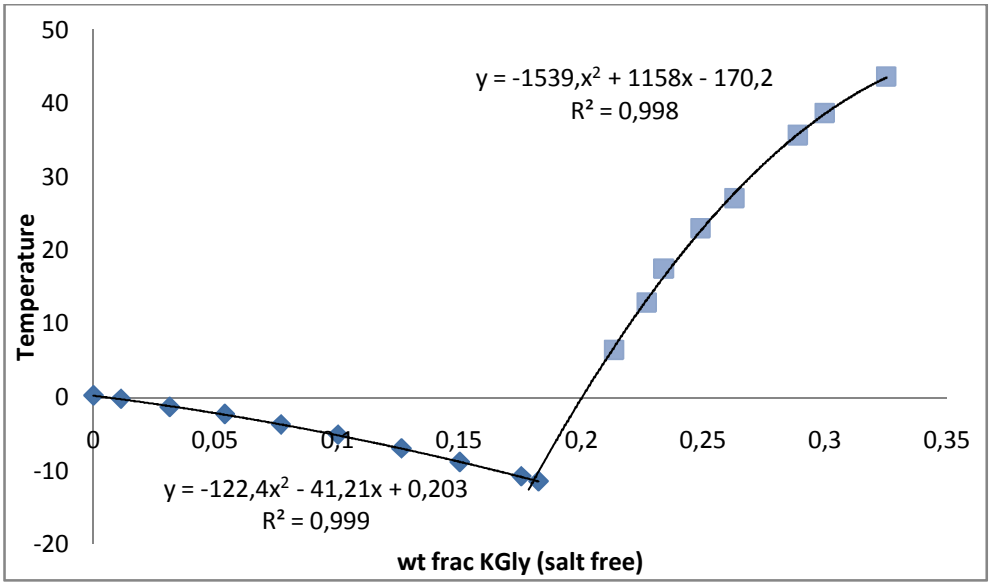

Figure 53. Temperatures measured for different KGly mass fractions for the KOH-Gly-H_2O system with an excess of glycine without taking into account the measurement at 20.03 wt% KGly.

Figure 53 shows the trendline of the phase diagram for the potassium hydroxide-glycine-water system (n_{KOH}/n_{Gly} 1/ 2). Both trendlines are polynomial, and the intersection between them is the point at 18.3 wt% KGly. The determined temperatures seem to follow fairly well the trend. According to this figure the temperatures measured in the laboratory were determined very accurately.

9.4.4.3. Relation of moles of KOH per moles of glycine 2 to 1.

Potassium glycinate mass fractions between 0 and 0.6671 were prepared and their freezing points were obtained. Results were shown in Table 26. From 0.5613 to 0.6671 KGly mass fraction the solutions needed to be warmed up in order to dissolve all the potassium hydroxide and glycine. Crystals for these experiments were amorphous at low KGly mass fractions (0.01-0.2236) and white at high mass fractions (0.4483-0.6671).

Table 26. Weights, temperatures and standard deviations for the mass fractions determined in the system KOH-Gly-H_2O with an excess of potassium hydroxide.

wt frac KGly, salt free	m H_2O (g)	m Gly (g)	m KOH (g)	Mean T (°C)	T Stddev (°C)
0.0000	5.000	0.000	0.000	0.057	0.009
0.0123	5.013	0.042	0.074	-0.63	0.003
0.0502	5.008	0.179	0.313	-3.40	0.002
0.1019	5.032	0.394	0.688	-8.54	0.015
0.1260	5.065	0.509	0.882	-11.62	0.023
0.1506	5.061	0.632	1.105	-15.28	0.032
0.1764	5.021	0.768	1.334	-19.58	0.035
0.2036	5.006	0.927	1.614	-24.92	0.018
0.2236	5.008	1.057	1.843	-29.62	0.032
0.2505	5.020	1.252	2.198	-	-
0.3008	5.018	1.669	2.911	-	-

0.3503	5.008	2.180	3.830	-	-
0.4004	3.014	1.714	3.004	-	-
0.4247	3.027	1.960	3.423	-	-
0.4483	2.035	1.500	2.631	10.11	0.727
0.4818	2.029	1.806	3.158	22.39	0.310
0.4997	2.028	2.007	3.510	28.46	0.343
0.5367	2.015	2.509	4.388	37.24	1.202
0.5613	2.041	3.004	5.262	42.26	0.675
0.5703	2.187	3.428	5.987	44.08	0.229
0.6008	1.008	2.005	3.512	48.78	0.356
0.6671	2.016	8.001	14.097	-	-

For the 25.05 wt% KGly I could not measure the freezing point because the cooling bath was limitated to -36°C. The freezing point seemed to be at -36°C, based on the other experiments, but no crystal formed.

Between 0.40 and 0.50 potassium glycinate mass fractions no need of heating was necessary, although the temperatures were on the solubility curve. For the 42.47 wt% KGly all the potassium hydroxide and glycine were dissolved, but I tried to determine the freezing point and I had no results. In the samples from 44.83 wt% KGly to 57.03 wt% KGly a lot of bubbles were formed in the glass beaker during the measurements.

There was some potassium hydroxide and glycine not completely dissolved in the sample of 0.5613 KGly mass fraction, so the solution needed to be heated; after that, at 19°C crystals appeared.

For the solution 66.71 wt% KGly was very difficult to obtain the correct temperature; after dissolving all the potassium hydroxide and glycine, crystals were formed when cooling the sample, but it was difficult to determine the solubility point (not all the crystals were homogeneously distributed in the sample).

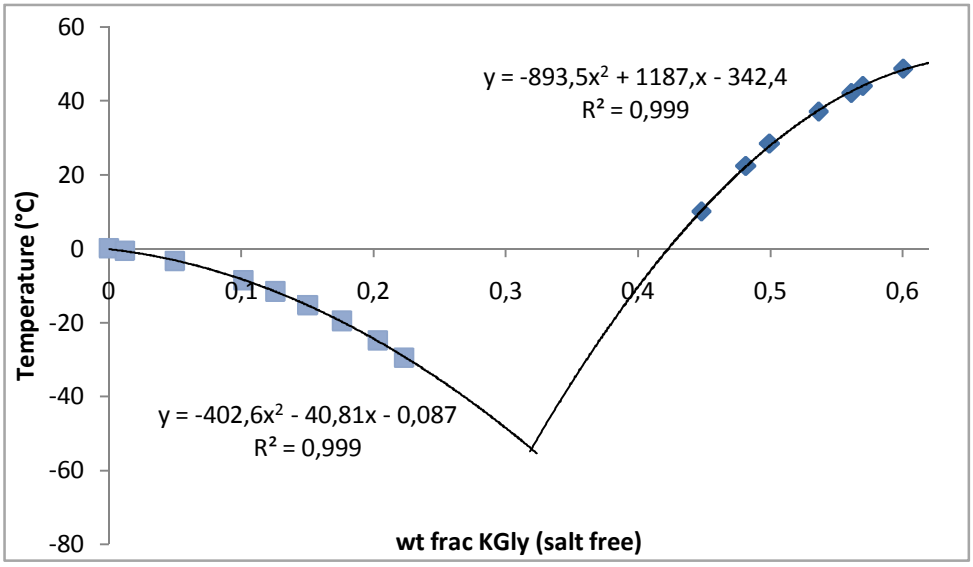

Figure 54. Temperature vs mass fraction diagram for the system KOH-Gly-H_2O with excess of KOH.

Figure 54 shows the freezing points for the system KOH-Gly-H_2O with an excess of potassium hydroxide. All the data seem to follow both trendlines (polynomial), so the R-squared values for both trendlines are very high, which may indicate that the data were taken very accurately. As shown in the figure, the eutectic point seems to be at 32.0 wt% KGly, and its temperature seems to be very low (about -58°C).

9.4.4.4. Relation of moles of KOH per moles of glycine 1 to 5.

Table 27 shows the obtained temperatures and the calculated standard deviations for all the KGly mass fractions analyzed. From 0.0784 KGly mass fraction the samples were needed to be warmed in order to dissolve all the glycine and potassium hydroxide not dissolved during the stirring. Crystals were amorphous (0.01-0.061 KGly mass fractions) and white (0.07-0.15 KGly mass fractions).

Table 27. Weights, mean temperatures and standard deviations for the KOH-Gly-H_2O system with an excess of glycine (n_{KOH}/n_{Gly} 1/5).

wt frac KGly, salt free	m H_2O (g)	m Gly (g)	m KOH (g)	Mean T (°C)	T Stddev (°C)
0.0000	5.000	0.000	0.000	0.220	0.020
0.0120	5.139	0.200	0.037	-0.95	0.004
0.0203	5.032	0.352	0.061	-1.76	0.003
0.0316	5.019	0.538	0.096	-2.74	0.007
0.0413	5.018	0.704	0.127	-3.54	0.004
0.0508	5.008	0.904	0.158	-4.64	0.005
0.0610	5.002	1.082	0.192	-5.14	0.230
0.0784	5.009	1.407	0.253	15.90	0.483
0.0887	5.037	1.658	0.292	24.48	0.703
0.1006	5.033	1.906	0.337	32.90	0.106
0.1066	5.030	2.053	0.360	37.44	0.476
0.1143	5.056	2.234	0.392	43.63	0.537
0.1272	5.003	2.502	0.440	53.48	0.287
0.1374	5.028	2.707	0.485	57.67	0.443
0.1446	5.018	2.918	0.515	63.77	0.637
0.1518	5.029	3.102	0.548	68.90	0.332

No problems were observed during the experiments. For the 0.0610 KGly mass fraction all the glycine and potassium hydroxide seemed to be dissolved. This sample was analyzed twice with two different methods: in the first analysis (freezing point depression) a mean temperature of -5.566 °C was obtained, but crystals were white. Then a second analysis was done by heating the sample and cooling it, and the mean temperature was -5.14 °C. So for both analyses the mean temperature was quite the same. Moreover, from KGly mass fractions 0.1272 to KGly mass fraction 0.1518, after heating the solutions to dissolve all the precipitate, crystals were formed at room temperature.

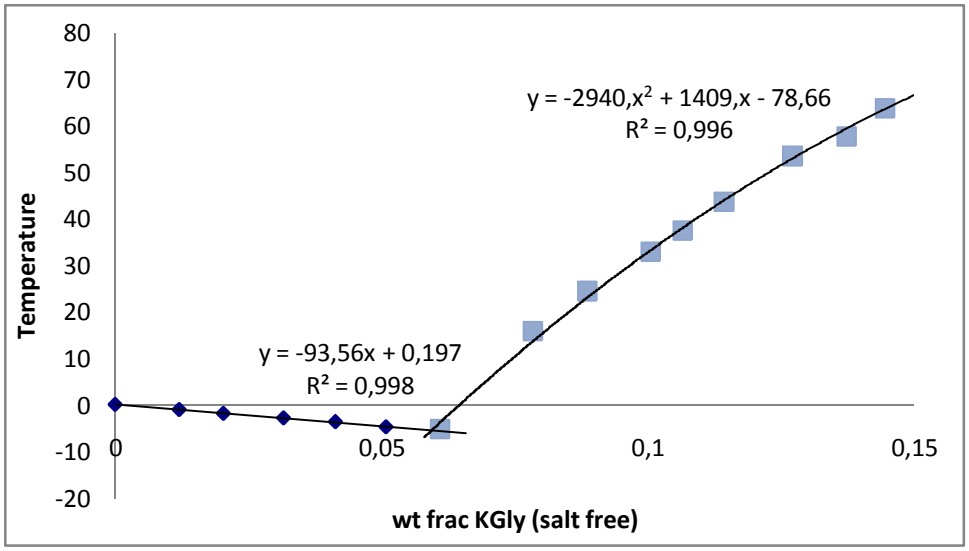

Figure 55. Temperature vs wt fraction KGly for the KOH-Gly-H_2O system with an excess of glycine (n_{KOH}/n_{Gly} 1/5).

Figure 55 represents the obtained freezing points for the respective potassium glycinate mass fractions. Tendencies for the freezing and the solubility curve are different: linear for the freezing curve, and polynomial for the solubility curve. The intersection between both curves (the eutectic point) is at 0.0593 KGly mass fraction. So the freezing point for the 0.0610 KGly mass fraction is in the solubility curve, and the correct mean temperature is the one obtained in the second analysis.

9.4.4.5. Relation of moles of KOH per moles of glycine 5 to 1.

Different solutions were prepared by mixing potassium hydroxide and glycine in a water solution, and their freezing points were determined. Table 28 shows the weights, mean freezing points for each mass fraction analyzed, and also standard deviations. From 0.3496 KGly mass fraction the samples needed to be warmed in order to dissolve all the potassium hydroxide and glycine present. Crystals were amorphous for low KGly mass fractions (0.01-0.33) and white for high KGly mass fractions (0.34-0.39).

Table 28. Weights, freezing points for the mass fractions analyzed and standard deviations for the KOH-Gly-H_2O system (n_{KOH}/n_{Gly} 5/1).

wt frac KGly, salt free	m H_2O (g)	m Gly (g)	m KOH (g)	Mean T (°C)	T Stddev (°C)
0.0000	5.000	0.000	0.000	0.161	0.016
0.0119	5.051	0.041	0.177	-1.86	0.004
0.0265	5.014	0.092	0.332	-3,69	0.009
0.0384	5.034	0.136	0.441	-5.00	0.002
0.0439	5.018	0.157	0.658	-8.05	0.007
0.0511	5.012	0.185	0.820	-10.39	0.010
0.0638	5.011	0.236	1.008	-13.52	0.002
0.0742	5.028	0.281	1.229	-17.32	0.009
0.0839	5.004	0.321	1.360	-20.79	0.014
0.1009	5.024	0.400	1.766	-	-
0.1263	5.011	0.525	2.280	-	-
0.1514	5.010	0.662	2.904	-	-
0.2017	5.034	0.990	4.297	-	-

0.2474	3.133	0.845	3.640	-	-
0.2747	3.037	0.982	4.296	10.35	0.809
0.2807	3.063	1.028	4.484	12.72	0.613
0.3023	3.002	1.155	5.015	19.80	0.371
0.3103	3.021	1.225	5.351	23.29	0.527
0.3312	3.022	1.401	6.143	29.15	0.652
0.3496	3.027	1.578	6.909	33.74	0.356
0.3604	3.027	1.690	7.368	39.33	0.808
0.3741	3.032	1.854	8.115	45.43	0.440
0.3868	3.017	2.006	8.773	51.42	0.529
0.3999	3.026	2.198	9.615	56.34	0.254

For the 0.1009 KGly mass fraction I could not reach a precipitation point. The main problem was that the freezing point seemed to be at a very low temperature. The cooling bath could not reach this temperature. I tried to cool the 0.2017 and 0.2474 KGly mass fractions to -31°C and -33°C respectively but no crystals were formed. This is due to the freezing point is very low outside the limit of cooling bath.

From 0.1009 to 0.3312 KGly mass fraction no need of heating the solution was necessary. But when the 0.3023 KGly mass fraction was prepared the solution seemed very thick. Furthermore, a lot of bubbles were formed during the manual stirring while measuring the freezing point, so the mean temperature obtained was not very accurate. It was difficult to determine the temperature due to bubbles. This phenomenon happened in all the samples from 0.3023 to 0.3868 KGly mass fraction. For the 0.3999 KGly mass fraction the temperature was very difficult to measure. This solution had a white color and was also very viscous, so the change of color could not be appreciated.

As shown in Table 28 standard deviations lower than 0.015°C were observed for low mass fractions (0-0.0839), but for the high concentration cases at the solubility curve 0.3°C were obtained.

When plotting the temperatures, two different trends can be seen in Figure 56 at high concentrations although it could just be a scatter in the data as shown in Figure 57.

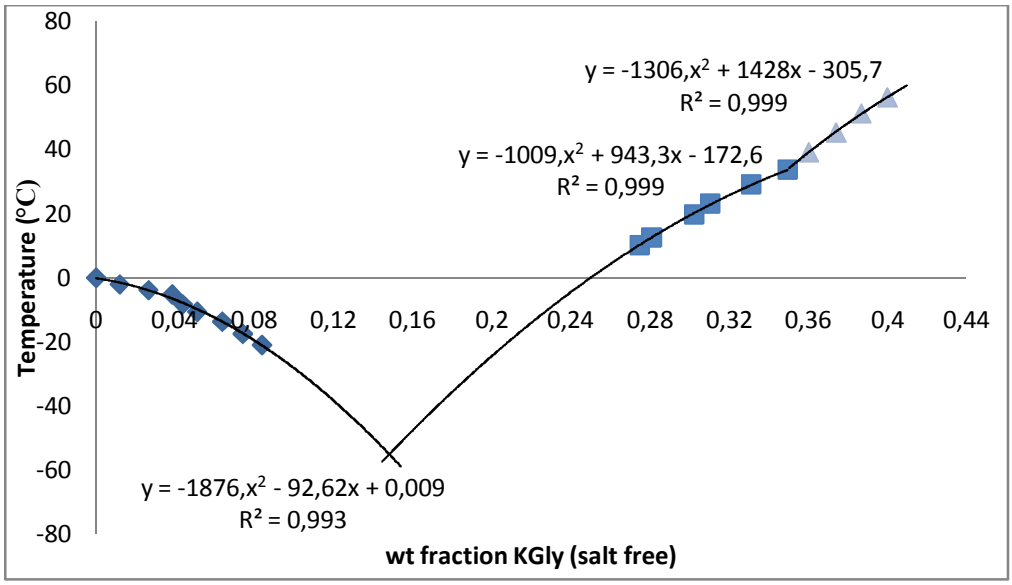

Figure 56. Temperatures for different KGly mass fractions for the n_{KOH}/n_{Gly} 5/1 relation when a scatter is considered.

No change was observed in the appearance of precipitate during the measurements, therefore phenomenon was considered to be scatter, corresponded to Figure 57.

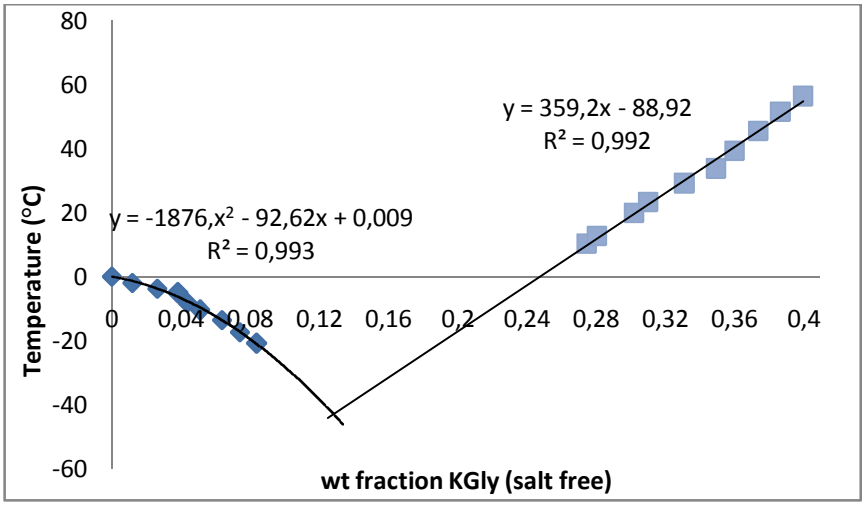

Figure 57. Temperatures for different KGly mass fractions for the n_{KOH}/n_{Gly} 5/1 relation without a scatter.

As shown in Figure 57, trendlines for both curves are different: for the freezing curve is polynomial, while for the solubility curve is linear. The data for low potassium glycinate mass fractions continue the trendline fairly well; with the exception of the 3.84 wt% KGly point which is probably scatter. At high KGly mass fractions (0.28-0.40), and consequently high temperatures, the trendline seems to be linear, but the values obtained during the measurements were less accurate due to high standard deviations and the points follows not as closely the trendline. In this figure the eutectic point seems to be at 0.128 KGly mass fraction.

9.4.4.6. Comparison between all the KOH-Gly-H_2O systems.

In this section all the results obtained for the potassium hydroxide-glycine-water systems is compared. Figure 58 shows the phase diagram for the cases containing excess of cation (excess of potassium hydroxide) at fixed stoichiometric relation between moles of potassium hydroxide and glycine.

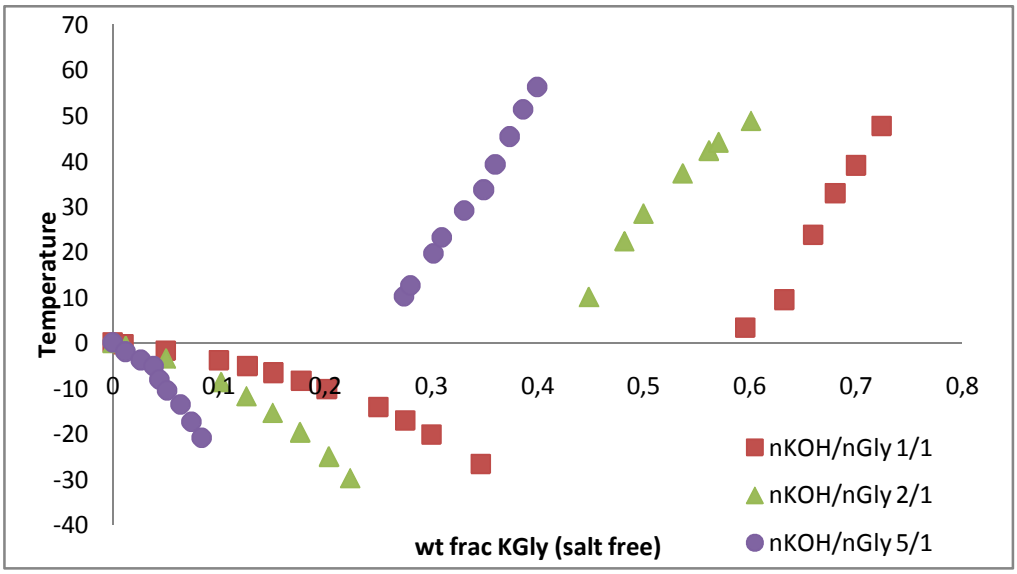

Figure 58. Comparison for the system KOH-Gly-H_2O with the stoichiometric molar relation and the systems with an excess of potassium hydroxide.

The curves tendency is the same for all the experiments compared in Figure 58, they are all polynomial. The more potassium hydroxide was added, the more compressed the curve becomes. It moves to the left in the diagram as shown in Figure 58.

The freezing points of the solutions decrease on addition of potassium hydroxide. For example, if we consider the 5 wt% KGly, the freezing points are: -1.627°C for the stoichiometric 1:1 n_{KOH}/n_{Gly} relation, -3.397°C for the 2:1 n_{KOH}/n_{Gly} relation, and -10.392°C for the 5:1 n_{KOH}/n_{Gly} relation.

The solubility curve behaves differently. It similarly moves to the left, but this indicates at constant temperature that the solubility decreases by adding potassium hydroxide.

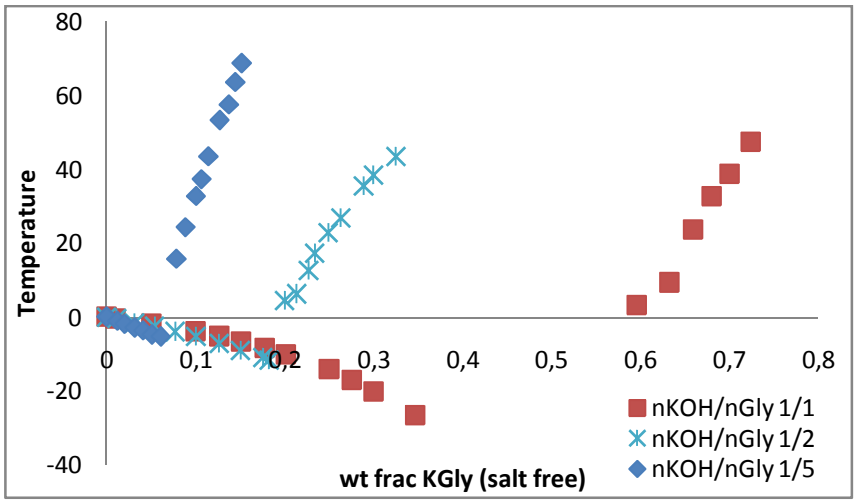

Figure 59. Comparison for the system KOH-Gly-H_2O with the stoichiometric molar relation and the systems with an excess of glycine.

Figure 59 shows the stoichiometric relation between moles of potassium hydroxide and glycine (n_{KOH}/n_{Gly}) with addition of excess glycine. The more moles of glycine were added, the more compressed the phase diagram was. By adding glycine the freezing decreases. For example, if we consider the 5 wt% KGly, the freezing points are: -1.627°C for the stoichiometric 1:1 n_{KOH}/n_{Gly} relation, -2.299°C for the 1:2 n_{KOH}/n_{Gly} relation and -4.639°C for the 1:5 n_{KOH}/n_{Gly} relation. The decrease in temperature is not at all as profound as shown in Figure 60 by addition of KOH as by addition of Gly.

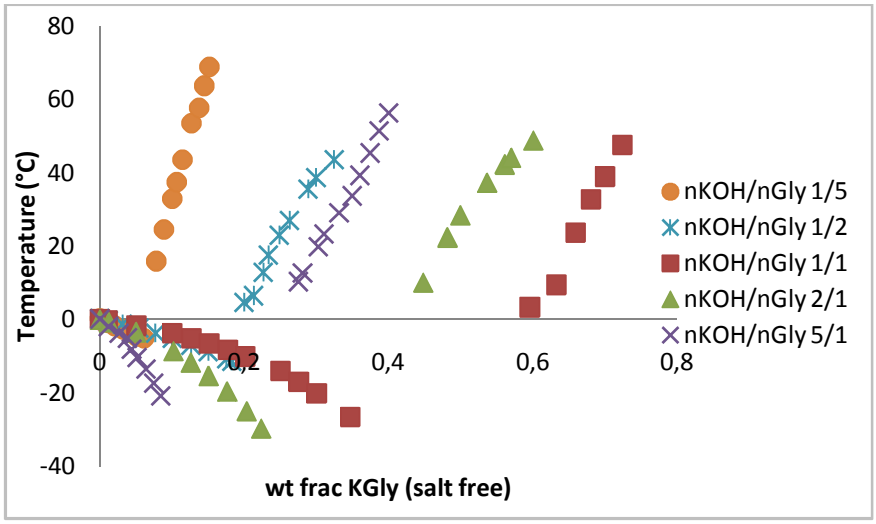

Figure 60. Comparison between the system potassium hydroxide-glycine-water in different nKOH/nGly ratios.

Figure 60 shows that the stoichiometric relation between moles of potassium hydroxide and glycine (n_{KOH}/n_{Gly} relation 1/1) has the highest solubility of all the systems. By adding either KOH or glycine, the solubility decreases.

As shown in Figure 58, Figure 59, and Figure 60 there is a gap in the figures due to not all the freezing points could be measured because of limitations in the equipment. Most of these mass fractions lay below -35°C.

9.4.5. Potassium bicarbonate-glycine-water system ($KHCO_3$-Gly-H_2O).

As in the case of the sodium bicarbonate, when potassium bicarbonate was mixed with glycine in an aqueous solution, potassium glycinate, carbon dioxide and water is formed.

Two different cases were under study: the main difference between them was the amount of moles of potassium bicarbonate added in comparison with moles of glycine added. The systems considered were n_{KHCO3}/n_{Gly} 1 to 1 (one mole of potassium bicarbonate per mole of glycine) and 3 to 1 (excess of potassium bicarbonate).

9.4.5.1. One mole of potassium bicarbonate per mole of glycine.

Different potassium glycinate mass fractions were prepared in order to determine their freezing points. The prepared KGly mass fractions and their freezing points are reported in Table 29. From 0.2496 KGly mass fraction the solutions were needed to be heated up in order to dissolve all the potassium bicarbonate present in the solutions. Up to 0.2496 KGly mass fraction, after heating the samples they were needed to be cooled to -13 or -19 °C (depending on the solution).

In this system, crystals were white, although for the KGly mass fractions up to 0.2496 crystals were whiter than the ones for the lower mass fractions. Bubbles were formed in all the samples, but the higher mass fractions were analyzed, the more bubbles were formed in the solution; this could explain some of the deviations for the temperatures obtained.

Table 29. Temperatures and standard deviation for the calculated mass fractions for the system sodium bicarbonate-glycine-water (1:1).

wt frac KGly, salt free	m H_2O (g)	m Gly (g)	m $KHCO_3$ (g)	Mean T (°C)	T Stddev (°C)
0.0000	5.000	0.000	0.000	0.133	0.032
0.0119	5.064	0.041	0.054	-0.38	0.003
0.0509	5.054	0.181	0.246	-1.86	0.009
0.0688	5.041	0.253	0.333	-2.51	0.004
0.1010	5.016	0.384	0.508	-3.75	0.005
0.1274	5.051	0.502	0.668	-4.82	0.003
0.1509	5.028	0.612	0.814	-5.78	0.001
0.1748	5.021	0.749	0.974	-6.98	0.003
0.1999	5.041	0.872	1.161	-8.22	0.008
0.2233	5.006	1.001	1.335	-9.69	0.010
0.2496	5.023	1.175	1.561	-10.41	0.166
0.2614	5.029	1.259	1.669	-11.49	0.135
0.2827	5.021	1.405	1.868	6.48	0.460
0.3001	5.021	1.540	2.044	8.41	0.470

0.3204	5.029	1.711	2.268	13.97	0.806
0.3499	5.023	1.962	2.616	19.88	0.464
0.3743	5.020	2.203	2.938	28.31	0.229
0.4002	5.010	2.484	3.309	31.90	0.229

At low KGly mass fractions (0-0.2233) standard deviations below or equal to 0.01°C were observed; but standard deviations up to 0.1°C were obtained for high mass fractions, when solubility points were determined.

The freezing point for the KGly mass fraction 0.2827 was very difficult to determine. Measurements were repeated twice: in the first time the mean temperature was 11.76°C, and in the second measurement the mean temperature was of 6.48°C. As the first measurement wasn't determined very accurately (high standard deviation) the measurement to take into account would be the second one. The same fact occurred for the 30.01 wt% KGly; in the first analysis the mean temperature obtained was -13.37°C, which had to be a metastable point, but when the measurements were repeated, the temperature obtained was in the solubility curve (8.41°C).

Regarding the 24.96 wt% and 26.14 wt% KGly freezing points, two different considerations could be taking into account while plotting the results: the first consideration is that both points were obtained wrongly (Figure 61), and the second case is that the 0.2496 KGly mass fraction was taken accurately, but the 0.2614 KGly mass fraction was not considered (Figure 62).

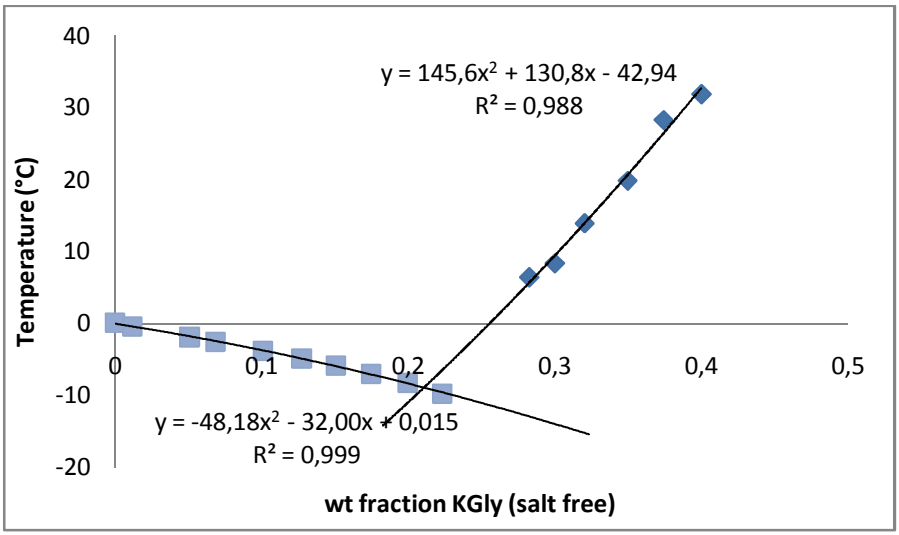

Figure 61. Freezing temperatures for the potassium bicarbonate-glycine-water system (one mole of $KHCO_3$ per mole of Gly) without the 0.2496 and 0.2614 KGly mass fractions.

In Figure 61 both freezing and solubility curves have polynomial tendencies. Finally the solubility curve has a concave shape instead of a convex shape, which is the expected one. According to both tendencies, the eutectic point seemed to be at 21.09 wt% KGly, so during the measuring of the 24.96 and 26.14 wt% KGly temperatures, metastable points were determined, the same as for the 22.33 wt% KGly. Furthermore in Figure 61 is shown that the solubility point for the 30 wt% KGly seems to deviate from the trendline; the same happens for the 37.43 wt% KGly.

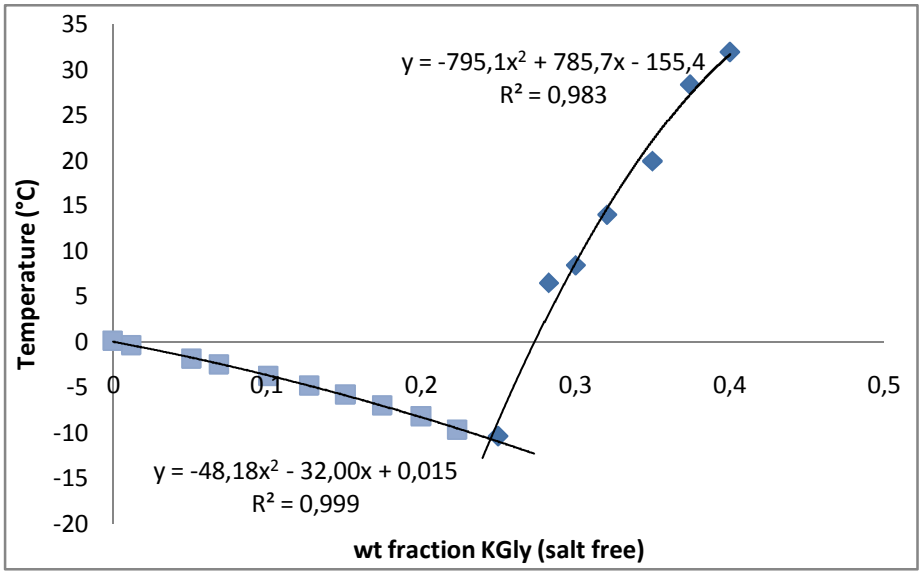

Figure 62. Freezing points for the potassium bicarbonate-glycine-water system (one mole of $KHCO_3$ per mole of Gly) without the 26.14 wt% KGly temperature.

As the previous case, the tendencies for both curves are polynomial, but the eutectic point seems to change: in this case it seems to be near the 24.5 wt% KGly.

As shown in Figure 62, temperatures for potassium glycinate mass fractions 0.2827 and 0.3499 seem to deviate from the tendency of the curve. This could be because the values were not taken very accurately, and their standard deviations (0.46 and 0.464 respectively) were higher than the normal standard deviations for the solubility points (0.15°C).

To sum up, the eutectic point seems to be between 0.20 and 0.25 potassium glycinate mass fractions. So the temperatures determined during the experiments for this average were very difficult to measure and the values can change a little; this is why there is a bit scatter in the results. As the solid phase after the eutectic point in the sodium system was glycine, we may assume the same for this system.

9.4.5.2. Three moles of potassium bicarbonate per mole of glycine.

An excess of potassium bicarbonate was considered, so more carbon dioxide was formed. In Table 30 all the measurements made in the laboratory were collected. From 11.23 wt% KGly samples were needed to be heated. Then, after the heating, they were cooled down to -10 or -13°C depending on the KGly mass fraction. Crystals for this experiment were also white, and as in the previous case, whiter when the solutions needed to be heated up (form 0.1123 KGly mass fraction). Once again bubbles appeared in all the samples, and as before more bubbles were formed from 11.23 wt% KGly. The bubbles may explain some of the deviations, and indicates that a small amount of CO_2 escaped.

Table 30. Results for the analyzed mass fractions for the system $KHCO_3$-Gly-H_2O with excess of potassium bicarbonate.

wt frac KGly, salt free	m H_2O (g)	m Gly (g)	m $KHCO_3$ (g)	Mean T (°C)	T Stddev (°C)
0.0000	5.000	0.000	0.000	0.202	0.001
0.0121	5.032	0.041	0.161	-0.99	0.003
0.0207	5.078	0.072	0.287	-1.83	0.004
0.0322	5.019	0.111	0.441	-2.68	0.003
0.0417	5.035	0.146	0.561	-3.40	0.002

0.0532	5.087	0.191	0.760	-4.45	0.005
0.0678	5.052	0.247	0.968	-5.52	0.007
0.0842	5.025	0.311	1.120	-6.19	0.006
0.0995	5.043	0.376	1.506	-8.16	0.002
0.1123	5.042	0.432	1.721	7.40	0.372
0.1285	5.016	0.503	2.007	18.33	0.662
0.1388	5.032	0.552	2.202	23.83	0.387
0.1508	5.063	0.614	2.442	28.94	0.320
0.1621	5.142	0.681	2.721	32.57	0.261
0.1804	5.017	0.759	2.926	38.78	0.408
0.2028	5.010	0.881	3.482	46.21	0.267

As shown in Table 30 standard deviations lower or equal to 0.007°C were observed at low KGly mass fractions (0-0.0995), but when mass fractions are higher and the solubility points were determined instead of the freezing points, standard deviations begin to be higher than 0.2°C. No problems were found analyzing these solutions.

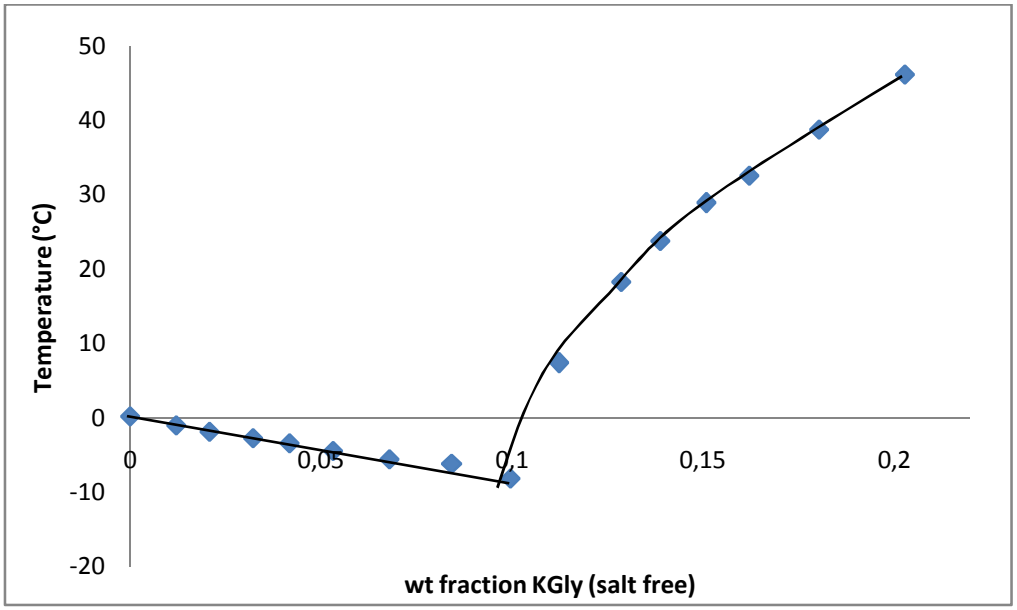

Figure 63. Freezing points for all the mass fractions determined for the system $KHCO_3$-Gly-H_2O with excess of potassium bicarbonate.

Figure 63 shows the diagram for this system as temperatures were determined. As it can be seen, the freezing curve has a linear tendency, but the solubility curve has a polynomial tendency. If tendencies are plotted with excel program, then the solubility curve changes a bit (Figure 64).

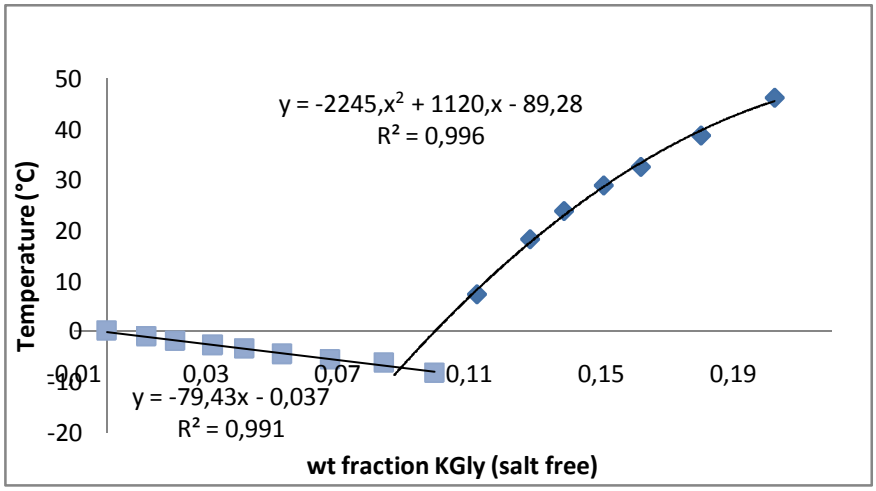

Figure 64. Temperature vs mass fractions for the studied system with excess of potassium bicarbonate.

In Figure 64 is shown the tendencies for both curves. As reported in Figure 63, the freezing curve tendency is linear; however the tendency of the solubility curve is polynomial. But this figure differs from the previous one about the eutectic point. The eutectic point in Figure 63 seems to be at approximately 10 wt% KGly, while in Figure 64 the eutectic point is at 8.93 wt% KGly. If the tendency of Figure 64 is taken into account, for the 0.0995 KGly mass fraction the metastable point was determined instead of the solubility point.

9.4.5.3. Comparison for the $KHCO_3$-Gly-H_2O systems.

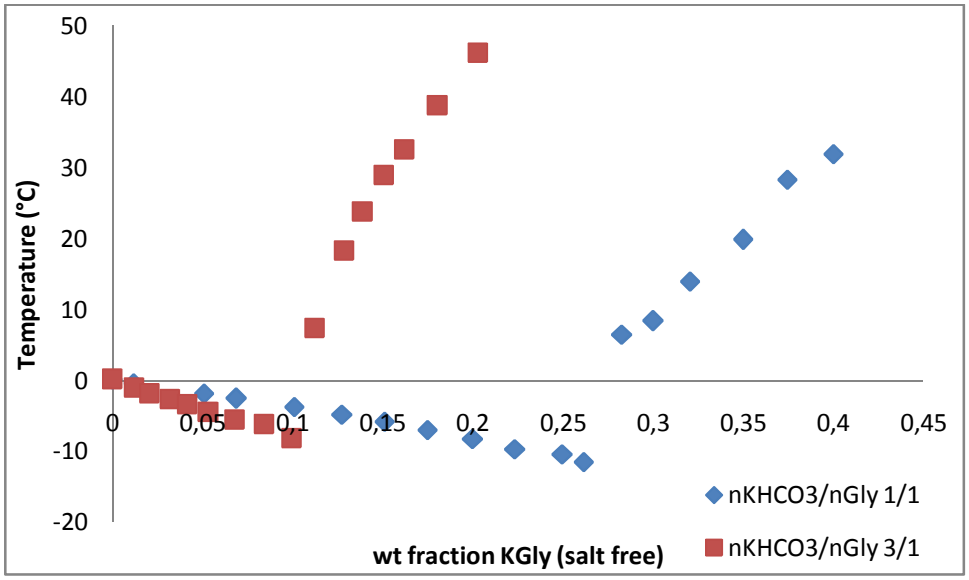

Figure 65. Comparison between both $KHCO_3$-Gly-H_2O systems.

Figure 65 represents a comparison between the systems containing potassium bicarbonate-glycine-water but with different amounts of potassium bicarbonate. Both curves have the same trend. The freezing point decrease on adding potassium bicarbonate and the solubility, at constant temperature, decreases.

There seem to be a bit more scatter in the 3:1 curve and these data may therefore be a bit more accurate, even though not enough to change the conclusions.

9.4.6. Potassium bicarbonate-potassium hydroxide-glycine-water system ($KHCO_3$-KOH-Gly-H_2O).

As in the sodium system, in this section the CO_2 formation was considered. Two different K:Gly relations were studied: 1 to 1 (even stoichiometric relation between potassium cation and glycine) and 2 to 1 (excess of potassium cation). For both K: Gly relations, different carbon dioxide loadings were considered: 0.1, 0.25 and 0.5.

9.4.6.1. Relation K: Gly 1:1.

9.4.6.1.1. CO_2 loading: 0.1.

Potassium glycinate mass fractions between 0.01 and 0.7632 were prepared in order to determine their freezing points. Table 31 shows the weights of the potassium bicarbonate, potassium hydroxide, glycine and water, the obtained freezing points and the calculated standard deviations for all the KGly mass fractions considered. From 60.14 wt% KGly solutions needed to be warmed up in order to dissolve all the potassium hydroxide, potassium bicarbonate and glycine present in the sample. Crystals for this system were amorphous at low KGly mass fractions (0.0296-0.3745) and white for high mass fractions (0.6014-0.7625).

Table 31. Weights, freezing points and standard deviations for the measured KGly mass fractions (CO_2 loading: 0.1).

wt frac KGly, salt free	m H_2O (g)	m Gly (g)	m $KHCO_3$ (g)	m KOH (g)	Mean T (°C)	T Stddev (°C)
0.0000	5.000	0.000	0.000	0.000	0.135	0.032
0.0296	5.015	0.102	0.017	0.080	-0.96	0.021
0.0523	5.002	0.198	0.025	0.147	-1.68	0.007
0.0772	5.009	0.290	0.039	0.223	-2.61	0.010
0.0993	5.189	0.399	0.052	0.307	-3.54	0.007
0.1268	5.017	0.501	0.069	0.404	-5.01	0.013
0.1545	5.030	0.637	0.088	0.505	-6.46	0.003
0.2037	5.040	0.911	0.142	0.724	-9.77	0.025
0.2520	5.018	1.219	0.172	0.957	-13.63	0.014
0.3021	5.021	1.607	0.216	1.270	-19.33	0.019
0.3549	5.017	2.105	0.281	1.666	-26.25	0.033
0.3745	3.040	1.420	0.189	1.109	-29.32	0.042
0.4022	3.019	1.606	0.214	1.265	-	-
0.4517	3.023	2.052	0.278	1.619	-	-
0.4758	3.003	2.305	0.308	1.817	-	-
0.5024	3.016	2.654	0.360	2.100	-	-
0.5202	3.112	3.010	0.412	2.375	-	-
0.6014	3.021	4.702	0.629	3.717	-	-
0.6427	2.170	4.513	0.605	3.553	-	-
0.6631	2.052	5.102	0.678	3.946	-	-
0.6860	2.002	6.006	0.808	4.743	17.35	0.352
0.6996	2.034	7.001	0.938	5.527	25.41	0.165
0.7190	1.047	4.511	0.601	3.552	35.34	0.132
0.7484	1.051	7.009	0.935	5.524	44.96	0.200
0.7625	1.018	9.008	1.206	7.108	48.33	0.632

Temperature standard deviations have very low values at low KGly mass fraction (below 0.05°C), so these experiments were carried out very accurately. But standard deviations up to 0.15°C were observed when solutions needed to be warmed up, so these temperatures were not taken with a high level of accuracy, but their values were not as high as for other systems (where standard deviations have values up to 0.4°C).

From 0.4022 KGly mass fraction to 0.6631 KGly mass fraction I could not obtain the freezing points due to there was no crystal formation. Even if the samples were cooled to -33°C was not enough for the formation of the crystals. Their freezing points must be at very low temperatures, and there were some limitations by the used ethanol bath, that could only get to -36°C. Furthermore, solutions were very viscous.

For the 60.14 wt% KGly the sample was needed to be cooled to -32.6°C in order to form crystals, but no crystals were formed, and the equipment could not cool the sample enough; besides the solution was very viscous. The same phenomena happened for the 0.6427 and 0.6631 KGly mass fractions. On the other hand, for the 68.60 and 69.96 wt% KGly the solutions had to be cooled to -13°C to have some crystals formed. The other samples did not need a lot of cooling, so the temperatures necessaries to obtain some crystals were temperatures up to 5°C.

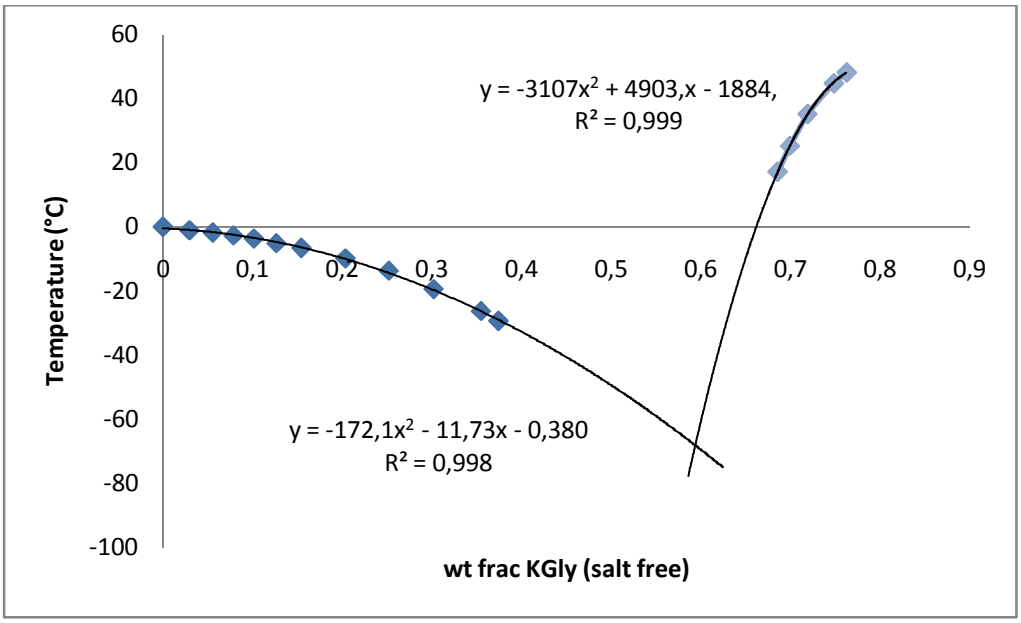

Figure 66. Temperature vs wt fraction KGly for the 0.1 CO_2 loading.

If two polynomial trendlines were plotted for these results in Figure 66, the intersection between both trendlines (eutectic point) should be at the KGly mass fraction of 0.594.

9.4.6.1.2. CO_2 loading: 0.25.

Different potassium glycinate mass fractions were prepared in order to determine their freezing points. Table 32 shows the mean temperatures and their standard deviation for all the KGly mass fractions prepared. From 0.3990 KGly mass fraction the solutions were needed to be warmed up. Crystals were amorphous at low potassium glycinate mass fractions (0.0242-0.3739) and white at high KGly mass fractions (0.3990-0.7046).

Table 32. Weights, mean temperature and standard deviations for 0.25 CO_2 loading.

wt frac KGly, salt free	m H_2O (g)	m Gly (g)	m $KHCO_3$ (g)	m KOH (g)	Mean T (°C)	T Stddev (°C)
0.0000	5.000	0.000	0.000	0.000	-0.297	0.031
0.0242	5.018	0.094	0.027	0.055	-0.66	0.005
0.0516	5.005	0.184	0.061	0.120	-1.57	0.013
0.1004	5.021	0.381	0.128	0.255	-3.50	0.004
0.1292	5.021	0.511	0.176	0.334	-4.75	0.002
0.1510	5.022	0.624	0.211	0.403	-5.99	0.009
0.1710	5.020	0.720	0.241	0.478	-7.03	0.006
0.2012	5.096	0.903	0.302	0.595	-8.93	0.006
0.2201	5.006	1.003	0.334	0.658	-10.21	0.014
0.2506	5.024	1.204	0.409	0.790	-12.43	0.011
0.3017	5.042	1.629	0.533	1.052	-17.27	0.023
0.3257	5.013	1.801	0.607	1.187	-19.77	0.039
0.3507	5.036	2.053	0.686	1.352	-22.83	0.031
0.3739	5.037	2.303	0.768	1.517	-26.20	0.042
0.3990	5.031	2.607	0.869	1.710	3.51	0.200
0.4210	5.043	2.905	0.975	1.908	-	-
0.4499	3.013	2.001	0.676	1.317	12.66	0.787
0.4787	3.007	2.315	0.768	1.516	-	-
0.5517	3.021	3.403	1.448	2.236	-	-
0.6158	3.019	5.007	1.672	3.288	-	-
0.6420	3.024	6.004	2.003	3.947	-	-
0.6689	2.049	5.008	1.675	3.289	-	-
0.7046	2.065	7.003	2.334	4.606	-	-

Temperature standard deviations lower than 0.5°C were observed at low KGly mass fraction (from 0 to 0.3990), and standard deviations up to 0.2°C were obtained at high potassium glycinate mass fractions (up to 0.3990 KGly mass fraction).

For the 39.90 wt% KGly the sample was needed to be heated in order to dissolve all the potassium bicarbonate, potassium hydroxide and glycine not dissolved while stirring the solution. Even if the solution was very viscous, by cooling it to -31°C crystals were formed and the mean temperature at which crystals disappeared was 3.51°C.

The 0.4210 KGly mass fraction was tried to be analyzed twice, but even if the solution was cooled to -33°C, the sample was very thick and no crystals were formed. But for the 0.4499 KGly mass fraction after cooling the sample to -29.5°C crystals were formed, so it was possible to determine the temperature at which crystals disappeared. From 0.4210 to 0.7046 KGly mass fractions (excluding the 0.4499 KGly mass fraction) no crystals were obtained even if the solution reached -33°C. Furthermore the solutions were very viscous.

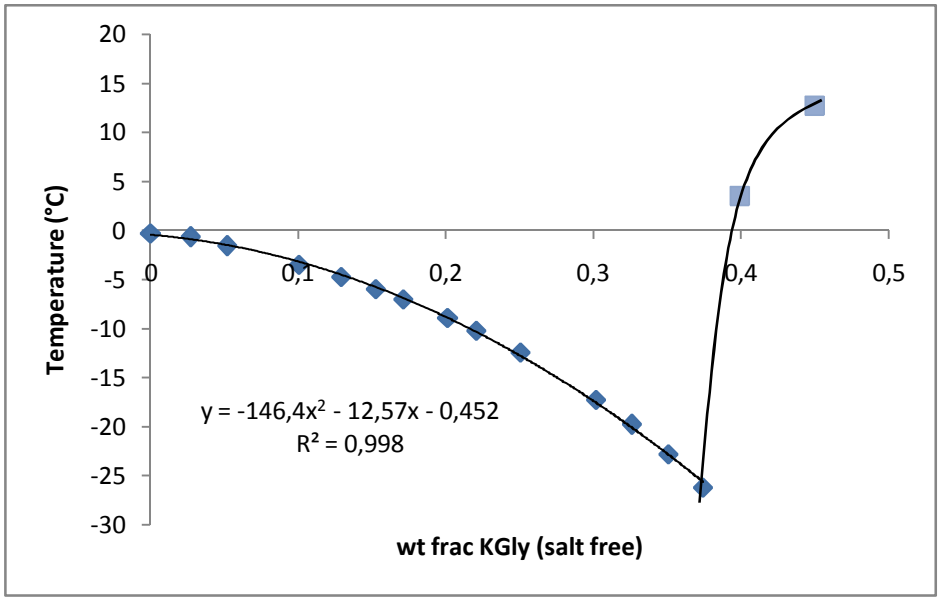

Figure 67. Freezing points for all the KGly mass fractions measured for the $KHCO_3$-KOH-Gly-H_2O system and 0.25 CO_2 loading.

Figure 67 shows all the obtained temperatures for the analyzed potassium glycinate mass fractions. No information can be obtained from the solubility curve. This curve was only represented by two points, but no more points could be determined because crystals could not be formed as the samples could not be cooled enough, so the trendline for the solubility curve was supposed as in the figure. According to these trendlines, the eutectic point seems to be at 0.3739 KGly mass fraction.

9.4.6.1.3. CO_2 loading: 0.5.

Different potassium glycinate mass fractions were analyzed. Table 33 shows the mean temperatures and the standard deviations obtained for the different KGly mass fractions. From 0.3225 KGly mass fraction the solutions were warmed up to dissolve all the potassium bicarbonate, potassium hydroxide and glycine that were in the samples. Then the solutions needed to be cooled to -17/-28 °C in order to notice the crystal formation. Crystals were amorphous (low KGly mass fractions) and white (high KGly mass fractions).

Table 33. Weights, measured temperatures and standard deviations for the $KHCO_3$:KOH:Gly:H_2O system (relation K:Gly 1:1 and 0.5 CO_2 loading).

wt frac KGly, salt free	m H_2O (g)	m Gly (g)	m $KHCO_3$ (g)	m KOH (g)	Mean T (°C)	T Stddev (°C)
0.0000	5.000	0.000	0.000	0.000	-0.116	0.045
0.0237	5.007	0.081	0.055	0.037	-0.65	0.012
0.0511	5.002	0.181	0.121	0.079	-1.54	0.008
0.1005	5.016	0.381	0.256	0.167	-3.31	0.006
0.1272	5.017	0.500	0.337	0.223	-4.37	0.010
0.1504	5.011	0.611	0.409	0.267	-5.26	0.011
0.1714	5.036	0.721	0.484	0.316	-6.25	0.012
0.2035	5.037	0.900	0.600	0.395	-7.76	0.007
0.2199	5.057	1.003	0.674	0.442	-8.79	0.016
0.2523	5.013	1.208	0.802	0.529	-10.87	0.012
0.2647	5.059	1.306	0.869	0.571	-11.65	0.008
0.2921	5.025	1.507	1.002	0.657	-14.60	0.019

0.3225	5.010	1.750	1.169	0.769	-14.80	0.195
0.3534	5.033	2.060	1.368	0.900	-18.73	0.056
0.3574	3.008	1.251	0.834	0.551	5.27	-
0.3733	3.009	1.352	0.905	0.595	11.58	0.790
0.4000	3.034	1.551	1.034	0.681	17.94	0.471
0.4277	3.001	1.758	1.167	0.770	27.00	0.770
0.4556	3.000	2.005	1.343	0.882	31.82	0.119
0.4995	3.018	2.503	1.667	1.099	41.74	0.177

For KGly low mass fractions (0.02-0.3225) standard deviations lower than 0.02°C were obtained, which indicate a good accuracy. But when KGly mass fractions increase (0.3534-0.4995) standard deviations up to 0.06°C were observed.

Two measurements were done for a KGly mass fraction near the 0.35 KGly mass fraction. In the first measurement (0.3534 KGly mass fraction) the freezing point was at a low temperature. But in the second measurements (0.3574 KGly mass fraction) a temperature above 0°C was obtained. This could explain that in the first experiment the temperature obtained indicates the metastable point, while the second temperature indicates the solubility point. Therefore it will be considered the 0.3574 KGly mass fraction as part of the solubility curve, and the 0.3534 KGly mass fraction will not be considered in the phase diagram. Furthermore it was very difficult to determine the exact temperature value as the wrong temperature was also obtained (metastable point).

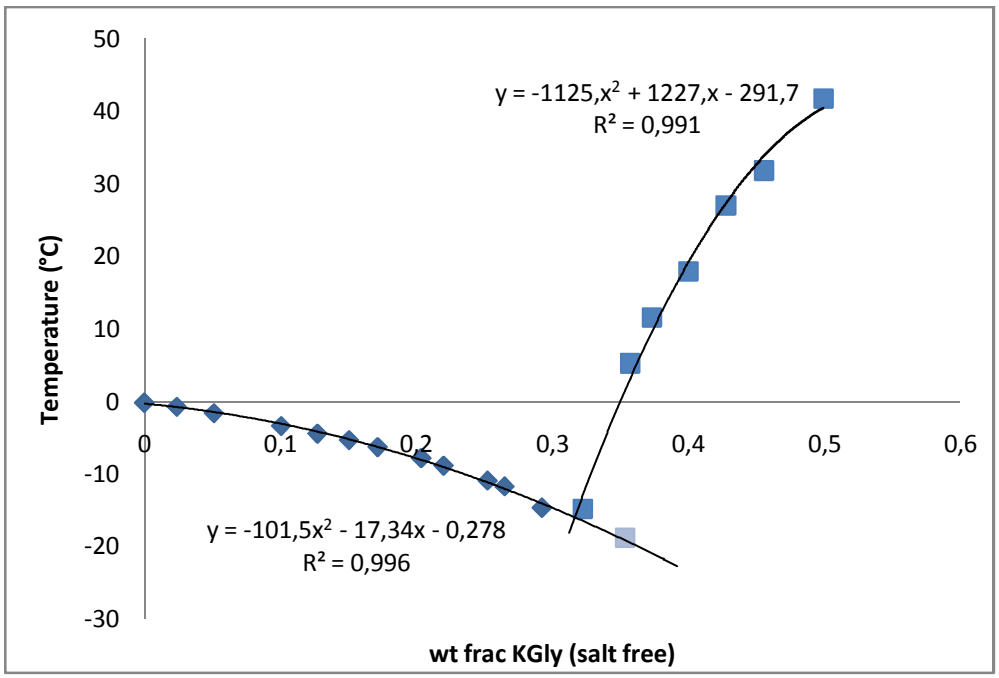

Figure 68. Temperature vs KGly mass fraction for the $KHCO_3$:KOH:Gly:H_2O system (relation K:Gly 1:1 and 0.5 CO_2 loading).

Figure 68 represents the obtained temperatures for the different potassium glycinate mass fractions. Tendencies for both freezing and solubility curves are polynomial. In Figure 68 it can be seen that the temperature for the 0.3534 KGly mass fraction is the lowest temperature of the system. Furthermore, this point is supposed to be in the solubility curve as the eutectic point is at approximately 0.3166 KGly mass fraction; so the point obtained is a metastable point.

9.4.6.1.4. Comparison for the $KHCO_3$: KOH: Gly: H_2O system (K:Gly relation 1:1).

In order to compare all the results obtained for this system, all the data are plotted in Figure 69. Furthermore, the zero CO_2 loading (potassium hydroxide-glycine-water system) and the 1 loading (potassium bicarbonate-glycine-water system) were also considered.

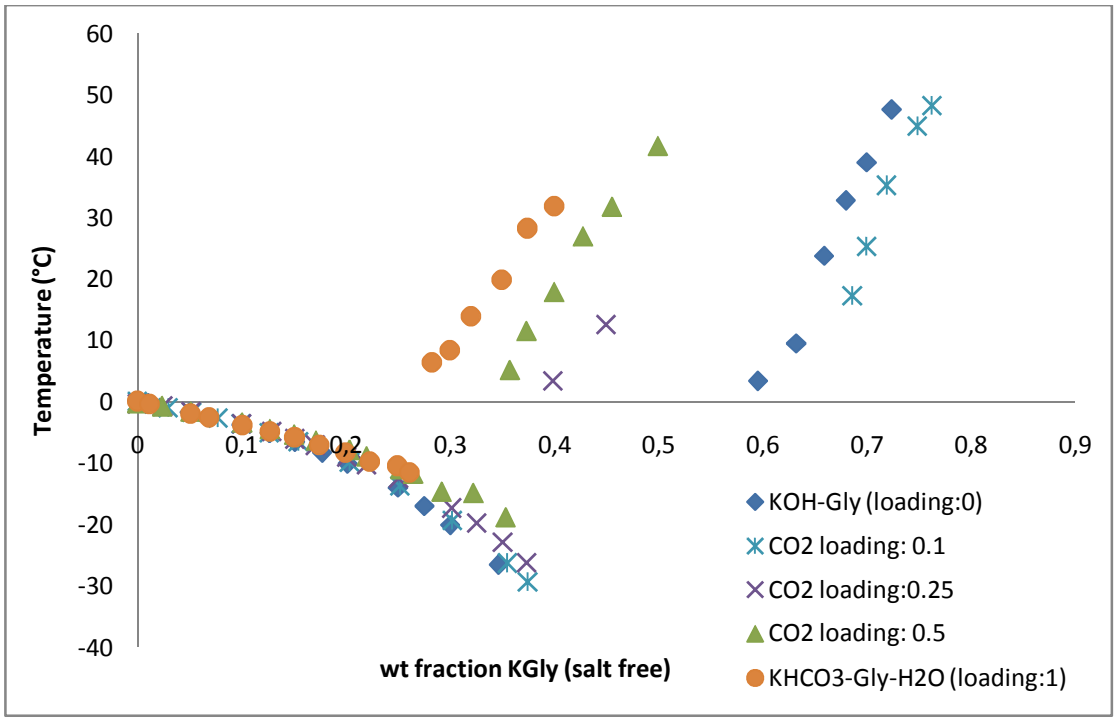

Figure 69. Temperatures and KGly mass fractions of the $KHCO_3$: KOH: Gly: H_2O system for the different CO_2 loadings, the KOH-Gly- H_2O system, and the $KHCO_3$-Gly- H_2O system.

Figure 69 represents the comparison between different systems with different CO_2 loadings. All the systems have the same tendency for both freezing and solubility curves. Comparing all the $KHCO_3$-KOH-Gly-H_2O systems for different CO_2 loadings, for low potassium glycinate mass fractions (from 0 to approximately 0.17 KGly mass fractions) the freezing points were obtained quite at the same temperatures. From 0.2 to 0.4 KGly mass fraction can be observed that the higher CO_2 loading is the nearer the freezing curve is to the x axis. Instead for the solubility curves the tendency is the same for all the systems, but the KGly mass fractions change. As the CO_2 loading increase, the solubility curve is compressed to the y axis.

To sum up, if the zero CO_2 loading is not taken into account, as the CO_2 loading increases the phase diagram is more compressed towards the y axis. The lower the CO_2 loading is considered the lower the freezing points are, and the bigger the KGly mass fractions are for the solubility curve.

9.4.6.2. Relation K:Gly 2:1.

9.4.6.2.1. CO_2 loading: 0.1.

Different potassium glycinate mass fractions were analyzed to obtain their freezing points. Table 34 shows all the freezing points for the solutions prepared and their standard deviations. From 0.4510 KGly mass fraction the solutions were needed to be warmed up to dissolve all the potassium bicarbonate, potassium hydroxide and glycine in the sample. Crystals for this system were amorphous at low KGly mass fractions (0.0193-0.2032) and white for high KGly mass fractions (0.4510-0.6475).

Table 34. Weights, Mean temperatures and standard deviations for the K: Gly relation 2:1 (0.1 CO_2 loading).

wt frac KGly, salt free	m H_2O (g)	m Gly (g)	m $KHCO_3$ (g)	m KOH (g)	Mean T (°C)	T Stddev (°C)
0.0000	5.000	0.000	0.000	0.000	0.260	0.025
0.0193	5.007	0.066	0.007	0.068	-0.60	0.002
0.0504	5.052	0.181	0.026	0.300	-3.40	0.013
0.0764	5.012	0.283	0.038	0.471	-5.71	0.023
0.1022	5.012	0.393	0.055	0.650	-7.96	0.015
0.1282	5.035	0.516	0.067	0.839	-10.71	0.023
0.1552	5.020	0.650	0.085	1.055	-14.53	0.018
0.2032	5.015	0.924	0.122	1.518	-22.98	0.023
0.2494	5.055	1.248	0.167	2.067	-	-
0.2997	5.021	1.653	0.223	2.755	-	-
0.3539	5.020	2.214	0.298	3.667	-	-
0.3773	5.043	2.518	0.336	4.168	-	-
0.3945	5.233	2.862	0.389	4.751	-	-
0.4510	3.027	2.241	0.302	3.700	5.16	0.870
0.4713	3.018	2.504	0.336	4.168	16.76	0.564
0.4993	3.026	2.952	0.393	4.922	37.12	0.726
0.5249	3.038	3.459	0.466	5.761	54.39	0.288
0.5494	3.016	4.021	0.538	6.702	66.79	0.115
0.5788	3.077	5.025	0.668	8.333	76.41	0.193
0.6045	3.005	6.005	0.803	9.999	83.94	0.255
0.6475	2.013	6.008	0.801	9.999	-	-

From 0.2494 to 0.3945 KGly mass fraction no crystals were formed even if the sample temperature was low (approximately of -33°C). This is because it was not possible to cool the solution enough to form the crystals. The cooling bath could not reach temperatures below -36 °C.

As shown in Table 34 standard deviations up to 0.1°C were observed for high KGly mass fractions (above 0.4510 KGly mass fraction). This is due to the difficulty to measure the temperature at which crystals disappeared. So these measurements were not very accurate, but standard deviations for low KGly mass fractions were lower than 0.03°C, and mean temperatures were obtained very accurately.

Taking the measurements for the 20.32 wt% KGly required a lot of time, but finally the freezing point was obtained; however for the 24.94 wt% KGly, after 30 minutes of cooling the sample no crystals were formed at -33°C. The same phenomena occurred for the potassium glycinate mass fraction 0.3539.

Analyzing the 0.2494 KGly mass fraction by microscope using liquid nitrogen in order to decrease the temperature of the sample, crystals were formed at approximately -32 °C (Figure 70).

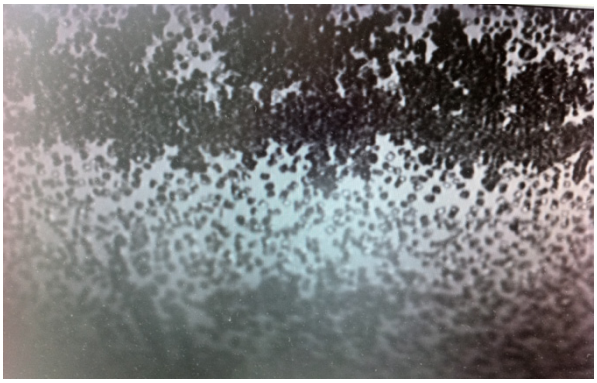

Figure 70. Crystals for the 0.2494 KGly mass fraction at approximately -32°C.

The rest of high KGly mass fractions needed to be cooled to different temperatures; for example, for the 0.4713 KGly mass fraction the sample was cooled to 17 °C, the 0.4993 KGly mass fraction was cooled to -0.1°C, and the 0.5788 KGly mass fraction was cooled to -18°C. For the 0.6475 KGly mass fraction was impossible to dissolve all the potassium bicarbonate, potassium hydroxide and glycine.

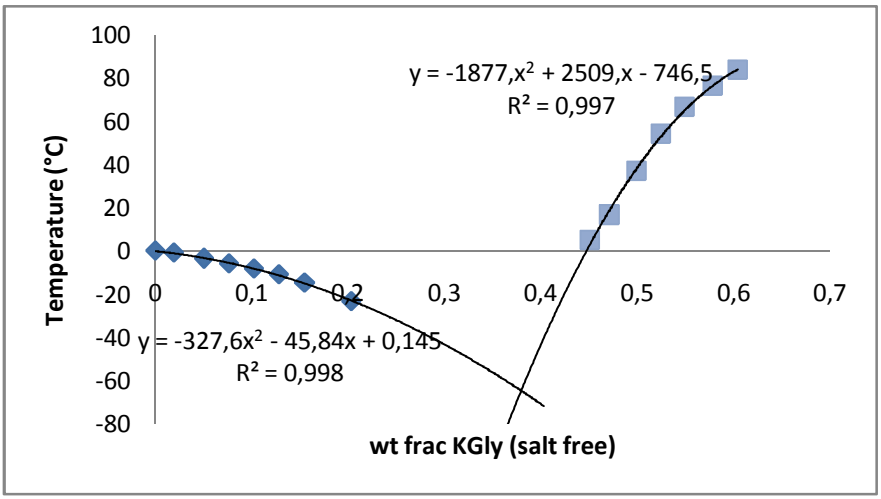

Figure 71. Phase diagram for the $KHCO_3$-KOH-Gly-H_2O system with a K:Gly relation 2:1 (0.1 CO_2 loading).

Figure 71 represents the freezing points for the analyzed KGly mass fractions. In this figure it can be seen the gap between 20 and 45 wt% KGly, and as explained above, the lack of results is due to the low temperatures required for these mass fractions. The eutectic point seems to be at a KGly mass fraction of 0.3797. Representing all the data of Table 34 the temperature for the 0.2494 KGly mass fraction was not considered due to this temperature was obtained by microscope and not with the freezing point depression method, but it can also be concluded that this point fits in the freezing curve trendline.

9.4.6.2.2. CO_2 loading: 0.25.

Potassium glycinate mass fractions between 0.0104 and 0.6078 were analyzed. Table 35 contains all the results for the measurements done in the laboratory. From the 0.4746 KGly mass fraction solutions were needed to be warmed in order to dissolve all the potassium bicarbonate, potassium hydroxide and glycine present in the sample. For this mass fraction, bubbles were formed during the stirring, and some crystals were formed at -18°C although the solutions were very viscous. Crystals were amorphous (0.01-0.2238 KGly mass fractions) and white (0.4746-0.6078 KGly mass fractions).

Table 35. Weights, mean temperatures and standard deviations for the following KGly mass fractions.

wt frac KGly, salt free	m H_2O (g)	m Gly (g)	m $KHCO_3$ (g)	m KOH (g)	Mean T (°C)	T Stddev (°C)
0.0000	5.000	0.000	0.000	0.000	0.096	0.011
0.0104	5.009	0.035	0.012	0.056	-0.37	0.011
0.0541	5.075	0.196	0.065	0.294	-3.06	0.003
0.0776	5.012	0.287	0.095	0.430	-4.84	0.002
0.1020	5.027	0.393	0.132	0.604	-7.01	0.003
0.1268	5.014	0.506	0.168	0.776	-9.50	0.005
0.1519	5.022	0.632	0.212	0.983	-12.95	0.013
0.2017	5.022	0.913	0.304	1.405	-20.73	0.007
0.2238	5.032	1.057	0.357	1.615	-25.54	0.040
0.2512	5.011	1.244	0.418	1.910	-	-
0.3009	5.042	1.661	0.554	2.544	-	-
0.4018	3.023	1.701	0.567	2.611	-	-
0.4330	3.017	2.001	0.668	3.069	-	-
0.4507	3.039	2.215	0.738	3.379	-	-
0.4746	3.017	2.510	0.834	3.846	33.43	0.782
0.4973	3.068	2.902	0.967	4.458	51.44	0.293
0.5196	3.023	3.259	1.089	4.996	64.83	0.788
0.6078	3.037	6.002	2.001	9.214	-	-

As shown in Table 35 from 0.2512 to 0.4507 KGly mass fraction no results were obtained for the freezing point. Standard deviations lower or equal to 0.04°C were observed for low KGly mass fractions (0.01-0.2238), and standard deviations up to 0.2°C were obtained for KGly mass fractions between 0.4746 and 0.6078.

For the 25.12 wt% KGly no crystals were formed during the measurements, but analyzing the sample in the microscope some crystals could be seen at approximately -29°C (Figure 72). So from 25.12 wt% KGly I could not reach the temperature at which crystals were formed, and besides solutions were very viscous.

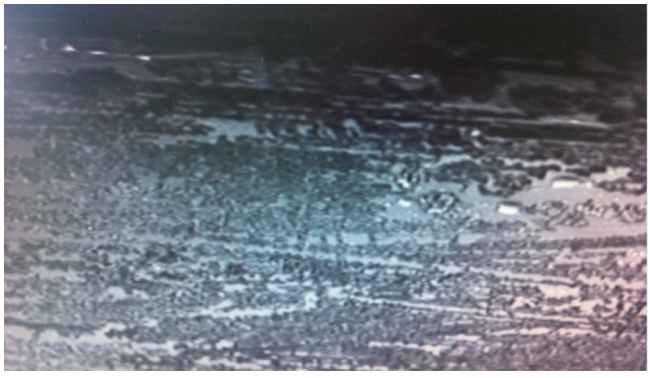

Figure 72. Crystals seen by microscope for the 0.2512 KGly mass fraction (CO_2 loading 0.25).

Also for the 0.4973 KGly mass fraction the solution was very thick, but it was cooled to -20°C. I could not dissolve all the sample of 0.6078 KGly mass fraction because it was very viscous.

Depending on the tendency of the solubility curve, two different trendlines can be plotted: a linear (Figure 73) and a polynomial (Figure 74) tendency.

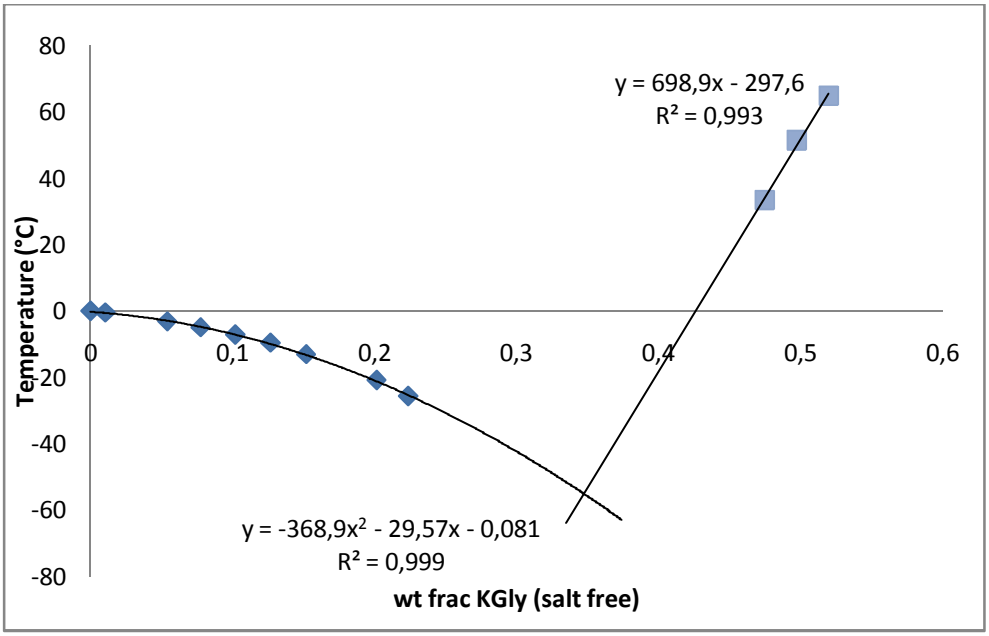

Figure 73. Temperature vs KGly mass fraction for the $KHCO_3$-KOH-Gly-H_2O system (K:Gly relation 2:1 and 0.25 CO_2 loading) with a linear tendency for the solubility curve.

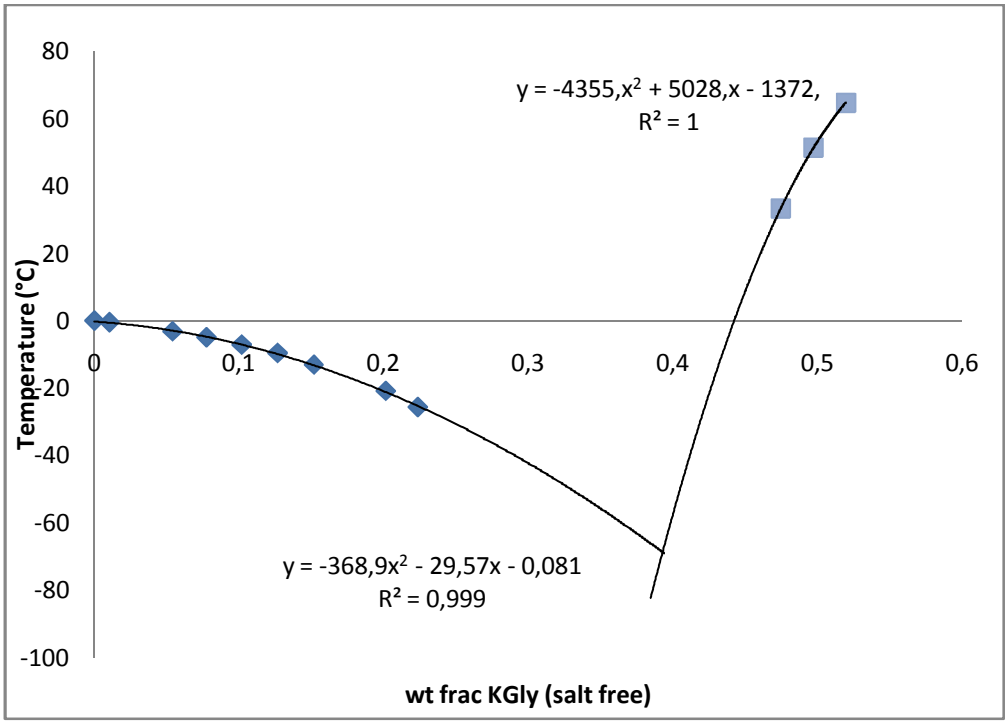

Figure 74. Temperature vs KGly mass fraction for the $KHCO_3$-KOH-Gly-H_2O system (K:Gly relation 2:1 and 0.25 CO_2 loading) with a polynomial tendency for the solubility curve.

Based on the two tendencies, the eutectic point is placed at a different potassium glycinate mass fraction: 0.347 KGly mass fraction (Figure 73) and 0.393 KGly mass fraction (Figure 74). As no other

temperatures were obtained for KGly mass fractions up to 0.6078 we could not tell if the solubility curve tendency is linear or polynomial.

9.4.6.2.3. CO_2 loading: 0.5.

Different potassium glycinate mass fractions were prepared to determine their freezing points. Table 36 shows all the data collected. From 0.5003 KGly mass fraction the samples needed to be warmed to dissolve all the potassium hydroxide, potassium bicarbonate and glycine. Then the samples were cooled to -21/-27°C to form some crystals. From 0.01 to 0.4559 KGly mass fractions crystals were amorphous, and they were white at KGly mass fractions up to 0.5003.

Table 36. Weights, Mean temperature and standard deviations for the 0.5 CO_2 loading of the system $KHCO_3$-KOH-Gly-H_2O (relation K: Gly 2:1).

wt frac KGly, salt free	m H_2O (g)	m Gly (g)	m $KHCO_3$ (g)	m KOH (g)	Mean T (°C)	T Stddev (°C)
0.0000	5.000	0.000	0.000	0.000	0.150	0.032
0.0103	5.053	0.035	0.030	0.047	-0.38	0.009
0.0538	5.018	0.192	0.127	0.251	-2.75	0.010
0.0762	5.022	0.282	0.192	0.372	-4.38	0.012
0.1018	5.073	0.394	0.263	0.516	-6.36	0.006
0.1266	5.013	0.503	0.337	0.663	-8.67	0.010
0.1526	5.033	0.634	0.428	0.833	-11.27	0.009
0.2037	5.021	0.920	0.608	1.202	-18.23	0.007
0.2248	5.019	1.053	0.705	1.380	-21.71	0.010
0.2523	5.012	1.243	0.836	1.642	-26.63	0.032
0.2986	5.147	1.656	1.107	2.174	-	-
0.4559	3.022	2.212	1.473	2.896	-	-
0.5003	3.004	2.803	1.872	3.686	49.80	0.520
0.5236	2.024	2.159	1.437	2.833	67.43	0.729
0.5538	2.034	2.606	1.743	3.426	-	-

As reported in Table 36 standard deviations lower than 0.03°C were observed for the measurements of the freezing points, and standard deviations up to 0.5°C were obtained for the solubility points.

For the 0.2986 KGly mass fraction no crystals were formed, so no freezing point could be determined. Besides for the 0.4559 KGly mass fraction was not possible to cool the solution enough to form crystals. Furthermore for the 55.38 wt% KGly the solution could not be dissolved, and it had a white color even before heating it.

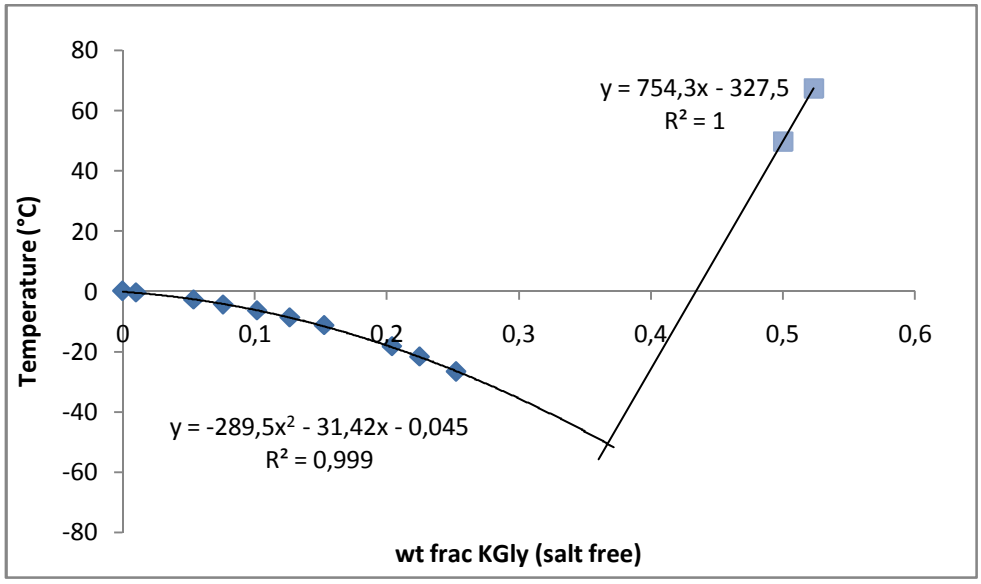

Figure 75. Phase diagram for the $KHCO_3$-KOH-Gly-H_2O system with a K: Gly relation 2:1 and a CO_2 loading of 0.5.

Figure 75 represents all the freezing and solubility points obtained during the laboratory experiments. As only two points were determined for the solubility curve, the tendency of this curve is linear, while the trendline for the freezing curve is polynomial. Both curves intersect at 0.3671 KGly mass fraction (eutectic point).

9.4.6.2.4. Comparison for the $KHCO_3$: KOH: Gly: H_2O system (K:Gly relation 2:1).

All the data measured for the potassium bicarbonate-potassium hydroxide-glycine-water system taking in consideration the K:Gly relation 2:1 were plotted in Figure 76.

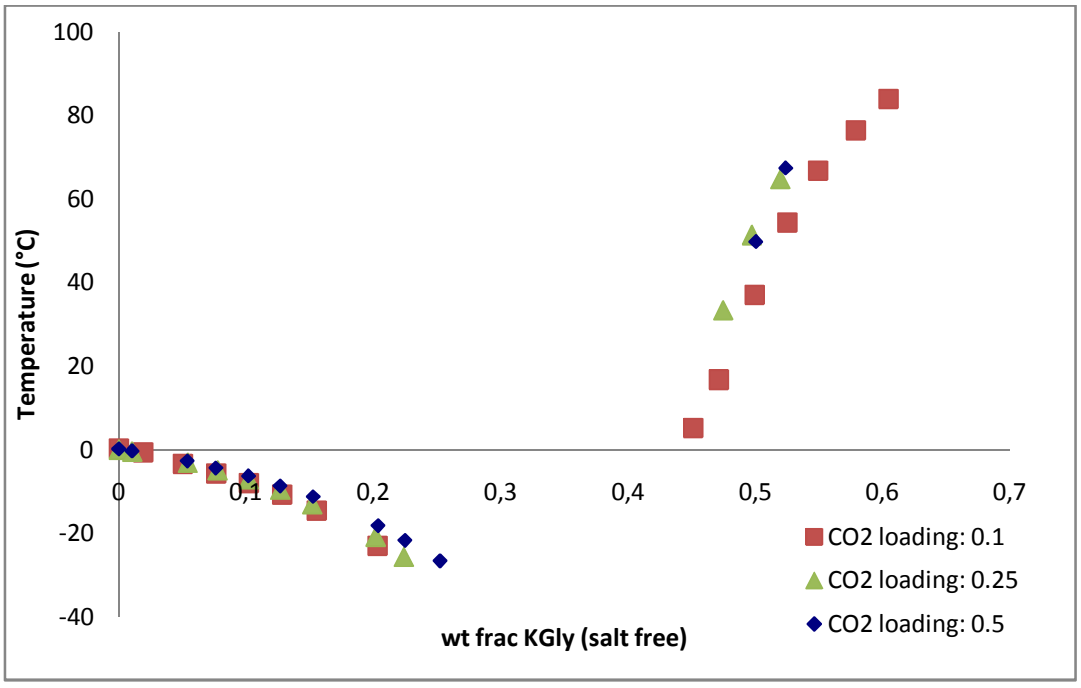

Figure 76. Comparison between the different CO_2 loadings for the $KHCO_3$-KOH-Gly-H_2O system (K:Gly 2:1).

As shown in Figure 76 at low KGly mass fractions (0-0.15) all the freezing points for all the studied CO_2 loadings were quite the same, so no notable difference can be seen in the figure on adding CO_2. From 0.2 to 0.27 KGly mass fractions the freezing points did not have the same value, although the difference between these temperatures was not very big. However for the solubility curve it can be seen that KGly mass fractions vary. Although no KGly mass fraction difference was obtained for 0.25 and 0.5 CO_2 loadings (blue and green points in Figure 76), a difference between these CO_2 loadings and the 0.1 CO_2 loading was clear. Taking into account a constant temperature, as CO_2 loading increases the KGly mass fraction is reduced, so the curve is more compressed.

Nevertheless the difference in KGly mass fraction for the different carbon dioxide loadings was not so big. So we can conclude that there is no effect of CO_2 in the $KHCO_3$-KOH-Gly-H_2O system with an excess of potassium cations.

9.4.6.3. Comparison between $KHCO_3$-KOH-Gly-H_2O systems with different K:Gly relations.

This section wants to examine the difference between adding an excess of potassium cation (K:Gly relation 2:1) and considering the stoichiometric K:Gly relation. Two different behaviors were found while comparing the K:Gly relations 1:1 and 2:1. Figure 77 and Figure 78 represent the different K:Gly relations for each CO_2 loading.

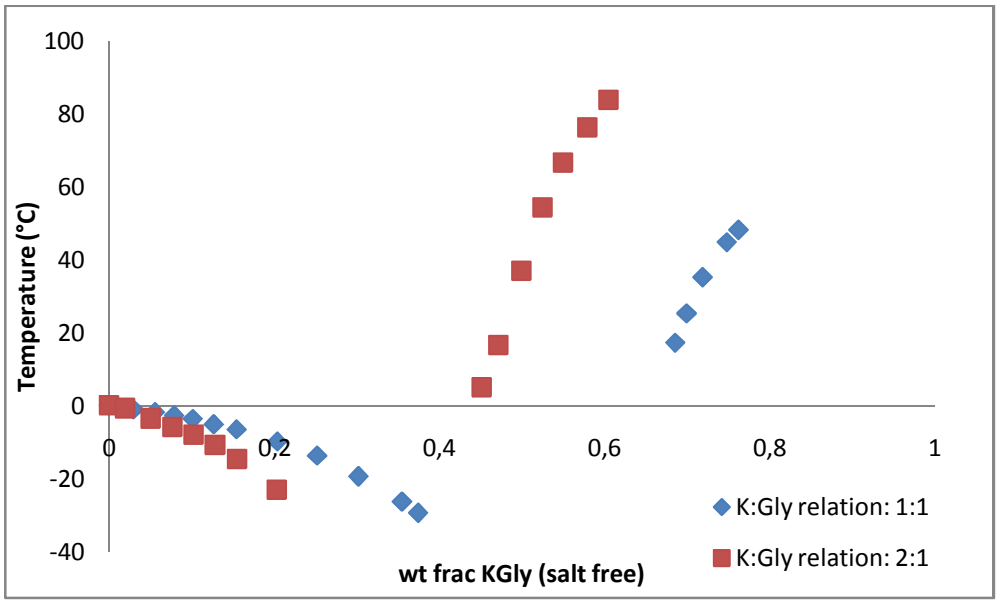

Figure 77. Comparison between the K:Gly relations 1:1 and 2:1 for the same 0.1 CO_2 loading.

Figure 77 compares both K:Gly relations for the same CO_2 loading (0.1). Regarding the freezing curve the more amount of potassium bicarbonate and potassium hydroxide was considered (more K, so the K:Gly relation 2:1), the lower the freezing points were. Considering the solubility curve, the more potassium bicarbonate and potassium hydroxide were considered (K:Gly relation 2:1), the lower KGly mass fractions were obtained. So the more potassium cation is considered, the more compressed the diagram is to the y axis.

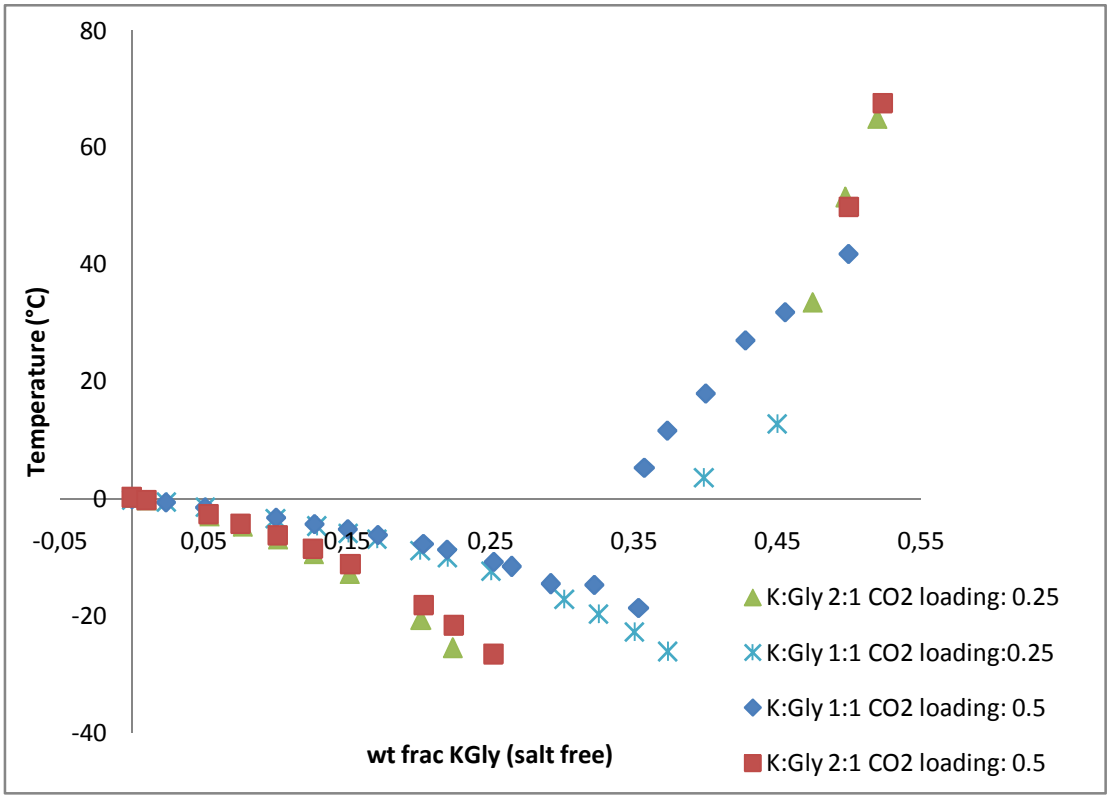

Figure 78. Comparison between the K:Gly relations 1:1 and 2:1 for the 0.25 and 0.5 CO_2 loadings.

In Figure 78, for the freezing curve the tendency of the curves was the same as for the 0.1 CO_2 loading: as the potassium cation increases (K:Gly relation 2:1) the freezing points are lower, so the freezing curve is nearer the y axis. But the behavior of the solubility curve cannot be determined as no points can be comparable.

9.5. Comparison between sodium and potassium systems.

In order to compare the SLE diagrams for both amino acids, sodium and potassium glycinate, a molal base was considered. The main objective of comparing the sodium systems with the potassium system is to determine if there are noticeable differences between the two system with respect to freezing point and solubilities.

In general, experiments with potassium bicarbonate and potassium hydroxide were easier to do, compared to the equivalent sodium systems. The solubility curve in the sodium system could not be determined for cases containing excess NaOH.

Figure 79 represents the phase diagram for NaOH-Gly-H_2O and KOH-Gly-H_2O systems for different (moles of NaOH (or KOH) per mole of Gly) relations.

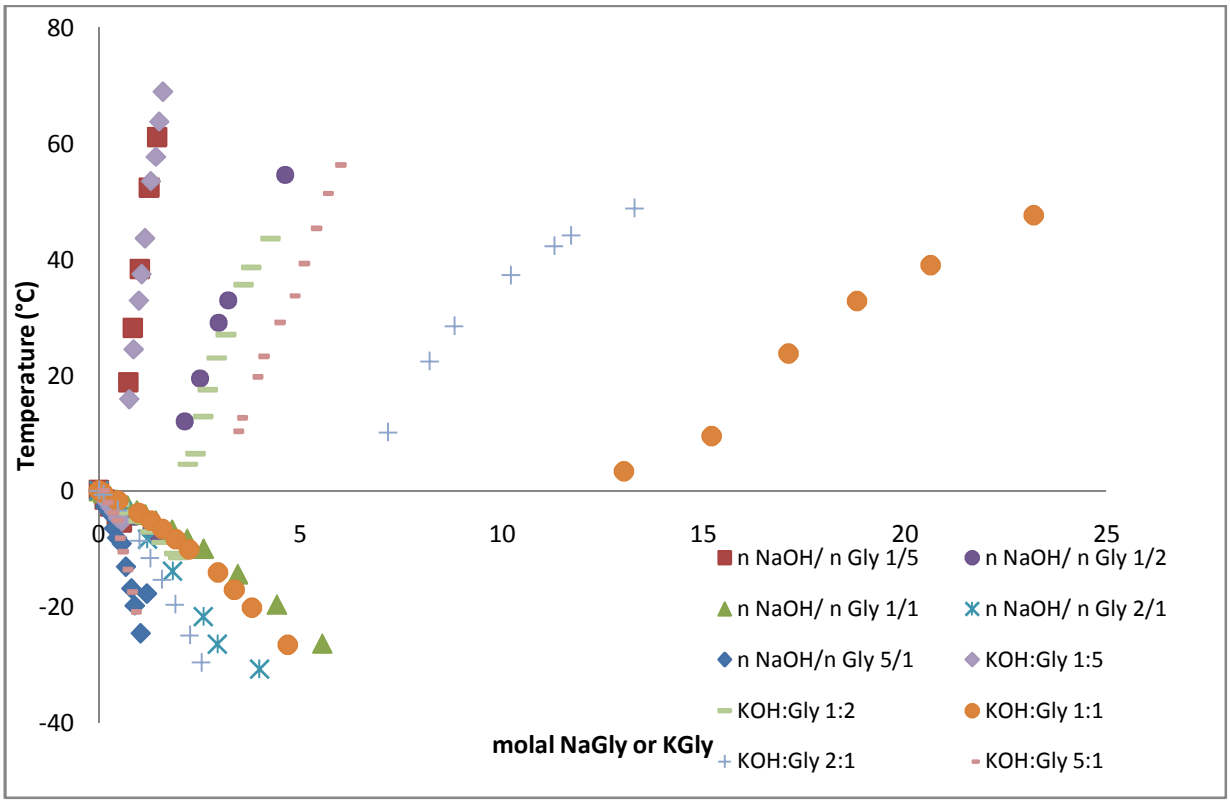

Figure 79. Comparison between NaOH-Gly-H_2O system and KOH-Gly-H_2O system for different n(NaOH or KOH)/n Gly.

Figure 79 shows that the lowest freezing points were obtained for the 5 to 1 relation between moles of NaOH or KOH and moles of glycine. The highest freezing points were obtained for the 1 to 1 NaOH or KOH per mole of glycine. The solubility curve looks very much the same. Almost no differences are observed between the sodium and potassium systems. The only exception in the cases for excess NaOH in which solubility could not be determined and the comparison to potassium is therefore not possible.

Figure 80 shows the results for the $NaHCO_3$-Gly-H_2O system and $KHCO_3$-Gly-H_2O system with different n$NaHCO_3$ ($KHCO_3$)/nGly ratios.

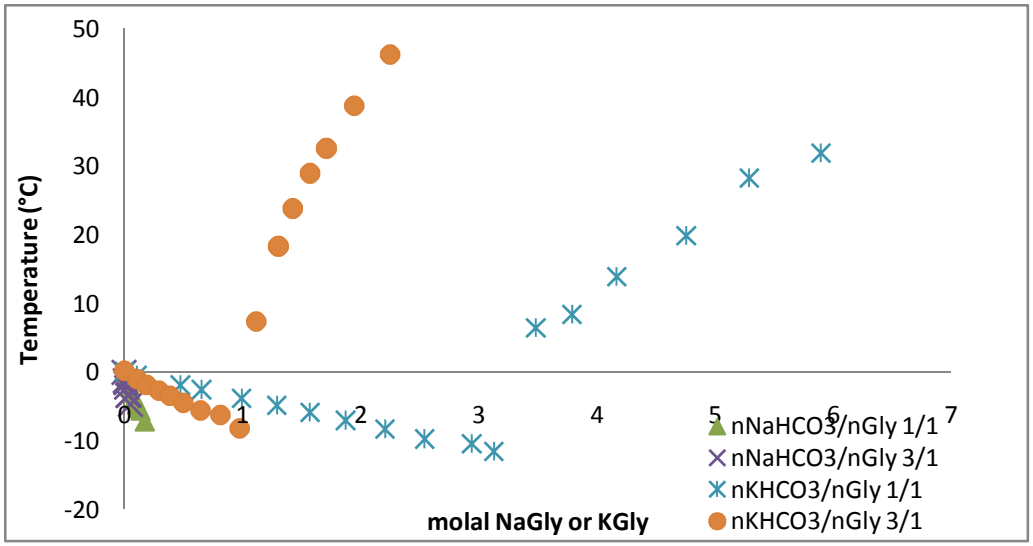

Figure 80. Comparison between $NaHCO_3$-Gly-H_2O system and $KHCO_3$-Gly-H_2O system with different $nNaHCO_3$ ($KHCO_3$)/nGly ratios.

The main difference between the sodium and the potassium systems is that the freezing point in the sodium system is much lower than the potassium system. But the tendency for the freezing points is the same for the four systems. No comparison can be made for solubility curves since was not possible to obtain measurements of the solubility in the sodium system.

Figure 81 shows all the data collected in this report for the sodium bicarbonate-sodium hydroxide-glycine-water system and the potassium bicarbonate-potassium hydroxide-glycine-water system.

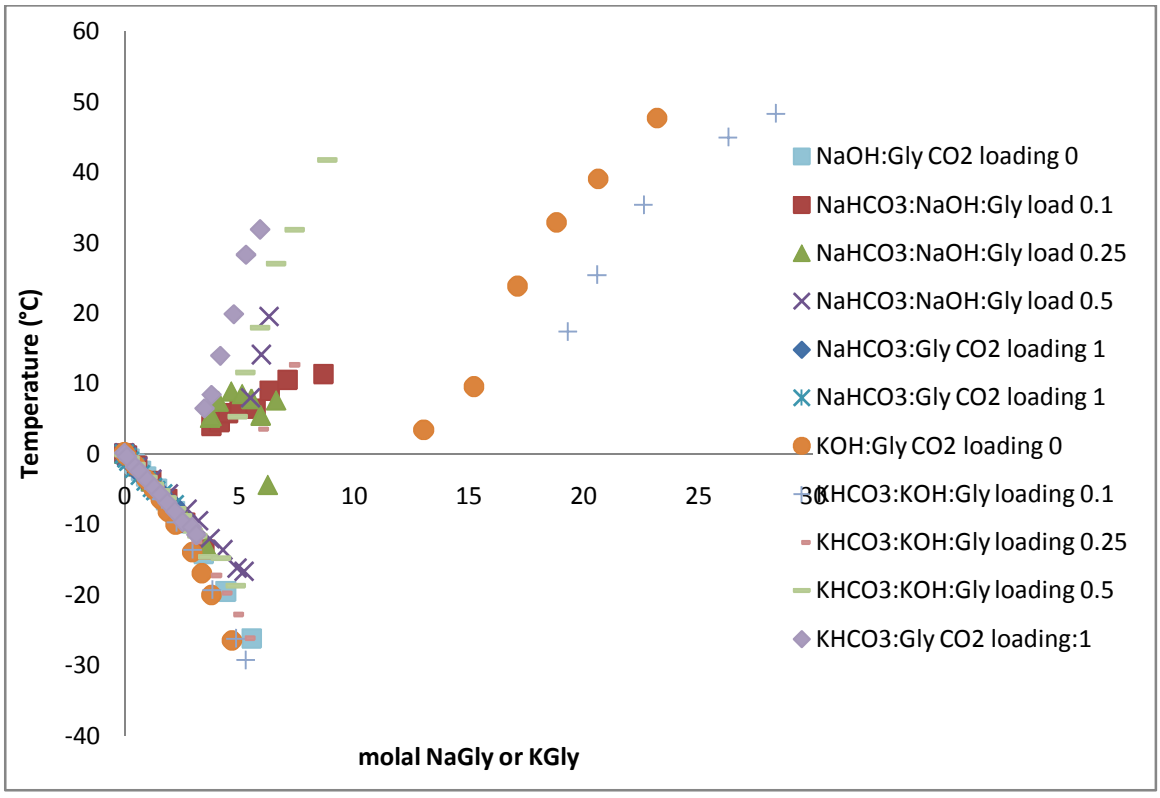

Figure 81. Comparison between $NaHCO_3$-NaOH-Gly-H_2O and $KHCO_3$-KOH-Gly-H_2O systems.

Freezing points for both systems and the different carbon dioxide loadings are quite the same at low molals. But from 2.5 to 4 molal NaGly or KGly the tendency changes a lot depending on the CO_2 loading and the amino acid. Regarding the solubility curve, different tendencies can be seen in Figure 81.

With the exception of the 0.1 loading, as the CO_2 loading increases the curves are more compressed, so the freezing points are higher and the solubility points are lower. So the 1 CO_2 loading for the potassium glycinate is the one that has a lower molal KGly.

9.6. Piperazine.

Piperazine (PZ) is an organic compound used as an accelerator (or activator) to remove carbon dioxide from process gases. Although piperazine is a colorless crystalline compound, at ambient temperature is a white solid.

Compared to other activators as MEA (monoethanolamine) piperazine has some advantages, although some disadvantages are also considered. Piperazine is more reactive with CO_2 than MEA (thirty times faster than MEA). In addition piperazine is more stable than MEA, so secondary environmental impact rates are reduced. Finally piperazine absorbs carbon dioxide 20% to 100% faster than MEA, and it can be also recovered by evaporation. As the boiling point of piperazine is lower than the boiling point of MEA it is more volatile, so this is a disadvantage when concentrations are big enough to obtain high capacity for CO_2 absorption. Furthermore piperazine is three to ten times more expensive than MEA [72].

In addition combinations of piperazine with MEA, MDEA or AMP (2-Amino-2-methyl-1-propanol) are also very promising as the reaction rate increases [73]. In the case of the piperazine-AMP system piperazine is a good promoter compared to MEA and DEA as is more effective than the other promoters.

A new aqueous solvent containing potassium carbonate and piperazine is under study for separating CO_2 from waste gas streams. In this study the potassium bicarbonate-piperazine-water system is under investigation.

Different molal (moles of piperazine/ kg water) ratios were analyzed: 2.2 and 3.6 molal PZ. In order to prepare these solutions, the solvent used during the measurements was prepared by mixing piperazine and water in different concentrations. Weighting piperazine and water was done, and the solution was stirred till all the piperazine was dissolved in water. Furthermore, another solvent was prepared, but this solvent was obtained by mixing potassium bicarbonate and water, so the molality ($KHCO_3$) of the final solution was 4.6.

The property studied for these systems was solubility. So the experimental method carried out was the same as the one explained in the section “8. Experimental method.” for solubility points. For most of the measurements temperatures (solubility points) were up to 0°C.

As most of the temperatures were up to 0°C, another setup different from the one used for obtaining freezing points was used. Also the temperature average varies, and because of that the calibration of the equipment was different. Calibration was made by other students, and the temperature average was 0-100°C. For these experiments the calibration data (M and B values) were M= 0.997796 and B=-0.248113.

During the measurements, from three to five temperatures were taken for each solution in order to obtain low standard deviations.

9.6.1. Solvent: 2.2 molal PZ.

First of all the solvent was prepared by mixing water and piperazine. In order to obtain a solution of 2.2 molal PZ, 168.1367 g of water and 31.8633 g of piperazine were mixed, so the solutions has a piperazine mass fraction of 0.1593. Table 37 shows the amount of water and piperazine weighted in the balance to obtain a 2.2 molal PZ solution.

Table 37. Measured amount of water and piperazine for the 2.2 molal PZ.

m water (g)	m PZ (g)	wt frac PZ	molal PZ
167.6993	31.8623	0.1596	2.2057

Different potassium bicarbonate mass fractions were prepared in order to obtain the solubility points. Solutions were made by mixing potassium bicarbonate and the solvent (2.2 moles PZ/kg water). When crystals were formed the solution had a white color.

Table 38. Weightings, measured temperatures and standard deviations using the 2.2 molal PZ solvent.

wt% $KHCO_3$	m solvent (g)	m $KHCO_3$ (g)	Mean T (°C)	T Stddev (°C)
0.000	9.0194	0.0000	23.74	0.108
2.054	9.0104	0.1890	24.09	0.069
3.989	9.0276	0.3751	24.53	0.113
5.974	9.0364	0.5741	24.26	0.128
7.976	9.0338	0.7830	23.61	0.291
9.982	9.0269	1.0010	19.66	0.099
11.996	9.0173	1.2292	17.55	0.119
13.977	9.0181	1.4653	15.21	0.091
15.953	9.0413	1.7161	11.64	0.187
17.913	9.0658	1.9783	8.73	0.190
19.966	9.0278	2.2521	2.52	0.096
21.979	9.0116	2.5386	-5.81	0.123
23.961	9.0199	2.8423	-14.77	0.162
25.983	9.0132	3.1640	-	-
27.996	9.0091	3.5028	-2.94	0.519
29.966	9.0151	3.8573	14.18	0.244

Standard deviations for these experiments are higher than for the previous experiments. Even though these values are lower than 0.2°C, with the exception of three cases.

Besides the stirring, after preparing the solutions there was a need of warming the samples in order to dissolve all the potassium bicarbonate in the solvent, even for the 0 wt% $KHCO_3$. This heat contribution was not needed for the 0.1791 and the 0.1996 $KHCO_3$ mass fractions as all the potassium bicarbonate was dissolved after stirring the solutions.

More time was needed to analyze the solutions from 22 wt% $KHCO_3$. For the 24 wt% $KHCO_3$ it took a long time to do the measurements. The sample was cooled down slowly to approximately -17.5°C, and crystals were formed at this temperature. But crystals for this solution were different from crystals of the rest of the solutions: they were tiny crystals and they were not white as the previous ones, but they were transparent.

For the 26 wt% $KHCO_3$ I could not determine the solubility point as the cooling bath only arrives to -21.1°C and this was not enough to form some crystals. The solubility point for the 28 wt% $KHCO_3$ was difficult to obtain; the solution was cooled to -16.3°C in order to form crystals.

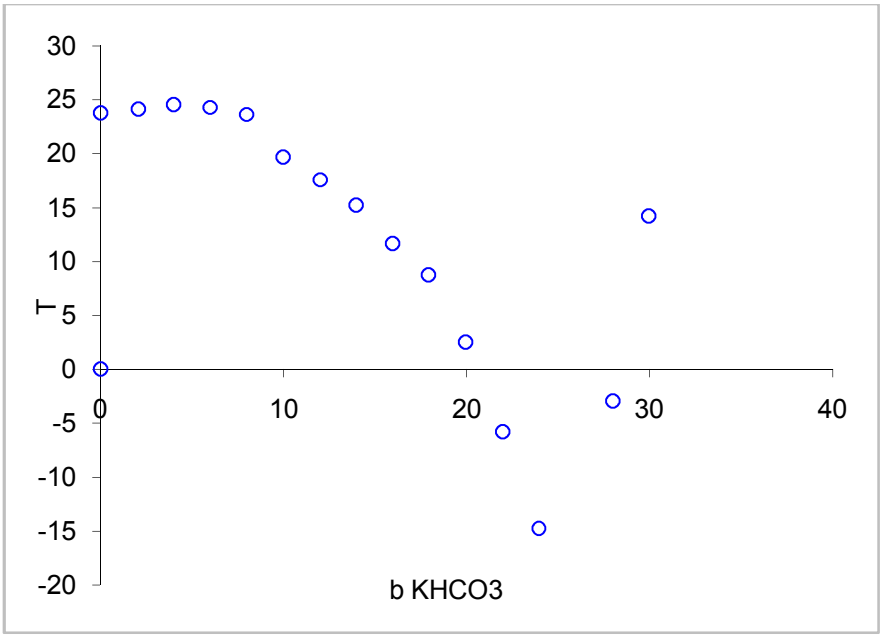

Figure 82. Temperature versus $KHCO_3$ mass fraction for the experiments carried out with the 2.2 molal PZ solvent.

Figure 82 shows the data obtained during the measurements. As shown in the figure, from 0 to 0.8 $KHCO_3$ mass fraction the temperature is quite the same, but then it begins decreasing until the temperature reached was approximately -15°C. From 25 to 28 wt% KHCO3 no data was obtained as it was not possible to form crystals. Then the temperature increases abruptly.

9.6.2. Solvent: 3.6 molal PZ.

First of all the solvent was prepared: water and piperazine were weighted so as the PZ molal concentration of the solution was 3.6. Table 39 shows all the weights taken in the laboratory.

Table 39. Measured amount of water and piperazine for the 3.6 molal PZ.

m water (g)	m PZ (g)	wt frac PZ	molal PZ
151.7239	47.3474	0.2378	3.6227

Then different solutions with a potassium bicarbonate mass fraction between 23 and 28 wt% $KHCO_3$ were prepared. After preparing all the solutions warming them was necessary in order to dissolve all the potassium bicarbonate present in the samples. All the weights and solubility points were collected in Table 40. The crystals observed in this system were white.

Table 40. Weightings, mean temperatures and standard deviations using the 3.6 molal PZ as a solvent.

wt% $KHCO_3$	m solvent (g)	m $KHCO_3$ (g)	Mean T (°C)	T Stddev (°C)
23.446	9.0308	2.7659	20.11	0.219
23.953	9.0239	2.8423	19.55	0.143
24.203	9.0242	2.8816	18.50	0.174
24.437	9.0324	2.9210	18.73	0.172

24.678	9.0359	2.9605	18.44	0.171
24.995	9.0038	3.0004	17.85	0.090
25.232	9.0236	3.0452	17.59	0.190
25.424	9.0387	3.0815	17.26	0.075
25.995	9.0041	3.1628	16.65	0.086
26.452	9.0307	3.2479	-	-
26.950	9.0236	3.3291	-	-
27.390	9.0502	3.4140	-	-
27.992	9.0084	3.5019	-	-

Table 40 shows that standard deviations for low $KHCO_3$ mass fractions are higher than standard deviations for high $KHCO_3$ mass fractions, which mean that the measurement of solubility points was more accurate when the potassium bicarbonate mass fractions were higher.

No problems were observed during the measurements of the samples with a potassium bicarbonate mass fraction between 23.5 and 26 wt%; the samples were cooled to 1-10.7 (depending on the sample) and when crystals were formed the solubility point was determined.

But from 26.5 to 28 wt%$KHCO_3$ the temperature could not be measured. When the samples were heated first the solutions were white, then at some point they turned transparent, and finally they turned white again.

Figure 83 (a) shows the solution for the 26.5 wt% $KHCO_3$ before the beaker glass was warmed up. As it can be seen not all the potassium bicarbonate was dissolved (bottom of the beaker glass), so warming the sample was needed. After warming the sample the solution became transparent but some tiny particles were observed floating in the beaker glass: some tiny crystals were formed. So when the solution in the beaker glass turned transparent, most of all the potassium bicarbonate was dissolved, but then crystals appeared and suddenly the solution became white again (Figure 83 (b)).

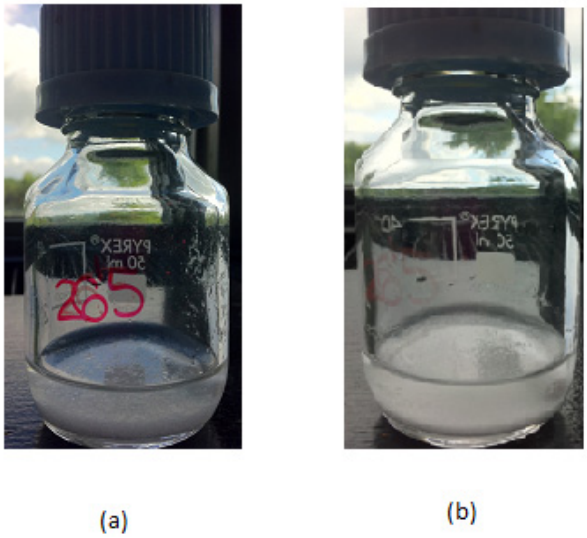

Figure 83. Photo of the solution 26.5 wt% KHCO3 before (a) and after (b) warming the sample to 99.5°C.

Figure 84 represents the 27 wt% $KHCO_3$ solution before (a) and after (b) warming the beaker glass. Before stirring the solution (Figure 84 (a)) it can be seen two different phases: the solvent and some precipitate; then when the solution was stirred a transparent phase was observed, but then the solution became white again, just as the previous $KHCO_3$ mass fraction. If the solution was left for some hours and

then it was warmed up again, no color change was observed: the solution remained white. Furthermore, the white color of the final solution was the same as the white color of the crystals obtained for the previous samples.

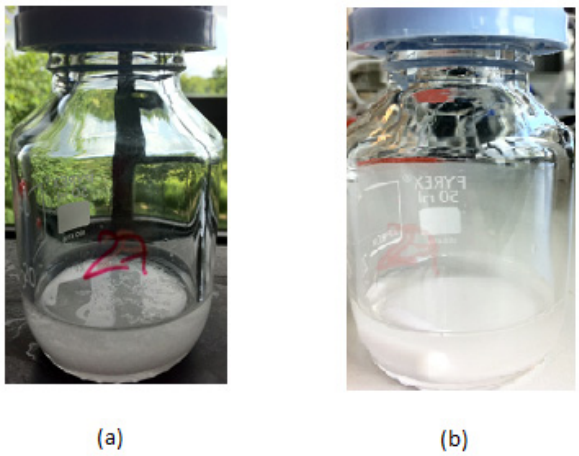

Figure 84. 27 wt% KHCO3 solution before (a) and after (b) warming to 27°C.

The 27.5 wt% $KHCO_3$ solution was warmed up, but the result of warming it was the same as for the previous solution. Furthermore the solution was left stirring the whole night, and as it is shown in Figure 85 the solution did not change, as it had the same white color as before leaving it stirring for a long time.

Figure 85. Solution of 27.5 wt% KHCO3 after stirring the sample night over.

Analyzing this potassium bicarbonate mass fraction by microscope some crystals were observed at room temperature, as shown in Figure 86. So the solution had some crystals at room temperature.

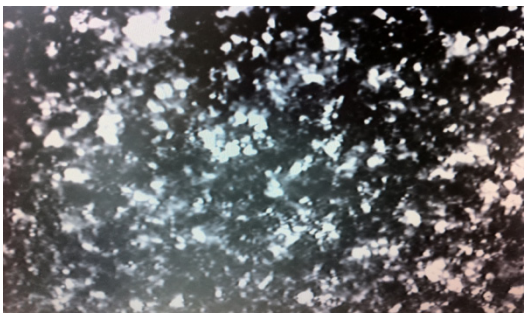

Figure 86. Crystals seen in the microscope for the solution 27.5 wt% $KHCO_3$.

Figure 87 shows the solutions after leaving them the whole night without stirring or warming. As it can be seen in the figure below, two different phases can be observed: a liquid one (water) and a precipitate (crystals). So the only thing that happened when the samples were warmed up and the solution turned white was trying to mix the different phases, but after leaving the samples for some hours these phases appeared again.

Figure 87. Some solutions after leaving them rest night over.

For the 28 wt% $KHCO_3$ the sample was not warmed up or stirred. Instead of it the solution was left the whole night in order to see the difference with the other solutions. Figure 88 shows the different phases observed in the solution: both in the upper part and in the bottom part of the beaker glass some crystals were formed, and between these layers a liquid phase (water) was observed.

Figure 88. Different phases observed in the solution 28 wt% $KHCO_3$.

The control of the temperature was not very accurate in the experiments. This was because we were not controlling the temperature accurately, as we were cooling and warming till crystals were formed or everything in the solution was dissolved. This was the problem why for high $KHCO_3$ mass fractions it was

not possible to determine the temperature at which crystals were formed and the temperature at which all the potassium bicarbonate was dissolved.

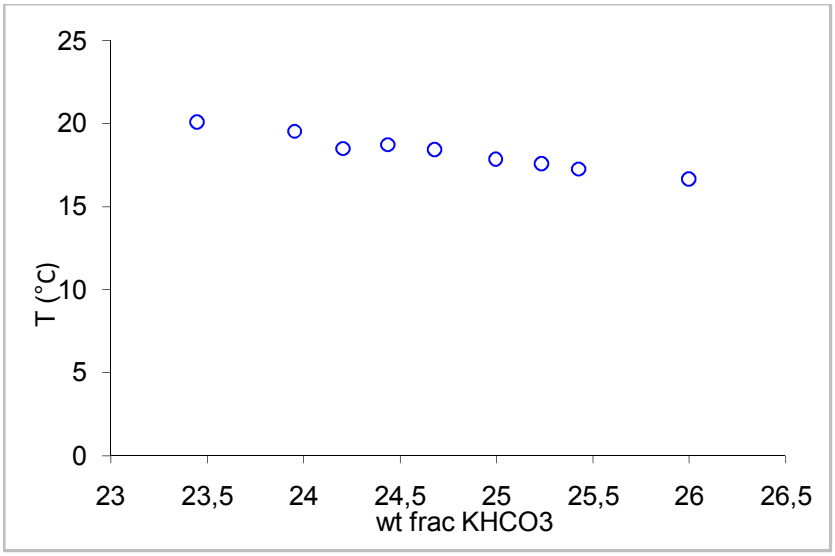

Figure 89. Temperature versus $KHCO_3$ mass fraction for the experiments carried out with the 3.6 molal PZ solvent.

As shown in Figure 89 both the temperature range and the $KHCO_3$ mass fraction range are not wide ranges. The temperature range in this graph is from 16 to 20°C, and the $KHCO_3$ mass fraction is form 0.253 to 0.26. First of all temperature decreases a little, then it seems that from 24.2 wt% $KHCO_3$ to 24.67 wt% $KHCO_3$ the temperature remains constant, and finally it decreases again.

9.6.3. Solvent: 4.6 molal $KHCO_3$.

Firstly the solvent was prepared. In this case, the solvent was different compared with the previous ones: the solvent was made by mixing water and potassium bicarbonate so that the $KHCO_3$ concentration was 0.3153 (or 4.6 molal $KHCO_3$). So 136.9366 g of water were mixed with 63.0634 g of potassium bicarbonate. Table 41 shows the experimental weights taken in the laboratory and the final molal $KHCO_3$ value.

Table 41. Measured amount of water and piperazine for the 4.6 molal $KHCO_3$.

m water (g)	m KHCO3 (g)	wt frac $KHCO_3$	molal $KHCO_3$
136.7529	63.0636	0.3156	4.6062

At room temperature some crystals were formed in the solution as shown in Figure 90, so the solvent was needed to be warmed up in order to get the crystals disappear.

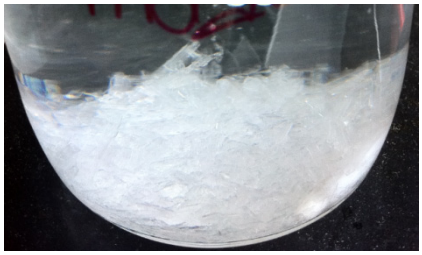

Figure 90. Crystals formed in the solvent at room temperature.

After preparing the solvent different solutions were prepared mixing the solvent with piperazine. Table 42 collects all the results for this system.

Table 42. Weightings, mean temperatures and standard deviations using the 4.6 molal $KHCO_3$ as a solvent.

wt% PZ	m solvent (g)	m PZ (g)	Mean T (°C)	T Stddev (°C)
11.979	9.0247	1.2282	-	-
12.839	9.1306	1.3450	-	-
14.465	9.0246	1.5262	6.10	0.143
15.684	9.0203	1.6779	10.64	0.099
17.673	9.0226	1.9368	19.47	0.121
19.955	9.0332	2.2519	25.16	0.198
21.552	9.0869	2.4964	66.61	1.986
23.232	9.0133	2.7276	90.24	0.187
23.994	9.0053	2.8428	93.33	0.424
24.708	9.0239	2.9613	92.25	0.289
25.483	9.0146	3.0828	-	-
26.191	9.0333	3.2055	-	-
26.989	9.0103	3.3307	-	-

Standard deviations up to 0.09°C were observed in Table 42, so the measurements were not taken very accurately, but we could not control the temperature very well.

The first two piperazine mass fractions (11.979 and 12.839 wt% PZ) were analyzed, but no crystals were formed even if the sample was at -17.5°C. The thermostatic bath with ethanol only arrives to -21.4°C, and this was not enough to cool the solution and get some crystals.

From 14.465 to 24.708 wt% PZ the solutions were needed to be cooled down to -13.1/14.3 (depending on the sample) and then warmed up till some crystals were formed. No problems were observed in these solutions, except from the 21.552 and 23.232 wt% PZ. In these cases the temperature was difficult to determine. For both cases at approximately 30°C there was a color change in the sample, but while observing it very carefully some tiny crystals were floating in the solution, and at 66°C and 93°C respectively these crystals disappeared. So the samples were needed to be warmed up a lot in order to get the solution without crystals.

For the 24.708 wt% PZ Figure 91 (a) shows some tiny particles floating in the solution, and as time passes the particles precipitate and deposit in the bottom of the beaker glass. In the case of the 25.483 wt% PZ not all the piperazine was dissolved correctly, even if the sample was warmed up to 100°C some particles were still floating in the solution (Figure 91 (b)). The same phenomenon occurred for the 25.191 wt% PZ.

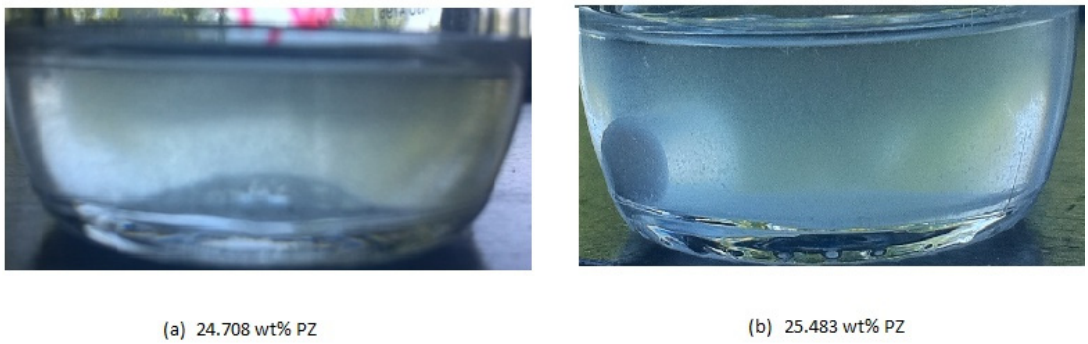

(a) 24.708 wt% PZ (b) 25.483 wt% PZ

Figure 91. Crystals floating in the solution 24.708 wt% PZ (a) and in the solution 25.483 wt% PZ (b).

For the 26.989 wt% PZ when the solution was observed after resting some time, two different phases were observed: some crystals were formed both in the upper part and in the bottom part of the beaker glass, and some water was in between (Figure 92). Furthermore, some crystals can be observed in Figure 92 on the walls in the upper part of the beaker glass (creeping).

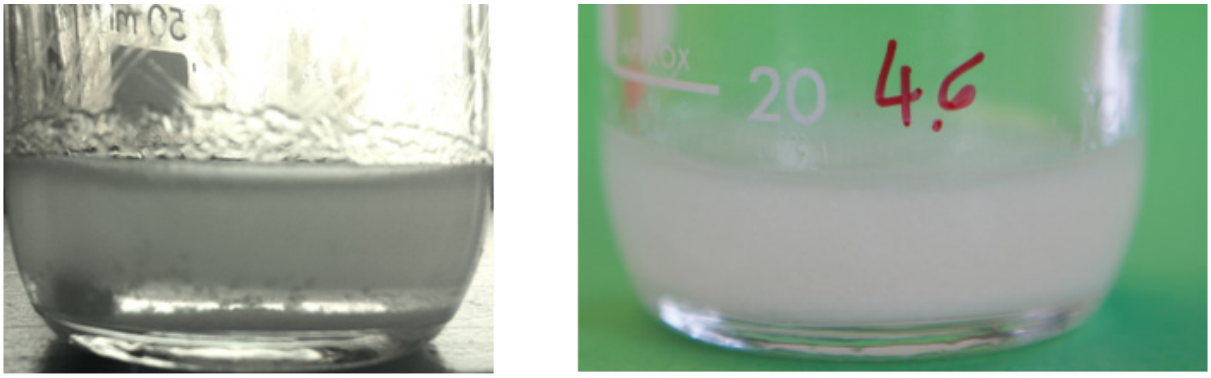

Figure 92. Different phases for the 26.989 wt% PZ (a) and the same solution after resting some hours (b).

Even if the 26.989 wt% PZ was warmed up, the solution did not change, so it was impossible to determine the temperature for this piperazine mass fraction.

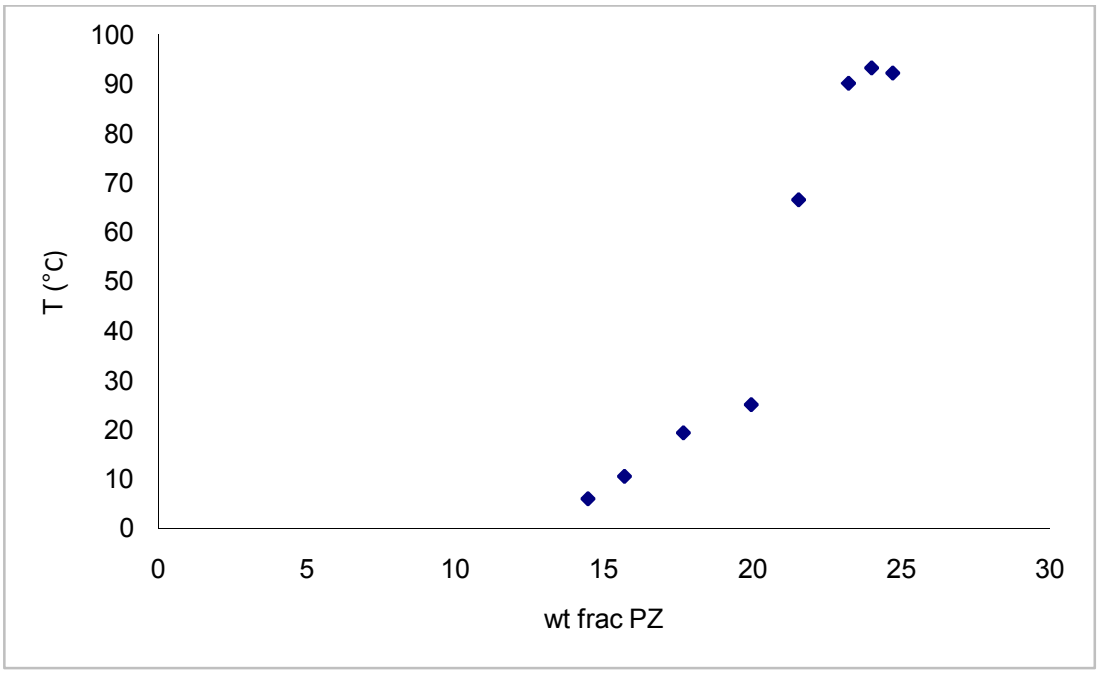

Figure 93. Temperature versus PZ mass fraction for the experiments carried out with the 4.6 molal $KHCO_3$solvent.

In Figure 93 it can be seen that the tendency of the solubility points is not the same as for the previous cases. In this case firstly temperature increases slightly, but then it increases very abruptly. Around 24 wt% PZ it reaches a maximum temperature, and then it seems that this temperature decreases.

10. Discussion and conclusions.

The industry burns fuels like coal, natural gas, or biomass to produce electricity. Chemicals, heat, or other similar large-scale products are produced. Post-combustion capture is a technique which enables these processes to become CO_2 neutral. The capture facilities require energy and this is an important reason why it is not used broadly today.

Chemical absorption is one of the most important post-combustion techniques used for separation of carbon dioxide from flue gases using solvents. Solidification of solvents as amino acids may be an important challenge for the industry. Solidification has two concerns. It can be either a benefit or a drawback. How it is viewed upon depends on the used equipment. If solidification of the solvents is not taken into account while using the scrubber, it may damage the equipment. On the other hand, it could also be used intentional to provoke precipitation to increase the CO_2 capture potential. Whatever method is used depends on the developed technology. It is important to be aware of the possible phase change.

To determine the solidification of amino acids we need to know the temperature at which crystals are formed.

The amino acids studied in this report are sodium and potassium glycinate; furthermore piperazine is also studied as an activator.

In this study freezing and solubility points were determined. Different systems were analyzed in order to study the influence of the various chemical species on CO_2 capture: glycine-water, sodium hydroxide-glycine-water, potassium hydroxide-glycine-water, sodium bicarbonate-glycine-water, potassium bicarbonate-glycine-water, sodium bicarbonate-sodium hydroxide-glycine-water, and potassium bicarbonate-potassium hydroxide-glycine-water. Furthermore, the effect of an accelerator as piperazine was also studied by mixing piperazine, potassium bicarbonate and water in different compositions.

Solutions were prepared and analyzed in the temperature range -35°C to 100°C. Freezing points were determined using a modified Beckmann apparatus.

Initially the equipment was calibrated. Solubility is often much higher than 0°C and freezing points are lower than 0°C. In order to increase accuracy two identical setups were used: one for freezing point determination and one for solubility determination. Each setup was calibrated accurately to the specific task at hand.

During the measurements the solutions were prepared, stirred and heated if needed in order to dissolve all the precipitate. Hereafter the freezing point or solubility points were determined using a previously developed method at DTU. Some samples were X-Rayed in order to determine the solid-phase type, and other samples were analyzed by microscope to obtain additional information on the precipitate.

Freezing and solubility points for potassium systems were easier to determine compared to sodium systems. Furthermore in both systems some solutions were very viscous and the measurements could not be performed. The viscous aspect of the solution is not a good property for CO_2 capture solvents. A very viscous liquid is not effective in a CO_2 absorber. The flow is simply to slow and the liquid films too thick. It basically reduces the performance.

In this study the experimental equipment is limited and may only measure freezing and solubility points down to -30°C approximately. Phase changes below this limit cannot be measured. This implies that parts of the freezing point curves and solubility curves appear undetermined in few of the plots. A section of the eutectic points lie in this concentration range and can consequently not be determined either.

On concluding whether the sodium or the potassium system is the better for CO_2 capture we need to use a general concentration scale for this. Therefore molal scale was used in this comparison instead of weight fraction.

The sodium glycinate system

In the sodium hydroxide-glycine-water system all the crystals formed had white color. By adding sodium hydroxide or glycine the freezing points were lower, so solidification is expected at lower temperatures. For the solubility curve, as more excess of glycine was considered (low solvent) the curve was more compressed in the SLE diagram.

For the loaded sodium bicarbonate-glycine-water system a high CO_2 loading was considered: 3 moles of sodium bicarbonate per one mole of glycine, although in industry scale this CO_2 loading is very high. By adding CO_2 freezing points are lower.

For the $NaHCO_3$-NaOH-Gly-H_2O system the freezing points and the solubility points were sometimes difficult to determine due to the viscosity and the impossibility of cooling the samples. As more amount of carbon dioxide is considered the solidification of sodium glycinate will be at higher temperatures. Therefore as the equipment has more carbon dioxide more problems can be expected in the equipment.

In order to obtain more information about the studied solutions for the sodium system, different samples were prepared and analyzed by microscopy at room temperature (approximately 20°C). For both 0.1 and 0.5 CO_2 loadings gamma-glycine and some impurities were present in the solutions. However solutions with 0.25 CO_2 loading melted very easily as freezing points (about 5-10°C) were lower than room temperature; therefore there was no possibility of analyzing these solutions. Furthermore, pure glycine seemed to have some impurities, and the sodium hydroxide contained water.

The potassium glycinate system

Most of the eutectic points in the analyzed potassium systems lie below -30°C and could not be determined by the used apparatus. Temperatures at about -70°C might be needed to fully determine the phase diagrams.

Observing the KOH-Gly-H_2O system the maximum solubility is obtained for the 1:1 nKOH/nGly relation. By adding an excess of glycine or potassium hydroxide, the solubility decreases. It is opposite for the freezing points. The 1:1 nKOH/nGly system has the highest freezing points adding an excess of potassium and glycine decreases the freezing points.

By adding CO_2, freezing points will decrease, and solubility points will decrease too.

Noticeably, there is no influence of carbon dioxide on systems containing excess of potassium (K/Gly relation 2 to 1).

In a broader perspective this means: to keep a high solubility a 1:1 K/Gly solvent should be used. Unfortunately it creates a solvent which has a relative high freezing point. Even as CO_2 is added the freezing point increases further. Note that the solubility also decreases on adding CO_2.

Consequently at low temperatures and high CO_2 loading, of a 1:1 K/Gly solvent, precipitation may occur. This could affect the bottom part of the absorber.

Comparison of the sodium and potassium glycinate systems

Comparing the sodium and the potassium systems we can conclude that the potassium glycinate is better than the sodium glycinate for CO_2 capture. The reason is that lower freezing points can be reached.

To sum up, by increasing the amount of sodium, potassium or glycine freezing points are lower; however if there is an increase in the CO_2 loading, freezing points are higher, so we need to reach a compromise between the amount of sodium, potassium or glycine and the amount of CO_2 in order not to have solidification of the amino acid. Furthermore we need to take into account the solubility curve, as if we add an excess of glycine the solubility curve is placed at low mass fractions.

Comparison to literature

Only one relevant study could be found in the literature which shows the aqueous solubility of sodium glycinate. There was no accordance between the literature and the determined solubility of this work. There seem to be a potential to scrutinize the glycinate chemistry.

More information about the solid-liquid equilibrium (SLE) phenomenon for amino acids is needed to be reported in order to have more information available in the literature and to see if the carbon dioxide capture systems can be enhanced.

The piperazine system

Piperazine is an organic compound used to accelerate the CO_2 removal from process gases. In this report piperazine was mixed with potassium bicarbonate and water in order to determine the influence of this accelerator in the process.

More time and heating were needed while measuring the solubility points in the systems in which piperazine was added. Unlike the sodium and potassium systems, when piperazine is considered in the system (for the 3.6 molal PZ and 4.6 molal $KHCO_3$) different phases can be seen in the beaker glass in some samples: a phase with crystals and a water phase between the two phases with crystals. Furthermore some crystals are creeping in the beaker glass.

11. Reference list.

[1] Reay, D.; Hogan, C. M. (2011).
Retrieved February, 2012, from http://www.eoearth.org/article/Greenhouse_gas.

[2] UNESCO. (2006). The global carbon cycle.
Retrieved February, 2012, from http://unesdoc.unesco.org/images/0015/001500/150010e.pdf.

[3] European Carbon Network. (2012).
Retrieved February, 2012, from http://www.co2net.eu/public/index.asp.

[4] ADEME; BRGM; IFP (2005). CO_2 capture and geological storage.The BRGM series "Geoscience issues". Pag. 7.

[5] (2009). Carbon Capture and Sequestration: Framing the Issues for Regulation: An Interim Report from the CCSReg Project. Retrieved February, 2012, from www.ccsreg.org/pdf/CCSReg_3_9.pdf.

[6] McGee, M. (2012). Retrieved February, 2012, from http://co2now.org/.

[7] United Nations Environment Programme (UNEP). Retrieved February, 2012, from http://www.unep.org/climatechange/mitigation/Introduction/tabid/29397/Default.aspx.

[8] Freund, P.; Adegbulugbe , A.; Christophersen, Ø.; Ishitani,H.;Moomaw, W.; Moreira, J. 1. Introduction. IPCC Special Report on Carbon dioxide Capture and Storage. Pag. 51-74.

[9]Greenhouse Gas Protocol (2011). Product Life Cycle Accounting and Reporting Standard. USA. No. ISBN 978-1-56973-773-6. Retrieved February, 2012, from http://www.ghgprotocol.org/standards/product-standard

[10] Red Europea del Dióxido de Carbono. (2005). Retrieved February, 2012, from http://www.co2net.eu/public/brochures/CO2NET-Public-Brochure-Spanish.pdf

[11] Hawkins, D. G.; Lashof, D. A.; Williams, R. H. (2006). What to do about coal. Scientific American.

[12] Gerlagh, R.; van der Zwaan, B. (2011). Evaluating uncertain CO_2 abatement over the very long term. Environ Model Assess, 17, 137-148.

[13] Forbes, S. M.; Verma, P.; Curry, T. E.; Bradley, M. J.; Friedmann, S. J.; Wade, S. M. (2008). Guidelines for carbon dioxide capture, transport, and storage. Washington, USA: World Resources Institute.

[14] Haszeldine, R. S. (2009). Carbon capture and storage: How green can black be? Science, 325 (no. 5948), 1647-1652.

[15] Bachu, S.; Bonijoly, D.; Bradshaw, J.; Burruss, R.; Holloway, S.; Christensen, N. P.; Mathiassen, O. M. (2007). CO_2 storage capacity estimation: Methodology and gaps. International Journal of Greenhouse Gas Control, 1(4), 430-443.

[16] Zakkour, P.; Haines, M. (2007). Permitting issues for CO_2 capture, transport and geological storage: A review of europe, USA, canada and australia. International Journal of Greenhouse Gas Control, 1(1), 94-100.

[17] IPCC. IPCC special report on carbon dioxide capture and storage. Retrieved February, 2012, from http://www.ipcc.ch/pdf/special-reports/srccs/srccs_chapter3.pdf.

[18] KBR. Retrieved February, 2012, from http://www.kbr.com/Technologies/Carbon-Capture-and-Storage/

[19] Royo, M. P. (2009). Evaluación de métodos para mejorar el comportamiento del óxido de calcio como sorbente regenerable en ciclos de carbonatación/calcinación aplicados a la captura de dióxido de carbono. Proyecto fin de carrera. Universidad de Zaragoza. 1-99.

[20] Morales, H.; Torres, C. (2008). Tecnologías de captura y secuestro de CO_2. Pontificia Universidad Católica de Chile.

[21] Zheng, L. (Ed.). (2011). Overview of oxy-fuel combustion technology for carbon dioxide (CO_2) capture.

[22] Otero Ventín, P. Tecnologías contra el cambio climático: Captura y almacenamiento de CO_2: Proceso de captura de CO_2 en oxicombustión.

[23] Adams, R. G.; Alin, J.; Biede, O.; Booth, N. J.; deMontigny, D.: Drew, R.; . . . Trunkfield, A. (2009). CAPRICE project—Engineering study on the integration of post combustion capture technology into the power plant gas path and heat cycle. Energy Procedia, 1(1), 3801-3808.

[24] Herzog, H.; Meldon, J.; Hatton, A. (2009). Advanced post-combustion CO_2 capture. Consultado en Febrero, 2012, de http://web.mit.edu/mitei/docs/reports/herzog-meldon-hatton.pdf.

[25] Herzog, H. (1999). An introduction to CO_2 separation and capture technologies. MIT Energy Laboratory.

[26] Abanades, C. (2005). Nuevas tecnologías de captura de CO_2. Carbonatación-calcinación.

[27] Galán, J. C. (2009). Estudio del efecto de la presencia de SO_2 sobre el comportamiento del CaO como sorbente regenerable para la captura de CO_2. Universidad de Zaragoza. 1-74.

[28] Figueroa, J. D.; Fout, T.; Plasynski, S.; McIlvried, H.; Srivastava, R. D. (2008). Advances in CO_2 capture technology—The U.S. Department of Energy's Carbon Sequestration Program. International Journal of Greenhouse Gas Control. 2, 9–20.

[29] Retrieved February, 2012, from http://www.powerplantccs.com/ccs/cap/fut/sns/sns.html.

[30] Ma'mun, S.; Svendsen, H. F.; Hoff, K. A.; Juliussen, O. (2007). Selection of new absorbents for carbon dioxide capture. Energy Conversion and Management, 48(1), 251-258.

[31] Lin, C.-Y.; Soriano, A. N.; Li, M-H. (2009). Kinetics study of carbon dioxide absorption into aqueous solutions containing N-methyldiethanolamine+diethanolamine. Journal of the Taiwan Institute of Chemical Engineers. 40, 403–412.

[32] Fosbøl,P. L.; Pedersen, M. G.; Thomsen, K. (2011). Freezing Point Depressions of Aqueous MEA, MDEA, and MEA-MDEA Measured with a New Apparatus. Journal of Chemical & Engineering Data. 56, 995–1000.

[33] Lee, S.; Song, H.-J.; Maken, S.; Park, J.-W. (2007). Kinetics of CO_2 Absorption in Aqueous Sodium Glycinate Solutions. Industrial & Engineering Chemistry Research. 46, 1578-1583.

[34] Versteeg, P.; Rubin, E. S. (2011). A technical and economic assessment of ammonia-based post-combustion CO_2 capture at coal-fired power plants. International Journal of Greenhouse Gas Control. 5, 1596–1605.

[35] Darde, V.; van Well, W. J.M.; Fosbøl, P. L.; Stenby, E. H.; Thomsen, K. (2011). Experimental measurement and modeling of the rate of absorption of carbon dioxide by aqueous ammonia. International Journal of Greenhouse Gas Control. 5, 1149-1162.

[36] Ma, J. ; Zhou, Z; Zhang, F; Fang, C; Wu, Y; Zhang, Z; Li, A. (2011). Ditetraalkylammonium Amino Acid Ionic Liquids as CO_2 Absorbents of High Capacity. Environmental Science & Technology. 45, 10627–10633.

[37] Aronu, U. E.; Svendsen, H. F.; Hoff, K. A. (2010). Investigation of amine amino acid salts for carbon dioxide absorption. International Journal of Greenhouse Gas Control. 4, 771–775.

[38] van Holst, J; Versteeg, G.F.; Brilman, D.W.F; Hogendoorn, J.A. (2009). Kinetic study of CO_2 with various amino acid salts in aqueous solution. Chemical Engineering Science. 64, 59-68.

[39] Jockenhoevel, T.; Schneider, R.; Rode, H. (2009). Development of an Economic Post-Combustion Carbon Capture Process. Energy Procedia. 1, 1043-1050.

[40] Portugal, A.F.; Derks, P.W.J.; Versteeg, G.F.; Magalhães, F.D.; Mendes, A. (2007). Characterization of potassium glycinate for carbon dioxide absorption purposes. Chemical Engineering Science. 62, 6534–6547.

[41] Majchrowicz, M. E.; Brilman, D.W.F.; Groeneveld, M. J. (2009). Precipitation regime for selected amino acid salts for CO_2 capture from flue gases. Energy Procedia. 979-984.

[42] Baek, J.-I.; Yoon,J.-H. (1998). Solubility of Carbon Dioxide in Aqueous Solutions of 2-Amino-2-methyl-1,3-propanediol. Journal of Chemical & Engineering Data. 43, 635-637.

[43] Lu, J.-G.; Fan, F.; Liu,C.; Zhang,H.; Ji, Y.; Chen, M.-D. (2011). Density, Viscosity, and Surface Tension of Aqueous Solutions of Potassium Glycinate + Piperazine in the Range of (288.15 to 323.15) K. Journal of Chemical & Engineering Data. 56, 2706–2709.

[44] Vaidya, P. D.; Konduru, P.; Vaidyanathan, M.; Kenig, E. Y. (2010). Kinetics of Carbon Dioxide Removal by Aqueous Alkaline Amino Acid Salts. Industrial & Engineering Chemistry Research. 49, 11067–11072.

[45] Simons, K.; Brilman, W.(D.W.F.); Mengers, H.; Nijmeijer, K.; Wessling, M. (2010). Kinetics of CO_2 Absorption in Aqueous Sarcosine Salt Solutions: Influence of Concentration, Temperature, and CO_2 Loading. Industrial & Engineering Chemistry Research. 49, 9693–9702.

[46] Tseng, H.-C.; Lee, C.-Y.; Weng, W.-L.; Shiah,I.-M. (2009). Solubilities of amino acids in water at various pH values under 298.15 K. Fluid Phase Equilibria. 285, 90–95.

[47] The Contactor^{TM}. (2010). Capturing CO_2 With Sodium Glycinate. Optimized Gas Treating, Inc. Volume 4, Issue 2.

[48] Salazar, V.; Sánchez-Vicente, Y.; Pando,C.; Renuncio, J. A. R.; Cabañas, A. (2010). Enthalpies of Absorption of Carbon Dioxide in Aqueous Sodium Glycinate Solutions at Temperatures of (313.15 and 323.15) K. Journal of Chemical & Engineering Data. 55, 1215–1218.

[49] Dietl,K.; Joos, A.; Schmitz, G. (2012). Dynamic analysis of the absorption/desorption loop of a carbon capture plant using an object-oriented approach. Chemical Engineering and Processing: Process Intensification. 52, 132–139.

[50] Goetheer, E.; Sanchez-Fernandez, E.; Mergler, Y. (2011). DECAB: process development of a phase change absorption process. Energy Procedia. Volume 4, Pages 868–875.

[51] Kumar, P. S.; Hogendoorn,J. A. ; Feron, P. H. M.; Versteeg, G. F. (2010). (2001). Density, Viscosity, Solubility, and Diffusivity of N_2O in Aqueous Amino Acid Salt Solutions.Journal of Chemical & Engineering Data. 46, 1357-1361.

[52] Lee, S.; Song, H.-J.; Maken, S.; Shin, H.-C.; Song, H.-C.; Park,J.-W. (2006). Physical Solubility and Diffusivity of N_2O and CO_2 in Aqueous Sodium Glycinate Solutions. Journal of Chemical & Engineering Data. 51, 504-509.

[53] Song, H.-J.; Lee, S.; Maken, S.; Park, J.-J.; Park, J.-W. (2006). Solubilities of carbon dioxide in aqueous solutions of sodium glycinate. Fluid Phase Equilibria. 246, 1–5.

[54] Harris, F.; Kurnia, K. A.; Mutalib, M. I A.; Thanapalan, M. (2009). Solubilities of Carbon Dioxide and Densities of Aqueous Sodium Glycinate Solutions before and after CO_2 Absorption. Journal of Chemical & Engineering Data. 54, 144–147.

[55] Mazinani, S.; Samsami, A.; Jahanmiri, A. (2011). Solubility (at Low Partial Pressures), Density, Viscosity, and Corrosion Rate of Carbon Dioxide in Blend Solutions of Monoethanolamine (MEA) and Sodium Glycinate (SG). Journal of Chemical & Engineering Data. 56, 3163–3168.

[56] Park, S.-W.; Son, Y.-S.; Park, D.-W.; Oh, K.-J. (2008). Absorption of Carbon Dioxide into Aqueous Solution of Sodium Glycinate. Separation Science and Technology. 43, 3003–3019.

[57] Lee, S.; Choi, S.-I.; Maken,S.; Song, H.-J.; Shin, H.-C.; Park,J.-W. ; Jang, K.-R.; Kim, J.-H. (2005). Physical Properties of Aqueous Sodium Glycinate Solution as an Absorbent for Carbon Dioxide Removal. Journal of Chemical & Engineering Data. 50, 1773-1776.

[58] Fosbøl, F. L.; Neerup, R.; Arshad, M. W.; Tecle, Z.; Thomsen, K. (2011). Aqueous Solubility of Piperazine and 2-Amino-2-methyl-1-propanol plus Their Mixtures Using an Improved Freezing-Point Depression Method. Journal of Chemical & Engineering Data. 56, 5088–5093.

[59] McCann, N.; Maeder, M.; Attalla, M. (2008). Simulation of Enthalpy and Capacity of CO_2 Absorption by Aqueous Amine Systems. Industrial & Engineering Chemistry Research. 47, 2002-2009.

[60] Park, S.-J.; Jang, K.-R.; Park, I. H. (2006). Determination and Calculation of Physical Properties for Sodium Glycinate as a CO2 Absorbent. Korean Journal of Chemical Engineering.Vol. 44, No. 3, 277-283.

[61] Song,H.-J.; Lee, S.; Park, K.; Lee, J.; Spah, D. C.; Park, J.-W. ; Filburn, T. P. (2008). Simplified Estimation of Regeneration Energy of 30 wt % Sodium Glycinate Solution for Carbon Dioxide Absorption. Industrial & Engineering Chemistry Research. 47, 9925–9930.

[62] Lee, S.; Song, H.-J.; Maken, S.; Yoo, S.-K.; Park, J.-W.;Kim, S.; Shim, J. G.; Jang, K.-R. (2008). Simulation of CO_2 removal with aqueous sodium glycinate solutions in a pilot plant. Korean J. Chem. Eng. 25(1), 1-6.

[63] Portugal, A.F.; Sousa, J.M.; Magalhães, F.D.; Mendes, A. (2009). Solubility of carbon dioxide in aqueous solutions of amino acid salts. Chemical Engineering Science. 64, 1993—2002.

[64] Hamborg, E. S.; van Swaaij, Wim P. M.; Versteeg, G. F. (2008). Diffusivities in Aqueous Solutions of the Potassium Salt of Amino Acids. Journal of Chemical & Engineering Data. 53, 1141–1145.

[65] Mergler, Y.; Rumley-van Gurp, R.; Brasser, P.; de Koning, M.; Goetheer, E. (2011). Solvents for CO_2 capture. Structure-activity relationships combined with Vapour-Liquid-Equilibrium measurements. Energy Procedia. 4, 259–266.

[66] Aronu,U. E.; Hoff, K. A.; Svendsen,H. F. (2011). Vapor–liquid equilibrium in aqueous amine amino acid salt solution: 3-(methylamino)propylamine/sarcosine. Chemical Engineering Science. 66, 3859–3867.

[67] Jakob,A. ; Joh,R.; Rose, C.; Gmehling, J. (1995). Solid-liquid equilibria in binary mixtures of organic compounds. Fluid Phase Equilibria. 113, 117-126.

[68] Mullin, J.W. (2001). "Crystallization". Fourth edition.

[69]The free dictionary. Retrieved May, 2012, from http://www.thefreedictionary.com/freezing+point

[70] Scorellano, M. (2004). Essential experiments for Chemistry. Sample experiment. Freezing point depression.

[71]Bishop, M. Acid-Base titration.
Retrieved May, 2012, from http://preparatorychemistry.com/Bishop_Titration.htm.

[72]Rochelle, G. T. Carbon dioxide capture by aqueous piperazine. Retrieved June, 2012, from de http://www.ideaconnection.com/technology-for-sale/6468-Carbon-Dioxide-Capture-by-Aqueous-Piperazine.html.

[73] Lensen, R. The promoter effect of piperazine on the removal of carbon dioxide. Consultado Retrieved June, 2012, from http://www.bsdfreaks.nl/files/hoofd6.pdf.